Politecnico di Milano

Scuola di Ingegneria Industriale e dell'Informazione

Ingegneria Aeronautica

Thermal Transpiration and Poiseuille Flow in a Knudsen Compressor

Supervisor / Relatore: Prof. Aldo Frezzotti

Advisor / Co-relatore: Prof. Kazuo Aoki

Student's Name / Nome dello studente: Timoteo Badalotti, 786512

Academic Year 2013/2014

Aknowledgements

I dedicate this thesis to all those without whose help I would have never made it to the end of this long journey, and whose support has been a spur never to give up. First of all, I ought to thank my parents who have always been encouraging me to deal with every problem that confronted me keeping in mind that the real aim of my studies and of my whole life is not merely that of acquiring knowledge but is to gain the personal and spiritual maturity that is required to face up to the many challenges of life. Then, I want to express my sincerest thanks to all the members of the Sauer family, my *adoptive* family. Apart from my *natural* family, they are those who had the greatest influence on my way of thinking. What I learned from them molded me permanently. I wish to thank my sister, my grandparents and my uncle's family. Then, I want to thank all those friends with whom I could share moments of joy as well as sorrowful thoughts whenever I felt dispirited in the past few years: Matteo Cestari, Naomi Arao, Hiroaki Kitagawa, Ray Sauer, Timmy Hinds, Tanner Hinds, Hattori Masanari, Ryo Kagaya, Tatsuo Shibata, Hiroyuki Kakiuchi, Yumiko Uchishiba. Three of them have been of great help whenever I was in need while doing research for this thesis: Hattori's *know-how* has proved essential; Kagaya let me use *mercilessly* the workstations he would have otherwise done calculations with; Shibata thought me the art of boning fish with chopsticks. As far as this thesis project is concerned, I have to thank also Professor Aldo Frezzotti for he gave the chance to go to Kyoto University, Japan, to undertake it. Finally, I basically owe my whole understanding of the Boltzmann equation to Professor Kazuo Aoki. His patience and perseverance make him a true *sensei*, a term that carries a broader meaning than just that of "teacher" or "professor". His ability to motivate me is undoubtedly worth of mention; whenever I had a question, his explananations could shed light on the dark spots of my understanding.

I truly hope the reader will enjoy this paper at least half as much as I did in writing it.

Contents

1 Abstract

The main objective of the present work is to analyze the opposing effects of thermal-transpiration flow and Poiseuille flow in a narrow conduit like the one employed in a Knudsen compressor or Knudsen pump. We will first introduce the basics about the Boltzmann equation (definition, brief physical intepretation, applicability, main issues, etc.). Then, the models used to describe the problem at hand, namely ES-Model and BKW-Model (also known as BGK-Model), will be explained alongside with all the information needed to apply them (simplifications deriving from the geometry of the domain and spherical simmetry of the collision operator). Thereafter, the setting of the problem will be detailed: what a Knudsen pump is and the particular kind of Knudsen pump we will deal with (basically one formed by two parallel plates and two tanks). The two kinds of flows that are to be found in the conduit of this pump will be then pointed out: the Poiseuille flow (well know from the fluid dynamics) and the more subtle thermal-transpiration (or thermal-creep) flow. Eventually, the problem will be solved by applying an asymptotical expansion: zeroth-oder solution, first-order solution and second-order solution. The zeroth-order solution has been analytically found. The first-order solution will be numerically computed after the application of a factorization and of the model equations. The second-order solution will not be explicitly computed but its analysis will lead to the characterization of the macroscopic quantities. Then, the unsteady case of flow between two tanks linked by a thin conduit will be considered. The final chapter will be dedicated to the data obtained and to the conclusions. The data obtained for the adimensionalized mass-flow rate are thought of as being more accurate than those previously available for the specific cases under consideration. The data obtained in case of accommodation coefficient different from 1 and in the unsteady case have not been computed before.

Keywords: Boltzmann Equation; ES-Model; BKW-Model; BGK-Model; Knudsen compressor; Thermal Transpiration; Numerical Kernel

Sommario

L'obiettivo principale di questo lavoro è quello di analizzare gli effetti contrastanti del flusso di traspirazione termica e del flusso di Poiseuille in un

condotto sottile come quello usato nella pompa di Knudsen. Come prima cosa verrà introdotta l'equazione di Boltzmann (definizione, breve descrizione fisica, applicabilità, principali problemi che presenta, etc.). In seguito verranno presentati i modelli usati per risolvere il nostro problema (Modello ES, Modello BKW, detto anche Modello BGK) assieme alle informazioni necessarie alla loro implementazione (semplificazioni derivanti dalla geometria del problema e dalla proprietà di simmetria sferica caratterizzante l'integrale collisionale). Successivamente, si presenterà il problema da risolvere: verrà spiegato che cos'è una pompa di Knudsen in generale e verrà presentato il funzionamento di quella che dovrà essere trattata (è una pompa formata da due piastre parallele e due serbatoi). Verranno evidenziati i due tipi di flusso che si incontrano in questo tipo di problemi: il flusso di Poiseuille (già noto dalla fluidodinamica) e quello meno evidente di traspirazione termica. Infine, il problema verra risolto applicando un'espansione asintotica: soluzione di ordine zero, soluzione di ordine uno e soluzione di ordine due. La soluzione di ordine zero è stata ricavata in modo analitico. La soluzione di ordine uno sarà trovata numericamente grazie all'applicazione di una fattorizzazione e delle equazioni modello. La soluzione di ordine due non viene calcolata ma la sua analisi porterà alla caratterizzazione delle quantità macroscopiche. Verrà poi considerato il caso di flusso instazionario tra due serbatoi connessi attraverso un condotto sottile. L'ultimo capitolo sarà dedicato ai dati ottenuti ed alle conclusioni. I dati ottenuti per il flusso di massa per unità di tempo adimensionalizzato sono considerati più accurati di quelli ottenuti precedentemente per i specifici casi in considerazione. I dati ottenuti in caso di coefficiente di accomodamento diverso da 1 e nel caso instazionario non sono stati ricavati precedentemente.

Keywords: Equazione di Boltzmann; Modello ES; Modello BKW; Modello BGK; Pompa di Knudsen; Traspirazione Termica; Numerical Kernel

2 Introduction to the Boltzmann Equation

2.1 Overview

"The first main open problem is to prove that positive, classical solutions of the Maxwell-Boltzmann equation corresponding to specified initial conditions and boundary conditions exist and are unique." [1]

This first introductory part is meant as a brief explanation of the Boltzmann equation. It goes without saying that neither a chapter nor a single book could ever be enough to introduce the Boltzmann equation both rigorously and completely. We'll just go through the formulation of the equation with its boundary conditions and then go on to analyze the model equations by explaining only what is strictly necessary to understand the main results of the present work. Broadly speaking, a problem is said to be well posed when the main equations and the boundary conditions have been specified, the boundary conditions are compatible with the equations and the solution has been proved to exist and be unique under the aforementioned boundary conditions. In the case of the Boltzmann equation, the proof of existence and uniqueness is not an easy task. Furthermore, were the two properties of uniqueness and existence are verified, there would still be the problem of finding an analytical solution. We will see in the next chapter that the use of model equations combined with a couple of clever tricks will greatly simplify the main problem of this paper and the existence and uniqueness of the solution will be dealt with quite easily. This brief introduction, though being not sufficiently detailed to reveal the meanders of the Boltzmann equation, should be just enough complete to cast some light on the basis upon which the kinetic theory stands and to explain the main results that will be useful later on in this paper. Other important aspects be illustrated on a need-to-know basis in the next chapter.

2.2 The Kinetic Theory for a Monoatomic Gas

"Maxwell's kinetic theory is a consequence neither of classical mechanics nor of the axioms of probability theory. Though it is motivated by a masterly and suggestive combination of

mechanical and stochastic ideas, it is an independent model of a gas. As such it is to be respected and studied mathematically. The proof of the model lies in its product. The two models of a dissipative fluid that have proved their value again and again are the Navier-Stokes theory of linearly viscous fluids and Maxwell's kinetic theory. [...] Each involves a special kind of non-linearity that seems somehow to reflect much, though by not means all, of the phenomena seen in natural fluids." [1]

The following explanation, scarce as it may seem at a first glance, should introduce the kinetic theory in the case of a monoatomic gas that has just one species, that is to say a simple gas. The main reference of this section is an enlightening book by Truesdell and Muncaster that step by step introduces this theory [1]. Basically, the kinetic theory of gases is a mathematical model in which the gas is envisaged as a collection of molecules that are subject to external forces, collide one with the other and impinge upon surfaces whose behavior has also to be modeled. Each molecule occupies a given position in the three-dimensional space domain and has a certain velocity at a given time. However, instead of following the motion of every single molecule, we will suppose that all the molecules are randomly distributed according to a specific rule. This rule is the molecular density F. Let us proceed by defining F. We first introduce the three main variables:

- $t \in \mathbb{T}$, a one-dimensional Euclidean space;
- $x \in \mathbb{X}$, a three-dimensional Euclidean space;
- $v \in \mathbb{V}$, a three-dimensional Euclidean space.

t is the time, x is the coordinate in the three-dimensional space domain and v is the velocity. $F = F(t, x, v)$ and $\int_{\mathbb{U}} \int_{\mathbb{B}} F(t, x, v) dx dv$, with $\mathbb{B} \in \mathbb{X}$ and $\mathbb{U} \in \mathbb{V}$, is interpreted as the expected number of molecules in $\mathbb{B}$ with velocities in $\mathbb{U}$ at the time$t$. The number density is defined by the formula $n = \int_{\mathbb{V}} F(t, x, v) dv$. Pay attention to the fact that the velocity domain is the whole space $\mathbb{V}$, in fact we want to find the expected number of molecules per unit point in a certain point at a fixed time including the molecules of any velocity whatever. Accordingly, we can conclude that the function $v \mapsto \frac{F(t,x,v)}{n(t,x)}$ is a probability density over $\mathbb{V}$. m is the constant bearing the unit of mass. We define the mass density ρas $\rho = mn$. Furthermore, the expectation $\overline{g}(t, x)$ of a function $g = g(t, x, v)$ is defined as $g \equiv \frac{1}{n} \int_{\mathbb{V}} F(t, x, v) g(t, x, v) dv$. We proceed by defining the following fields:

- gross velocity field $u \equiv \overline{v}$ (the random velocity c is defined as $c = v - u$),
- pressure tensor field $M \equiv \rho \overline{c \otimes c}$,
- pressure deviator field $P \equiv M - \frac{1}{3}(trM)I$,

- energy flux vector $q \equiv \frac{1}{2}\rho\overline{c^2 c}$,

and the following scalars:

- pressure $p = \frac{1}{3}\overline{c^2}$,

- expected random kinetic energy (interpreted as the energetic) $\varepsilon = \frac{1}{2}\overline{c^2}$.

To quote Truesdell, "The entire purpose of the kinetic theory is to relate the 13 scalar fields ρ, u_k, M_{pm} and q_r to various circumstances of the kinetic gas."

So far, we have defined only the quality we want to find but we haven't specified how to determine F. The earliest kinetic theorists tried to solve the problem by assuming that F has certain properties in some given conditions. Also Maxwell, at first, tried to do the same. The theory derived by Maxwell following this fashion is called by Truesdell first kinetic theory. However, the theory that we wish to introduce in this basic chapter is named Maxwell's second kinetic theory. The axiom laid down by Maxwell that we are about to explain is the first necessary step to justify the Maxwell-Boltzmann Integro-Differential Equation. We know that there are two kind of forces that modify the trajectory of the particles in our domain: a body force$b$, which is an extrinsic force per unit mass, and a mutual force due to the collisions of the molecules. Analytical dynamics would require us to treat the two forces together by summing them up whereas Maxwell's assumption was that the two forces be considered separately: the body force is treated as Newtonian mechanics would require while the mutual force is approximated with a stochastic model. This assumption yields a model that is neither coherent with the laws of dynamics nor completely suitable to be described by purely statistical methods. Let us now take into consideration only the body force b. As Truesdell shows, we can easily find the trajectory of every single particle and define an operator dependent upon s, called retrogressor, whose effect on the function defining the trajectory is that of retrieving the position and velocity of the particle s units of time before the actual time t. Analogously, we could define the transform R_s dependent upon s, also called retrogressor, whose effect if that of evaluating the value of a given function s units of time before the actual time t by going back along the trajectory. The trajectory considered by omitting the term related to the mutual interaction of the particles is called the extrinsic trajectory, and, if there were no mutual interaction, the extrinsic trajectory would coincide with the actual trajectory of each particle. Therefore, we can say that all the expectations remain unchanged along the trajectory. We require that

$$F(t,x,v) = R_{t-t_0}F(t,x,v) \tag{2.1}$$

for some fixed time $t_0$and for every t, x and v. A dynamically coherent approach would require us to sum the effect of collisions to the right hand side of this equation. Let us take, for instance, the case of elastic and inelastic collisions: the collision follows certain rules and its effect are given by adding a force to the right hand side. Generally, an impact would disrupt the smoothness of the trajectory. In Maxwell's model, the mutual forces between particles are thought to "appear and disappear instantly at (t,x,v) at a rate that depends on some specified way on F". The operator specifying this rate is called collision operator and denoted by $\mathbb{C}$. The effect of collisions have to be "accumulated". By doing so we may state Maxwell's Equation of Evolution:

$$F(t,x,v) = R_{t-t_0}F(t,x,v) + \int_{t_0}^{t} R_{t-s}(\mathbb{C}F)(t,x,v)ds \tag{2.2}$$

Even though much could be said about the agreement between this theory and fluid mechanics, we go on and spend a few words on the dynamics of encounters. Whatever be the molecules constituting the body of gas that we are to describe, the encounters are always taken to be binary. This is somewhat coherent with the assumption that the gas under consideration is rarefied. A binary encounter is supposed to be subject to conservation of energy and momentum. The mutual forces may have an infinite range in space of may be forces instantly exerted during a collision.

$$v + v_\star = v' + v'_\star \tag{2.3}$$

$$v^2 + v_\star^2 = v + v_\star'^2 \tag{2.4}$$

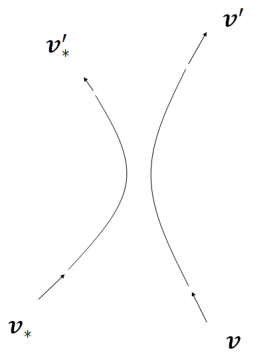

Figure 2.1: Velocities of Two Colliding Molecules

Let us introduce the notion of summational invariant. A real-valued function C on $\mathbb{V} \times \mathbb{V}$ satisfying the condition $C(v, v_\star) = C(v', v'_\star)$ for all $(v, v_\star)$ and $(v', v'_\star)$ related through the conservation laws is called a collisional invariant. Analogously, a real-valued function S on $\mathbb{V}$ such that $S(v)+S(v_\star) = S(v')+S(v'_\star)$ for all $(v, v_\star)$ and $(v', v'_\star)$ related through the conservation laws is called a summational invariant. The subspace of summational invariants has dimension 5 as stated by the Boltzmann-Gronwall Theorem on Summational Invariants (whose proof can be found in the aforementioned book): A measurable function S over $\mathbb{V}$ is a summational invariant if and only if it is an affine combination of momentum and energy: $S(v) = \alpha v^2 + \mu \cdot v + \beta$, α and β being scalars and μ a vector.

A further definition needs mentioning, as it will be useful later on. The elements of the basis of the space of the summational invariants are called principal invariants I_α.

$$I_\alpha \equiv \begin{cases} 1 & \alpha = 0, \\ v_\alpha & \alpha = 1, 2, 3, \\ v^2 & \alpha = 4. \end{cases} \tag{2.5}$$

The next step is the solution of the encounter problem. Truesdell, after listing a few properties that an encounter is supposed to satisfy, presents three solutions, the last of which has been found taking into consideration the "physical process", quoting Truesdell himself. The leads to the definition of an encounter operator $\mathbb{E}$. What we want to point out in this meager explanation is that this operator, which may be defined a priori (given that it satisfies certain properties), determines $v'$and $v'_\star$once v, $v_\star$, r and ζ have been assigned, r and ζ being respectively the distance and angle used to define

in radial coordinates the vector whose origin corresponds to the position (x) of the molecule under consideration, which is considered at rest, and that points to the point of intersection between the trajectory that the colliding molecule would have if no mutual forces were present and the plane P, which we are about to define. The molecule that is about to collide with the one under consideration has a trajectory which features an asymptote at $t = -\infty$. P is the plane normal to this asymptote to which x belongs. Actually, in the case of mutual forces of finite range, the collision occurs only if the point of intersection lies in a certain portion of the plane P, defined as cross-section$S$. We say that in the case of infinite-range forces S corresponds to $\mathbb{R}^2$. Furthermore, S may be a function of given parameters, such as the diameter of the molecules for an hard-sphere model of the gas. m, $\mathbb{E}$, and S are called Constitutive Quantities of the Kinetic Theory. The force b, which is regarded as "external rather than constitutive", to quote Truesdell, is taken to be a prescribed function of place alone. It is interesting that the focus is shifted from the two-body problem to the problem of encounter as defined through the constitutive quantities of the kinetic theory.

Let us point out a few further important hypotheses justifying the definition of the Maxwell Collision Operator that is about to be introduced:

- At a given place and a given time, the velocities of the molecules colliding are instantly changed. In classical mechanics a number of molecules interacting have trajectories resulting from all the interactions for all time. The conversion of velocities if instantaneous and discontinuous.

- The colliding molecules do not occupy the same position but they are supposedly so close to each other that the molecular density is not a function of the position.

- The assumption of stochastic independence is the most delicate one: "Maxwell assumed that the probability density for a pair of molecules with velocities v_1 and v_2 at (t, x) was proportional to $F(t, x, v_1)F(t, x, v_2)$", to quote Truesdell once again. This is what is called "molecular chaos" and Truesdell himself uses the term "fading memory" between quotation marks to give an idea of what molecular chaos is. This is far from being a self-contained assumption. This hypothesis has an overwhelming influence on the problem which is pointed out by Cercignani [2]. Let us focus on the case of hard-sphere molecules (they are modeled as hard, elastic and perfectly smooth spheres). The Boltzmann equation is strictly valid in the case in which $N \to \infty$,$\sigma \to 0$ and $N\sigma$ is finite, where σ is the diameter of the molecules (Boltzmann-Grad limit). The Boltzmann-Grad assumption is related to the fact that $\sigma \to 0$ in order for the first assumption to be valid. Cercignani points out that

we cannot expect every initial state to be a solution of the Boltzmann equation in the Boltzmann-Grad limit. We need a special initial state which verifies this assumption. Indeed, we want this assumption to be verified for all time. Furthermore, it cannot hold everywhere. If it did, the molecular density would not evolve in time. It has to be verified only for molecules which are about to collide!

Let us introduce an useful notation for a function $g = g(t, x, v)$:

- g stands for $g(t, x, v)$;
- $g_\star$ stands for $g(t, x, v_\star)$;
- g' stands for $g(t, x, v')$;
- $g'_\star$ stands for $g(t, x, v'_\star)$.

It is high time that we introduced the Collision Operator. There is not a better way than to use Truesdell's words.

"According to Maxwell's picture of a gas, the density of the rate of decrease of F at (t, x) due to collisions with molecules of velocity $v_\star$ is proportional to $FF_\star$ evaluated at (t, x). On the other hand, molecules of velocity v are being produced as the result of collisions. Since the equations of analytical dynamics are invariant under time reversal, the pair of velocities $(v, v_\star)$ results as the outcome of a collision between molecules of velocities $(v', v'_\star)$ as determined by the encounter operator $\mathbb{E}$. Thus the density of the rate of increase of F at (t, x) due to collisions is proportional to $F'F'_\star$, evaluated at (t, x). The net rate of increase in the density of molecules with velocity v by collisions is proportional to the difference $F'F'_\star - FF_\star$, weighted by an appropriate factor to convert it into a molecular density, and the integrated over all velocities $v_\star$ and all possible relative positions."

This factor is the wdS, in which w is the magnitude of the relative velocity of the approaching molecule. This is justified by the fact that in the time dt the oncoming molecule travels a distance wdt, and so the volume swept out in that time by that molecule is $(\int_{\mathbb{S}} wdS)dt$. We now define the Collision Operator as follows.

$$\mathbb{C}F \equiv \int_{\mathbb{V}} \int_{\mathbb{S}} w(F'F'_\star - FF_\star) dS dv_\star \tag{2.6}$$

An underlying hypothesis is that of convergence of this operator. We should eventually stress that this is a definition, and as such it does not require all the previous analysis to be complete. Even though what has been

said before might be useful to figure out the applicability of this operator to describe physical phenomena, this operator has been arbitrarily defined. That is why we do not expect the results obtained in the kinetic theory to be the same as those obtained in fluid dynamics. Truesdell dedicated a chapter and several other sections of his book to this topic, that is to say the comparison of the results obtained in the two theories.

In order to define the Boltzmann equation, Trusdell defines mild, weak and strong solutions. We say that H is differentiable along the extrinsic trajectories if for fixed t, x, and v the function $s \mapsto R_s H(t,x,v)$ is differentiable. On the space of such functions we define the mild derivative as follows: $\mathrm{D}H \equiv -\frac{d}{ds} R_s H|_{s=0}$. Analogously, we define the strong derivative as $\mathfrak{D}H \equiv \partial_t H + v \cdot \partial_x H + b \cdot \partial_v H$. Together with the basic properties of the mild derivative, it is easy to show that $\mathrm{D}H \equiv \mathfrak{D}H$. A molecular density that is differentiable along trajectories and satisfies the functional-differential equation $\mathrm{D}H = \mathbb{C}F$ is called a mild solution. It can be also derived that on an extrinsic trajectory such as to make the mapping $s \mapsto R_{t-s}\mathbb{C}F(t,x,v)$ continuous, the equation of evolution is equivalent to the functional-differential equation $\mathrm{D}H = \mathbb{C}F$. On the other hand, a molecular density that is smooth and satisfies the functional-differential equation $\mathfrak{D}H = \mathbb{C}F$ is called a strong solution. A mild solution can be promptly proved to be a mild solution but generally the converse is not the case. In general it might be complex to say under which restrictions the converse is true. An interesting comment by Truesdell proves itself really useful to clarify the physical applicability of the assumption of smoothness: "Whenever we use it [with reference to the equation of evolution] we shall assume implicitly that F is smooth, even though to assume outright that it is reflects no physical principle and is in no way natural in a theory employing ideas associated with probability". We want also to point out one more feature of the equation of evolution: it does no impose any restrictions on the value of F at some fixed time t_0. It is from the definitions of strong derivative, strong solution and collision operator that we derive the Maxwell-Boltzmann Equation:

$$\mathfrak{D}H \equiv \partial_t H + v \cdot \partial_x H + b \cdot \partial_v H = \int_{\mathbb{V}} \int_{\mathbb{S}} w(F'F'_\star - FF_\star) dS dv_\star = \mathbb{C}F \quad (2.7)$$

Truesdell proves also one property that is of overwhelming importance: its absence would imply a dramatic failure of the whole theory. That property is the validity of the Principle of Frame-indifference for the collision operator $\mathbb{C}$: the collision operator $\mathbb{C}$ is invariant under rigid changes of framing.

We now proceed by defining

$$\bar{\mathbb{C}}_F \equiv \int_{\mathbb{V}} g\mathbb{C}F = \int_{\mathbb{V}}\int_{\mathbb{V}}\int_S wg(F'F'_\star - FF_\star)dSdv_\star dv \tag{2.8}$$

A major result is the Boltzmann Monotonicity Theorem:

$$\bar{\mathbb{C}}_F \log F \leqq 0 \tag{2.9}$$

for all F;

$$\bar{\mathbb{C}}_F \log F = 0 \tag{2.10}$$

if and only if $F = F_M \equiv ae^{-b|v-u|^2}$.

Being a molecular density, F_M must be positive on an essential domain and integrable over $\mathbb{V}$; for this conditions to be fulfilled it is necessary that $a > 0$ and $b > 0$. This two inequalities, if verified, imply that F_M shall be a positive, integrable function.

Another major result is Maxwell's Assertion: $\mathbb{C}F = 0$ if and only if $F = F_M$. The Maxwellian density has several interesting properties and is necessary to discuss the problem of Kinetic Equilibrium. The definition of equilibrium itself requires a detailed discussion: Truesdell uses Wang definition ($F = F(x, v) = F(x, -v)$) and the proves Maxwell-Boltzmann-Wang Theorem on Kinetic Equilibrium. The strong relationship between the Gross Equilibrium (that is to say the equilibrium as defined in fluid dynamics) and the Kinetic Equilibrium is also an interesting topic that Truesdell deals with. We just point out that the kinetic equilibrium implies the gross equilibrium but that the converse if false.

We remark that $\bar{\mathbb{C}}_F S = 0$ for all F if S is a summational invariant. The converse has not been proved to be generally true. In a few special cases also the converse is verified.

The last point in this section is probably the most meaningful one because it is necessary to explain why the ES-Model is a good model in a sense. First, we should introduce the field h, then compare it with the specific entropy η, then analyze the conditions under which this comparison make sense. Thereafter, we ought to introduce the flux of h (that is to say s). The next step would be that of introducing the quantity $H \equiv \int_B \rho h dV$, where B is a

portion of volume. Soon after, two theorems about the evolution of H would follow: the Formal Broad H-Theorem and the Formal Narrow H-Theorem. Then, at that point, a comparison between these theorems and the Clausius-Duhem inequality and the heath-bath inequality of thermomechanics. After taking into consideration the boundary conditions, we would finally try to draw a few conclusions about the relationship between the behavior of H and the trend to kinetic equilibrium. In the case of formal narrow H-theorem, we would obtain that its validity is not a sufficient condition for the strict trend to equilibrium. In fact, even if we could prove that F tends to a given local Maxwellian, the theorem "gives no clue to the transition from local to absolute Maxwellian". The formal broad H-theorem is even more complex to interpret. The best way to understand all this material is to read to book by Truesdell. We will deal later on with the H-Theorem in a more concise way. However, a good understanding of what Truesdell wrote about this subject may be really useful to grasp the meaning of this much discussed theorem. We now go on with different matters. Several other topics discussed by Trusdell, especially the collision operator and the exact solution for moments of order 0 to 3 in the case Maxwellian molecules, in the same book are surely good to fully understand what is to follow.

2.3 The Kinetic Theory as Developed for Molecules Different from Hard Spheres

The reference for this section is the already mentioned book by Cercignani [2]. The way in which Cercignani introduces the Boltzmann equation is slightly different due to a different variable choice used to model the collision. His description is more general and it encopasses several different kind of molecules (e.g. those different from hard spheres) and polyatomic molecules. It is enough to say that in the case of a general monoatomic gas w is substituted by $B(\theta, w)$, where θ is the angle between the unit vector $\mathbf{n}$ with origin in the central point of the molecule and pointing toward the gas and the velocity v of the molecule approaching the molecule under consideration (the latter being still considered at rest). The integral has to be performed over the whole hemisphere $\boldsymbol{B}_-$, which is the hemisphere corresponding to $v \cdot n < 0$. We have that

$$\frac{\partial P^{(1)}}{\partial t} + v_1 \cdot \frac{\partial P^{(1)}}{\partial x_1} = N \int_{\mathbb{R}^3} \int_{\mathbf{B}_-} (P^{(1)\prime} P_\star^{(1)\prime} - P^{(1)} P_\star^{(1)}) B(\theta, w) dv_\star d\theta d\epsilon \quad (2.11)$$

where ϵ is the angle that, together with θ, identifies $\mathbf{n}$. N is the total number of molecules in the body of gas under consideration. The notation has been slightly changed to suit that used so far. P has been used instead of F: F is a molecular density whereas P is a probability density. In the first section a different probability density over $\mathbb{V}$ was introduced. The function $v \mapsto \frac{F(t,x,v)}{N}$ is a probability density over $(\mathbb{B}, \mathbb{V})$. In fact, $N \equiv \int_{\mathbb{B}} n(t,x)dx$. The superscript 1 means that P^1 is the probability related to the molecule under consideration and not to the molecule colliding with the former one. The same reasoning holds for the subscript 1 for the vectors v_1 and x_1. The external force may be added to yield a formula similar to the one previously explained in the last section. Here, the domain of integration for the velocity is $\mathbb{R}^3$. $B(\theta, w)$ acquires a special form in the case of hard-sphere molecules. After having clarified the difference of notation to show the coherence of the two models, we can go on to generalize what was claimed in the last section to be true in the special case of a monoatomic gas. Almost all the theorems explained and the conclusions drawn in the previous section still hold, after having substituted the former definition of the collision operator with the latter. However, there are certain exceptions, like the degree to which thermodynamics and kinetic theory yield the same result, the equilibrium and the H-theorem. Actually, the same results could hold but the author of the present paper has assumed this not to be the case in general, given that some of these results where found after the definition of the collision operator in the gas of a monoatomic gas. A more detailed analysis should be carried out.

What we have to do is to formally introduce the H-theorem. Just for the sake of generality, we define a bilinear operator $\mathbb{C}(G, H)$ as

$$\mathbb{C}(G,H) \equiv \frac{1}{2}\int_{\mathbb{R}^3}\int_{\mathbf{B}_-} (G'H'_\star + G'_\star H' - GH_\star - G_\star H)B(\theta, w)dv_\star d\theta d\epsilon \quad (2.12)$$

where G and H are any such as to render the integral convergent. This definitions might appear a sophistication at first but it proves useful for later developments. We have that

$$\mathbb{C}(G,H) = \mathbb{C}(H,G) \quad (2.13)$$

and

$$\mathbb{C}F = \mathbb{C}(F,F) \quad (2.14)$$

The Boltzmann equation may be rewritten as:

$$\frac{\partial F}{\partial t} + v \cdot \frac{\partial F}{\partial x} = \mathbb{C}(F, F) \tag{2.15}$$

Let us multiply the two sides of the equation for $\log f$ and integrate with respect to the velocity on the whole domain of the velocity. This is what we obtain:

$$\frac{\partial (nh)}{\partial t} + \frac{\partial}{\partial x} \cdot S = \Sigma \tag{2.16}$$

$$\text{where } h \equiv \tfrac{1}{n} \textstyle\int_{\mathbb{R}^3} F \log F dv,\ S \equiv m \int_{\mathbb{R}^3} vF \log F dv \text{ and}$$
$$\Sigma \equiv m \textstyle\int_{\mathbb{R}^3} \log FCF dv.$$

We are using Truesdell's notation instead of the one introduce by Cercignani or other authors. We will be consistent with this notation throughout the whole paper unless otherwise specified. Here S is strictly related to the flux S of the field h introduced by Truesdell. Because of the Boltzmann monotonicity Theorem, we know that $\Sigma \leqq 0$ for all F and $\Sigma = 0$ if and only if F is a Maxwellian. In the case of space-homogeneous solutions we have that $\frac{\partial (nh)}{\partial t} = \Sigma \leq 0$. Intuitive reasoning could lead us to conclude that $nh \to (nh)|_{F_M}$ for a certain Maxwellian molecular density. Once again, we fill tempted to draw erroneous conclusions about the trend to equilibrium but we refrain with difficulty from doing that because we have no grounds for claiming that. What we do now is to integrate over the whole space domain mnh, we get that $H \equiv m \int_{\mathbb{B}} nh dV$. We get that $\frac{\partial H}{\partial t} \leq \int_{\partial \mathbb{B}} S \cdot n d\sigma$, where n is the inward normal and $d\sigma$ the normal element on $\partial \mathbb{B}$. The definition of H given by Cercignani coincides with this one, except for the fact that it is divided by m. It looks crystal clear that H determines some kind of irreversibility, which does not contradict the reversibility of the laws of dynamics. It should be rather regarded as an irreversibility like that of the entropy η. Indeed, in a special case the which is in some special cases the entropy η is proportional to h, the constant of proportionality being negative. This irreversibility, under special boundary conditions and with a few more

restrictions, will determine a trend towards equilibrium, which is ascribable to a trend toward an absolute Maxwellian, which might follow an intermediate state of local Maxwellians. However, the general meaning of this quantity has not a direct counterpart in thermomechanics. Unfortunately, a sweeping generalization will not yield satisfactory results whereas the application of strict boundary conditions will deliver good but sometimes useful results. At first, by studying this topic, it might seem that the field h is an useless sophistication. Furthermore, it the case of a polyatomic gas, the H-theorem has to be dealt with differently! Boltzmann, too, had some trouble trying to prove it: he erroneously was deceived into thinking that the proof given in the case of a monoatomic gas could be applied to a polyatomic gas whereas this is not the case! Soon after, as Cercignani tells us, Lorentz found this error and Boltzmann found a proof that was right but not satisfactory because based on the idea that the final state after an encounter be achieved by a sequence of collisions. Cercignani gives a proof of the H-theorem also in this general case but the author of the present paper, drove into a state of despair due to the striking complexity of the interpretation of this theorem, hasn't had enough time to go through this proof yet.

The time has come to introduce a further generalization, that of a polyatomic gas. "The molecule is a dynamical system, which differs from a point mass by having a sequence of internal states, which can be identified by a label, assuming integral values", as Cercignani himself points out. This internal state might be one and might be described by the energy E. The fact that we can use just one state is subject to an hypothesis commented upon by Cercignani. The most interesting point of this generalization is the distribution of the energy between the translational and internal degrees of freedom after a collision. The energy is conserved in the collision. Two assumptions have to be made: one about the scattering kernel and the other is that "the redistribution of energy among the various degree of freedom only depends upon the ratios of the various energy to the total energy", quoting Cercignani. Then, a distinction between elastic and inelastic collisions should be made. However, we will use the ES-Model, in which the energy is already distributed in a given way.

2.4 Boundary Conditions

As far as the boundary conditions are concerned, many models are available, few of which are physically justifiable. The interaction between the molecules and the boundary theoretically should be modeled by applying to the surface of the boundary a model similar to that of the Boltzmann equation, which

is practically not an achievable aim, due to the complexity of this kind of interaction: when a molecule impinge upon a surface, it may be absorbed by the surface itself, give rise to chemical bonds, dissociate, etc. Indeed, even if we could model this way the boundary, such a precise scheme would require to know the surface finish, its cleanness and its temperature, which are data that cannot be measured with the required precision. A detailed description of possible choices of boundary conditions models is given by Cercignani. A scattering kernel is used just as in the case of the formulation of the Boltzmann equation (the definition of scattering kernel is given both by Truesdell and Cercignani). It should meet certain requirements. We will use the Maxwell-type boundary conditions omitting a detailed analysis. This will be enough. The author of the present paper has to admit that has never read a single paper in which different boundary conditions have been applied since the beginning of the the study of the Boltzmann equation a few months ago. As Cercignani points out, this model is the only one that appeared in literature before the late 1960s. Basically, this model requires that a fraction of the molecules undergo a specular reflection while the others are reflected with the Maxwellian distribution of the wall uniformly in any direction (diffuse-reflection boundary condition). This fraction is determined by α, named accommodation coefficient. A specular reflection is a kind of interaction that modifies only the component of velocity that is normal to the surface, that is, at every point upon a wall:

$$F(v_i) = F(v_i - 2[(v - u_{wall}) \cdot n]n_i) \tag{2.17}$$

$$\text{if } (v - u_{wall}) \cdot n > 0$$

where u_{wall} is the velocity of the wall and n is the unitary vector normal to the boundary that points toward the gas.
This property implies no shear stress at the boundary. It just prevents the gas from going past the surface of the boundary. The full expression of the Maxwell-type boundary condition is:

$$F(v_i) = (1-\alpha)F(v_i - 2[(v - u_{wall}) \cdot n]n_i) + \alpha \frac{\rho_w}{(\pi T_w)^{\frac{3}{2}}} \exp(-\frac{(v_j - u_{wall_j})^2}{T_w}) \tag{2.18}$$

$$\text{if } (v - u_{wall}) \cdot n > 0.$$

2.5 Model Equations: the Taming of the Collision Operator

It goes without saying that it is the collision operator that make the Boltzmann equation so complex. "When one is not interested in fine details", quoting Cercignani, model equations can be applied. They are equations that retain the qualitative and average properties of the collision operator but are in a sense more easy to deal with. We approximate $\mathbb{C}(F,F)$ with $\mathbb{J}(F)$. The two models used in this paper are the BKW-Model, also called BGK-Model, and the ES-Model. The first one, proposed by Bathnagar, Gross and Krook, is largely employed in actual computations. Welander proposed it independently at about the same time.

$$\mathbb{J}(F) = \nu(\rho, T)(F_M(v) - F(v)) \tag{2.19}$$

$$\text{where } F_M = \frac{\rho}{(2\pi RT_w)^{\frac{3}{2}}} \exp(-\frac{(v_j-u_j)^2}{2RT}).$$

F_M is the local Maxwellian with the same density ρ, temperature T and bulk velocity as F. The choice of ρ and T is not obvious. They are to be chosen in such a way that for any summational invariant $S(v)$ we have that $\int_{\mathbb{R}^3} S(v)F_M(v)dv = \int_{\mathbb{R}^3} S(v)F(v)dv$. If this property is satisfied, then F_M and F have the same density, temperature and bulk velocity. Furthermore, mass, momentum and energy are conserved, that is, for any summational invariant $\int_{\mathbb{R}^3} S(v)\mathbb{J}F(v)dv = 0$ (this equivalence between these two properties may be verified by substituting the principal invariants into the last equation). We must be careful because a summational invariant as defined bu Truesdell coincides with a collision invariant as defined by Cercignani. Furthermore, the Boltzmann monotonicity theorem holds even if we replace $\mathbb{C}(F)$ with $\mathbb{J}(F)$:

$$\int_{\mathbb{R}^3} (\log F(v))\mathbb{J}(F)dv \leqq 0 \tag{2.20}$$

$$\text{for all } F;$$

$$\int_{\mathbb{R}^3} (\log F(v))\mathbb{J}(F)dv = 0 \tag{2.21}$$

$$\text{if and only if } F = F_M \equiv ae^{-b|v-u|^2}.$$

From the equation $\int_{\mathbb{R}^3} S(v)\mathbb{J}F(v)dv = 0$ we derive a method to check the error of our computations. In fact, approximations and computational will yield a result that is not identically zero. The error that we get might be useful as an estimate of the precision of the results obtained by applying this model. The same method can be used with the ES-Model. The BKW-Model has two advantages: "for any given problem one can deduce integral equations for ρ, v and T that can be solved with moderate effort on a computer", quoting Cercignani, and its linearized form is extremely useful. Its disadvantage consists in the fact that $\mathbb{J}F = 0$ contains F in both the numerator and denominator of an exponential, whereas the nonlinearity of the collision operator is only quadratic.

The main problem of the BKW-Model is that, in order to have a complete agreement with the Navier-Stokes equations, we should be able to set both the viscosity μ and the heat conductivity κ but we can modify just one parameter, that is to say the collision frequency. We cannot assign an arbitrary value to those two parameters. This fact implies that we cannot set whatever value we will for the Prandtl number ($Pr = \frac{\mu}{c_p\kappa} = \frac{\gamma}{\gamma-1}\frac{R\mu}{\kappa}$). According to the BKW-Model, the Prandtl number for a monoatomic gas is 1, whereas its value according to the kinetic theory is $\frac{2}{3}$, as shown by Trusdell. Therefore, another model, the so called ES-Model (Ellipsoidal Statistical Model), also called BGK-Gaussian model, has been proposed. While the BKW-Model is based upon the relaxation toward local Maxwellians, in the ES-Model the local equilibrium Maxwellian is substituted with a Gaussian G ($G = G(t, x, v)$ in the monoatomic case; $G = G(t, x, v, \mathcal{E})$. In the polyatomic case, a polyatomic Maxwellian $M = M(t, x, v, \mathcal{E})$ has to be defined. However, as proved in this paper, if $H(G) = H(f)$ then $f = M$. In this model one parameter ν is used in the monoatomic case ($-\frac{1}{2} \leq \nu < 1$) and two parameters, that is to say ν and θ, are used in the polyatomic case ($-\frac{1}{2} \leq \nu < 1$ and $0 < \nu \leq 1$). In the case of a monoatomic gasν and θ, which are called relaxation coefficients, reduce to one, which is ν. This is perfectly coherent with what has been explained by Truesdell, that is to say "The kinetic gas, insofar as it is a linearly viscous fluid, has bulk viscosity zero". The bulk viscosity λ of the book by Truesdell coincides with the second viscosity $\alpha\mu$ used in this paper. An important point is that the Prandtl number is derived through a Chapman-Enskog expansion at the first order! All these model, by themselves, do not give any specifications as to how to derive it. The author cannot refrain from suggesting to read the paper by Pierre Andries, Patrick Le Tallec, Jean-Philippe Perlat and Benoît Perthame [3] about the ES-Model that comprises:

- the proof of the validity of the H-theorem for this model in the monoatomic case;
- the same proof in the polyatomic case (there's an additional internal state, that is the energy);
- the steps that yield the Navier-Stokes system with a polytropic law for the pressure ($P = \rho RT = (1-\gamma)\rho e$), viscosity $\mu = \mu(T)$, second viscosity $\alpha\mu$, and thermal conductivity $\kappa = \kappa(T)$.
- a different formulation of the method employing two different distribution functions, one for mass and the other for internal energy (this reduction cannot be performed in the case of Boltzmann's quadratic collision operator).

As far as the second-last point is concerned, for the sake of clarity we rewrite here Proposition 4.1.

Proposition 4.1: For the Gaussian-BGK model [that is to say the ES-Model], we obtain in the Chapman-Enskog expansion the Navier-Stokes system (2) [this is a reference to the system rewritten at the beginning of the paper] where the viscosity tensor is given by

$$\sigma_{ij} = \mu(\partial_{x_j} u_i + \partial_{x_i} u_j - \alpha\delta_{ij}\mathrm{div}u) \tag{2.22}$$

Moreover the second viscosity coefficient α and Prandtl number $Pr = \frac{\gamma}{\gamma-1}\frac{R\mu}{\kappa}$ are given by

$$\alpha = (\gamma - 1) - \frac{1-\theta}{\theta}(1-\nu)(\frac{5}{3} - \gamma) \tag{2.23}$$

$$Pr = \frac{1}{1-\nu+\theta\nu} \tag{2.24}$$

δ is the additional number of degrees of freedom of the gas related by $\gamma = \frac{\delta+5}{\delta+3}$. For a diatomic gas $\delta = 2$ and $\gamma = 1.4$. By setting the only available relaxation coefficient in the monoatomic case and the two relaxation coefficients in the polyatomic case, we can fix a value for the Prandtl number. Later on, after having introduce the linearized collision operator, we will see what the linearized BKW-Model and ES-Model look like. The latter is a generalization of the former. The aforementioned paper is the key to understand the ES-Model, which will be heavily employed in the present work.

2.6 Adimensionalization and Linearization

The linearized collision operator is defined by Cercignani as

$$\mathcal{L}F = \frac{2}{F_M}\mathbb{C}(F_M, F) \tag{2.25}$$

Let us consider the Hilbert space of square summable functions endowed with a scalar product weighted with the Maxwellian function $(G, H) = \int_{\mathbb{R}^3} \bar{G}HF_M dv$, where the bar denotes complex conjugation. Here some confusion may arise due to the use of the word "scalar product" used by Cercignani. The definition previously given does not satisfy the properties of a scalar product. Indeed, it is an inner product, that is to say a particular Hermitian form. Cercignani uses the term scalar product because, in our analysis, the functions are defined on a real domain and yield real values. In this particular case the inner product correspond to the scalar product. $\mathcal{L}$ is symmetric in this space, that is to say $(G, \mathcal{L}H) = (\mathcal{L}G, H)$. Furthermore, it is nonpositive, that is to say $(H, \mathcal{L}H) \leq 0$, where the equality sign holds if and only if H is a summational invariant. We have now to introduce the reference book that will be empolyed in the next section. This book, largely used at Kyoto University, is the book by Professor Yoshio Sone [4]. In the first sections of the first chapter Sone introduces the concept of linearized adimensionalized equations. He is really precise and the steps are all extremely detailed. In order to give a form of the adimensionalized linearized Boltzmann equation, we have to explain what we mean by adimensionalization. The body force is assumed to be null.

The first adimensionalized form is basically a rescaled form, obtained by substituting in the equation the following dimensionless variables:

- $\hat{t} = t/t_0$;
- $\hat{x} = x/L$ (where L is the reference length);
- $\hat{v} = v/(2RT_0)^{1/2}$;
- $\hat{F} = \frac{(2RT_0)^{3/2}}{\rho_0}F$ (where ρ_0 is the reference density);
- $\hat{\rho} = \rho/\rho_0$;
- $\hat{u} = u/(2RT_0)^{1/2}$;
- $\hat{T} = T/T_0$;
- $\hat{p} = p/p_0$ where p is the pressure and $p_0 = R\rho_0 T_0$ the reference pressure;

- $\hat{p}_{ij} = p_{ij}/p_0$.

R is the gas constant k_b per unit mass, that is to say $R = k_b/m$.

The macroscopic quantities are expressed in the following ways as functions of the adimensionalized variables:

- $\hat{\rho} = \int_{\mathbb{R}^3} \hat{F} d\hat{v}$;
- $\hat{u} = \frac{1}{\hat{\rho}} \int_{\mathbb{R}^3} \hat{v}\hat{F} d\hat{v}$;
- $\hat{T} = \frac{2}{3\hat{\rho}} \int_{\mathbb{R}^3} (\hat{v}_j - \hat{u}_j)^2 \hat{F} d\hat{v}$;
- $\hat{p} = \hat{\rho}\hat{T}$;
- $\hat{p_{ij}} = 2 \int_{\mathbb{R}^3} (\hat{v}_i - \hat{u}_i)(\hat{v}_j - \hat{u}_j)\hat{F} d\hat{v}$.

which is the one we assume the body force to be null and express the variables as perturbations of the equilibrium state.

From now on, $a = \sqrt{a_1^2 + a_2^2 + a_3^2}$, unless otherwise specified. The second adimensionalized form is given by expressing the variables as perturbations of an equilibrium state at rest, given by a Maxwellian that is proportional to $E(v) = \pi^{-3/2} \exp(-\hat{v}_i^2)$. "At rest" is a specification that is no longer necessary as long as you define the equilibrium as Wang did. The nondimensional perturbed variables are chosen in the following way:

- $\phi = \frac{\hat{F}}{E} - 1$;
- $\omega = \hat{\rho} - 1$;
- $\tau = \hat{T} - 1$;
- $P = \hat{p} - 1$;
- $P_{ij} = \hat{p}_{ij} - \delta_{ij}$.

If we assume the absolute values of all these quantities to be small, their products may be neglected and we obtain that:

- $\omega = \int_{\mathbb{R}^3} \phi E d\hat{v}$;
- $\hat{u} = \int_{\mathbb{R}^3} \hat{v}\phi E d\hat{v}$;
- $\hat{\tau} = \frac{2}{3} \int_{\mathbb{R}^3} (\hat{v}_j^2 - \frac{3}{2})\phi E d\hat{v}$;
- $P = \omega + \tau$;

- $P_{ij} = 2\int_{\mathbb{R}^3} \hat{v}_i \hat{v}_j \phi E d\hat{v}$.

Accordingly, the Boltzmann equation is given as

$$Sh\frac{\partial \phi}{\partial \hat{t}} + \hat{v}_i \frac{\partial \phi}{\partial \hat{x}_i} = \frac{1}{k}[\mathcal{L}(\phi) + \mathcal{J}(\phi, \phi)] \tag{2.26}$$

$$\mathcal{L}(\phi) = \int_{\mathbb{R}^3} \int_{\mathbf{B}_-} E_\star(\phi' + \phi'_\star - \phi - \phi_\star)\hat{B} dv_\star d\theta d\epsilon \tag{2.27}$$

$$\mathcal{J}(\phi, \psi) = \frac{1}{2}\int_{\mathbb{R}^3} \int_{\mathbf{B}_-} E_\star(\phi'\psi' + \phi'_\star\psi'_\star - \phi\psi - \phi_\star\psi_\star)\hat{B} dv_\star d\theta d\epsilon \tag{2.28}$$

where

- $\hat{B} = \frac{B}{B_0}$, B being defined as before and B_0 in the following way $B_0 = \frac{1}{\rho_0^2}\int_{\mathbb{R}^3}\int_{\mathbf{B}_-} F_0 F_0 B(\theta, w) dv_\star d\theta d\epsilon$ ($F_0 = \frac{\rho_0}{(2\pi R T_0)^{\frac{3}{2}}} \exp(-\frac{v_j^2}{2RT_0})$);
- $Sh = \frac{L}{t_0 (2RT_0)^{\frac{1}{2}}}$ is named the Strouhal number;
- $k = \frac{\sqrt{\pi}}{2} Kn$, Kn being the Knudsen number being defined as $Kn = \frac{l_0}{L}$ (l_0 is the mean free path, which is a measure of the distance covered on average by a molecule before a collision occurs).

Before proceeding, we must point out that the phenomena that fluid dynamics is meant to model are those in which the mean free path is small if compared to the reference length L, which implies a relatively small Knudsen number. On the contrary, the kinetic theory is thought to be more suitable to describe the behavior of a rarefied gas, in which case the Knudsen number is quite big. These two parameters are two of the three similarity parameters of the Boltzmann equation. Furthermore, it will be useful later to mention the following two properties:

- $2\mathcal{J}(1, \phi) = \mathcal{L}(\phi)$;

- $E\mathcal{J}(\phi,\psi) = \hat{\mathbb{C}}(E\phi, E\psi)$, where $\hat{\mathbb{C}}(\hat{F},\hat{G}) = \frac{1}{2}\int_{\mathbb{R}^3}\int_{\mathbf{B}_-}(\hat{F}'\hat{G}' + \hat{F}'_\star\hat{G}'_\star - \hat{F}\hat{G} - \hat{F}_\star\hat{G}_\star)\hat{B}dv_\star d\theta d\epsilon$.

These properties hold also in the case of the model equations we will introduce.

Analogously, also the Maxwell-type boundary condition must undergo the same procedure and it is to be transformed into the following equations:

$$E(v)[1+\phi(x_i,v_i,\hat{t})] = (1-\alpha)E(\check{v})[1+\phi(x_i,\check{v}_i,\hat{t})]+\alpha E(v)[1+\phi_e(\check{\sigma_w},u_{w_i},\tau_w)] \tag{2.29}$$

if $[(v_j - u_{w_j})n_j > 0]$, where

$$\phi_e = \frac{1}{E}\frac{1+\omega}{\pi^{\frac{3}{2}}(1+\tau)^{\frac{3}{2}}}\exp(-\frac{(v_j-u_j)^2}{1+\tau}) - 1 \tag{2.30}$$

$$\check{\sigma}_w = -2(\frac{\pi}{1+\tau_w})^{\frac{1}{2}}\int_{(v_j-u_{w_j})n_j<0}(v_j-u_{w_j})n_jE(v)[1+\phi(x_i,v_i,\hat{t})]dv-1 \tag{2.31}$$

$$\check{v}_i = v_i - 2(v_j-u_{w_j})n_jn_i \tag{2.32}$$

$$\tau_w = \frac{T_w}{T_0} - 1 \tag{2.33}$$

where T_w is the temperature of the wall.

By neglecting the nonlinear term in the previous equation, we get the linearized Boltzmann equation:

$$Sh\frac{\partial\phi}{\partial\hat{t}} + \hat{v}_i\frac{\partial\phi}{\partial\hat{x}_i} = \frac{1}{k}\mathcal{L}(\phi) \tag{2.34}$$

The same reasoning may be followed in the case of model equations. In the case of the BKW-Model, we get that all the preceding formulas remain the same, we just rename them by removing the caps:

- $\omega = \int_{\mathbb{R}^3} \phi E dv$;
- $u_i = \int_{\mathbb{R}^3} v_i \phi E dv$;
- $\tau = \frac{2}{3} \int_{\mathbb{R}^3} (v^2 - \frac{3}{2}) \phi E dv$;
- $P = \omega + \tau$;
- $P_{ij} = 2 \int_{\mathbb{R}^3} v_i v_j \phi E dv$.

The final linearized equation to be solved reads:

$$Sh \frac{\partial \phi}{\partial t} + v_i \frac{\partial \phi}{\partial x_i} = \frac{1}{k} [-\phi + \omega + 2 v_i u_i + (v^2 - \frac{3}{2}) \tau] \tag{2.35}$$

The Maxwell-type boundary condition for the linearized Boltzmann equation and for the linearized BKW-Model is the following:

$$\begin{gathered} \phi(x_i, v_i, t) = (1-\alpha)(\phi(x_i, v_i - 2(v_j - u_{w_j}) n_j n_i, t) + 4 v_j u_{w_k} n_j n_k) + \\ + \alpha [\check{\sigma}_w + 2 v_j u_{w_j} + (v^2 - \tfrac{3}{2}) \tau_w] \\ \text{if } [(v_j - u_{w_j}) n_j > 0], \end{gathered} \tag{2.36}$$

where

$$\check{\sigma}_w = \sqrt{\pi} u_{w_j} n_j - \frac{1}{2} \tau_w - 2\sqrt{\pi} \int_{(v_j - u_{w_j}) n_j < 0} v_j n_j \phi E dv \tag{2.37}$$

$$\tau_w = \frac{T_w}{T_0} - 1 \tag{2.38}$$

where T_w is the temperature of the wall.

In the case of the ES-Model, its linearized form reads [5] (caps have been removed)

$$\begin{gathered} Sh \tfrac{\partial \phi}{\partial t} + v_i \tfrac{\partial \phi}{\partial x_i} = \tfrac{1}{k} \{ -\phi + \omega + 2 v_i u_i + (v_i^2 - \tfrac{3}{2}) [(1-\eta) \tau_{tr} + \eta \tau] + \\ + (\mathcal{E} - \tfrac{\delta}{2}) \tau_{rel} + (1-\eta) \nu [P_{ij} v_i v_j - (\omega + \tau_{tr}) v^2] \} \end{gathered} \tag{2.39}$$

with

- $\omega = \int_{\mathbb{R}^3} \int_0^\infty \mathcal{E}^{\frac{\delta}{2}-1} \phi E d\mathcal{E} dv$;
- $u_i = \int_{\mathbb{R}^3} \int_0^\infty v_i \mathcal{E}^{\frac{\delta}{2}-1} \phi E d\mathcal{E} dv$;
- $\tau_{tr} = \frac{2}{3} \int_{\mathbb{R}^3} \int_0^\infty v^2 \mathcal{E}^{\frac{\delta}{2}-1} \phi E d\mathcal{E} dv - \omega$;
- $\tau_{int} = \frac{2}{\delta} \int_{\mathbb{R}^3} \int_0^\infty \mathcal{E}^{\frac{\delta}{2}} \phi E d\mathcal{E} dv - \omega$;
- $\tau = \frac{3\tau_{tr}+\delta\tau_{int}}{3+\delta}$;
- $\tau_{rel} = \eta\tau + (1-\eta)\tau_{int}$;
- $P_{ij} == \int_{\mathbb{R}^3} \int_0^\infty 2 v_i v_j \mathcal{E}^{\frac{\delta}{2}-1} \phi E d\mathcal{E} dv$.

Accordingly, the Maxwell-type boundary condition is ($\tau_w = \hat{T} - 1$, where $\hat{T}_w$ equals $\hat{T}$ evaluated at the wall)

$$\begin{gathered} \phi(x_i, v_i, t) = (1-\alpha)\phi(x_i, v_i - 2v_j n_j n_i, t) + \\ +\alpha[2\sqrt{\pi} \int_{(v_j - u_{w_j})n_j < 0^3} \int_0^\infty v_j \mathcal{E}^{\frac{\delta}{2}-1} \phi E d\mathcal{E} dv + (v^2 - 2 + \mathcal{E} - \tfrac{\delta}{2})\tau_w] \\ \text{if}[(v_j - u_{w_j})n_j > 0]. \end{gathered} \tag{2.40}$$

2.7 Discontinuity: an Outcome of Gas-Surface Interaction

So far, solutions of the Boltzmann equation have been assumed to be smooth or smooth enough to be acted upon by certain operators. Unfortunately, the solution generally is not smooth at the boundary. The problem of finding a suitable function space in which to seek the solution present a major concern. Let us now add one more hypothesis: the problem is stationary. By looking at the Maxwell-type boundary conditions, we notice that an integral equation specifies the way in which the impinging particles bounce off the surface.

In the case of pure specular reflection, the solution on the boundary is symmetric with respect to some of the three spatial coordinates, that is to say that it is an even function with respect to those coordinates, which implies that it is continuous in the origin. The molecular distribution does not vary with respect to the other spatial coordinate or coordinates. We may say that, is the molecular density of the impinging particles if smooth, then the molecular density of the particles leaving the boundary is smooth too. If we applied an accommodation coefficient without including the second member of the boundary condition, that is to say $F(v_i) = (1-\alpha)F(v_i - 2[(v-u_{wall})\cdot n]n_i)$, $(v-u_{wall})\cdot n > 0$, we would have that a discontinuity would appear in the origin. The boundary would serve as a mirror that reflects the molecules after having rescaled the molecular density.

On the other hand, in the case of particles that are emitted with the molecular density of the surface, we might have whatever molecular distribution we will applied to the impinging molecules, but the molecular distribution of the molecules directed away from the surface will be always a given Maxwellian. This behavior implies a discontinuity in the spatial domain in the origin in the general case.

The discontinuity presents us with a major concern:

What is the functional space in which the solution is to be found?

In order to draw some comparisons between fluid dynamics and kinetic theory, assumptions have been made by Truesdell as to the asymptotic behavior of the molecular density with respect to the velocity, like supposing that it is a $O(v^n)$. Furthermore, we may have discontinuities located in given portions of the domain. The problem is still different when the problem is not stationary (though not always). From now on, we will JUST ASSUME THE FUNCTION TO BE PIECEWISE CONTINUOUS! An informal all-caps statement is definitely compulsory for such a forceful assumption.

After having ascertained that a discontinuity generally occurs, we have to know how to treat it in our calculations. Indeed, the finite-difference method is largely employed to solve the Boltzmann equation, and a discontinuity may bring about large errors. At first, the author of the present paper thought of using a dense distribution of grid points close to the boundary. However, that does not yield good results unless the solutions is smooth enough. If fact, usually, the solution is shaped like a bell with a peak in the origin in such a way that a change of the molecular density close to the origin means the integrals giving the value of the moments greatly vary. This is due to the fact that the area underlying the molecular density around the origin has a greater size than the area underlying the lateral slopes away from it. Therefore, even if the grid points have been densely laid down but, a a small error around

the origin bring forth a huge error in the evaluation of the moments. The best thing to do is to use two different points: 0^+ and 0^-. The molecular distribution is evaluated on a domain comprising two different points that are infinitely close to zero. With the addition of a denser distribution for grid points around zero, the result get much better. This problem was first encountered by the author when carrying out his first numerical simulation of the Boltzmann equation. After having discretized the space domain to apply a finite-difference method, assembling the solving matrix, he couldn't get the right number of linearly independent equations. After having added one more point in which to impose the Boltzmann equation and the boundary conditions, he obtained a determinate system. We will see later on how the problem was solved. The author first came to know about this discontinuity thanks to a fruitful conversation with Professor Kazuo Aoki so this section has no reference to any books. For what concerns the numerical analysis, it was Masanari Hattori (PHD student at Kyoto University) who shared with the author his numerical know-how by explaining him that the best way to solve the problem was to use these two grid points and what function was most suitable to dispose the grid points around the origin. The problem to be solved in this paper is stationary, so we won't include the time variable. As far as the internal state $\mathcal{E}$ that plays a role in the case of a polyatomic gas, no discontinuities are present with respect to this variable.

2.8 Similarity Solutions

The reference to this last section comprises Appendixes 2.5, 2.6 and 5 of the aforementioned book by Sone [4]. A few steps have two be followed to explain what we mean by similarity solutions.

1. Put $f(v_i) = \mathbb{O}(\phi_1(v_i), \phi_2(v_i), ...)$, where $\mathbb{O}$ is an operator and $\phi_n(v_i)$ are functions of v_i. Take the functions $\phi_{n_R}(v_i) = \phi_n(l_{ij}v_i)$, in which $l_{ik}l_{jk} = \delta_{ij}$ is a three-dimensional orthogonal transformation matrix. The operator $\mathbb{O}$ is said to be isotropic if and only if $f(l_{ij}v_j) = \mathbb{O}(\phi_{1_R}(v_i), \phi_{2_R}(v_i), ...)$. $\mathbb{C}(G(v_i), H(v_i)) = \mathbb{C}_{G,H}(v_i)$ and $\mathcal{L}(F(v_i)) = \mathcal{L}_F(v_i)$ can be proved to be isotropic operators.

2. A tensor field $f_{i_1,i_2,...,i_m}(v_i)$ is called spherically symmetric if and only if $f_{i_1,i_2,...,i_m}(l_{ij}v_j) = l_{i_1j_1}l_{i_1j_2}...l_{i_1j_m}l_{i_2j_1}l_{i_2j_2}...l_{i_2j_m}...l_{i_mj_m}f_{j_1,j_2,...,j_m}(v_i)$.

3. Thanks to the bilinearity of $\mathbb{C}(G(v_i), H(v_i)) = \mathbb{C}_{G,H}(v_i)$ with respect to $G(v_i)$ and $H(v_i)$ and to the linearity of $\mathcal{L}(F(v_i)) = \mathcal{L}_F(v_i)$ with respect to $F(v_i)$ and two the property of isotropicity of these two operators, they can be shown to be spherically symmetric.

4. A tensor field $f_{i_1,i_2,\ldots,i_m}(v_i)$ is said to be axially symmetric if and only if it is spherically symmetric l_{ij} satisfies the following relation: $a_i = l_{ij}a_j$.

5. In a few special cases, the number of independent variables may be reduced by employing the spherical symmetry of the collision operator and of the linearized collision operator.

6. The approximation of the collision operator in the BKW-Model and ES-Model are spherically symmetric as well.

In order for a function to be a solution, it must be compatible with the Boltzmann equation or the model equation equipped with boundary conditions. If this happen to be the case, the problem greatly simplifies. We will see later on the importance of the similarity solutions.

3 The Knudsen Compressor and Setting of the Problem

3.1 Overview

"In practical applications, slightly rarefied gas flows (gas flows with small Knudsen numbers) are often analyzed by the use of the Navier-Stokes equations and the slip boundary conditions. However, much attention is not paid to the validity of the use of this system. Furthermore, it is rather surprising that the formulas of the slip conditions derived by means of the elementary kinetic theory very long time ago are still in use." [6]

In this chapter, we will go through the theoretical background that will open the way to the formulation of the problem. The Knudsen compressor or Knudsen pump is named after Martin Hans Christian Knudsen, a Danish physicist who passed away around the middle of the twentieth century. However, its feasibility has been recently verified thanks to recent studies. The comeback of the Knudsend pump, justified by a number of possible applications, could be viewed as the practical reason of the present study. The investigation of its working will be focused on the analysis of the thermal transpiration effect. The main reference paper that will be used throughout the first three sections of this chapter is a text by Kazuo Aoki and Shigeru Takata [6]. Being this paper quite complete, there is no need to be too specific: we will just summarize a couple of notable results. A detailed description can be found in the paper and in the reference papers cited therein. We must be aware of the fact that different notation will be used in the main papers that will be introduced later in this dissertation. Once again, Truesdell's notation will always be employed for the sake of clarity.

3.2 Asymptotic Theory for Small Knudsen Numbers

First of all, we point out that the Mach number ($M = \frac{U}{a}$, where U is the reference value of the flow speed and a is the reference value of the sound speed) is proportional to the Reynolds number ($Re = \frac{\mu_0 U L}{\rho_0}$, where μ_0 is the

reference viscosity) and to the Knudsen number. Note that $a_0 = (5RT_0/3)^{\frac{1}{2}}$.

We have now to introduce one of the most delicate aspects of this theory. Let us focus on the stationary case and diffuse-reflection boundary condition. We will consider only "slightly" rarefied flows, that is those whose Knudsen number is "slightly" small. We can differentiate the analysis according to the Reynolds number. The aforementioned reference paper has a whole chapter dedicated to this point, which is completely (presuming that a complete analysis can ever be made) dealt with in the book by Sone. In the case of $Re = O(1)$ and $Ma = O(Kn)$ (the case of $Re \ll Kn \ll 1$ is first taken into consideration), the Mach number is pretty small, which implies a slight deviation of the macroscopic quantities from their reference values, which is the equilibrium state at rest. Accordingly, these deviations (not the macroscopic quantities) can be expanded in power series of $k = \frac{\sqrt{\pi}}{2}Kn$, as defined by Sone [4]. As explained by Sone in the chapter about slightly rarefied gas of the previously mentioned book, the smaller the mean free path gets, the more the collision terms plays a dominant role over the other terms, which means that the velocity of approach of a Maxwellian distribution is faster. Therefore, the deviation from the equilibrium state at rest is smaller and the distribution function may be described as a function of the macroscopic variables. Even though this might appear intuitive at a first glance, it is far from being banally explainable in a few lines. We just point out that, in the stationary case, only one correction near the boundary should be applied, but it will be omitted in the present work. The Stokes system of equation may be derived and the boundary conditions have to be appended to these system. What we would get is that a flow is generated that goes from the colder part to the hotter: this is the thermal creep flow, also called thermal transpiration. Chapter 5 of the book by Sone is basically dedicated to this flow, which is somewhat counter-intuitive. An interesting experiment is that of the radiometer, whose windmill rotates due to the thermal creep flow (its rotation, in the case of high pressure in the chamber, is due also to natural convection). The author had a first hand experience of this during an introductory seminar by Professor Shigeru Takata held at Kyoto University. Broadly speaking, we could give a reason that justifies qualitatively this flow. If we consider a boundary whose behavior is described by pure Maxwellian diffusion of the molecules ($\alpha = 1$ in the Maxwell-type boundary condition), we get that the molecules leaving the boundary are scattered around uniformly whereas those approaching the boundary might have substantially different velocities. The average speed of the molecules coming from the hotter region is greater than that of the molecules coming from the colder one, which gives rise to a thermal creep flow on the boundary. This effect is restricted to the case of slightly rarefied gas. Otherwise, the Poiseuille flow,

that is the flow driven by pressure difference, overwhelms the thermal creep flow. This reasoning is approximate and qualitative but might be a good argument to justify the presence of this flow in the case of slightly rarefied gases. Furthermore, there are some related flows. This effect is restricted to the case of slightly rarefied gas. Otherwise, the Poiseuille flow, that is the flow driven by pressure difference, overwhelms the thermal creep flow. This reasoning is approximate and qualitative but might be a good argument to justify the presence of this flow in the case of slightly rarefied gases. Furthermore, there are some related flows.

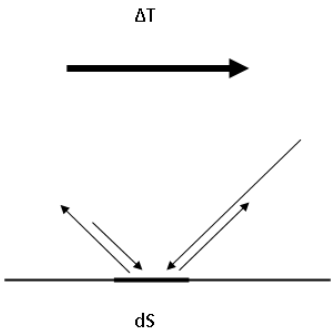

Figure 3.1: Thermal Transpiration

As Kazuo Aoki and Shigeru Takata pointed out, the asymptotic expansion without the proper Knudsen-layer correction "gives the correct overall bevahior of the gas up to $O(Kn^2)$". This correction has to be introduced when the physical quantities near the boundary are required. Given that the author has not had enough time to study how to apply this correction and that it does not appear in the formulation of the problem, we will insensitively neglect this correction.

Moreover, the analysis holds as long as the flow is subsonic. As the Knudsen number and the Mach number increase, the thermal-transpiration flow becomes less relevant: it occurs only in the case of slightly rarefied gases at low Mach numbers. The main results will be given as functions of the Knudsen number ($Kn \propto Re \times Ma$). However, their validity is subject to small Mach numbers ($Ma < 1$). We will discuss this hypothesis from an experimental point of view in section 3.5. This relevance of this hypotheses lies in the fact that these parameters play a predominant role when results obtained from the kinetic theory are compared with those obtained through a fluid-dynamics analysis.

3.3 The Knudsen Compressor

The Knudsen compressor is a pump whose working is based on the thermal creep effect (we will focus on what is called first category of Knudsen compressors). In order to make the pump drive fluid in the right direction in the most efficient way, throughout the last decades several different mechanisms have been devised. The main idea is that of applying a constant gradient of temperature through a channel. If this channel, which most of the times is a straight conduit, were a single tube with constant diameter, the difference of pressure at its ends should be too large to make it feasible. Therefore, a cascade structure of alternating tubes has been applied.

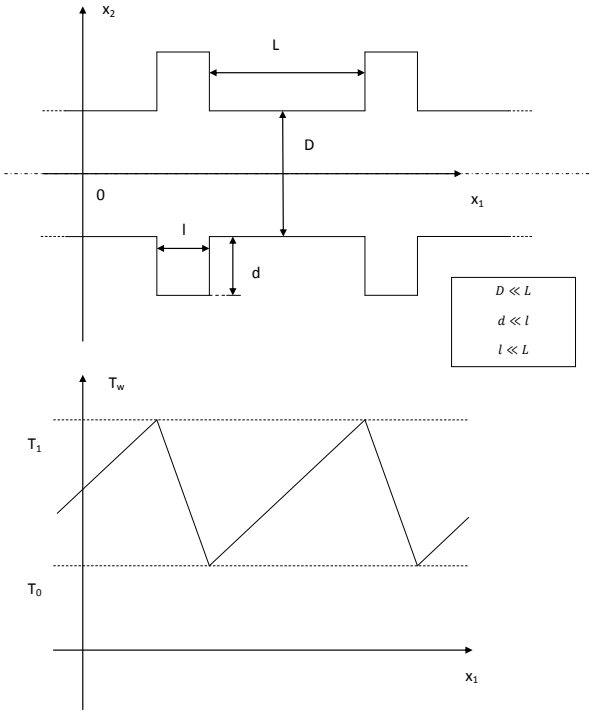

Figure 3.2: Knudsen Compressor

Different kinds of compressors have been ideated and studied:

- the channel can be bent and the diameter can be kept constant;
- shelves may be introduced;
- the so-called "accommodation pumps" may be used.

3.4 Setting of the Problem

In the present study, we will focus on the behavior of a slightly rarefied gas between two parallel plates, which constitute a single section of the Knudsen pump, without caring about what happens at the junction between two sections. The main reference paper is a paper by Shigeru Takata, Hitoshi Funagane and Kazuo Aoki [7]. Once again, we will summarize only the results needed. Let us state all the hypotheses behind our model:

- We consider a rarefied diatomic gas (Nitrogen gas, $\delta = 2$, $\nu = -0.50$, $\eta = 0.46$, $Pr = 0.787$) between to extremely long parallel plates $D \ll L$;
- The behavior of the gas can be described using the ES-Model.
- The wall may be modeled with the Maxwell-type boundary condition.
- The channel is so thin that the temperature is uniform in the cross section. It can be easily proved that the pressure is also constant (see the aforementioned paper).
- The problem is two-dimensional.
- The imposed pressure gradient a and the temperature gradient β are small.

In order to solve this problem, an asymptotic expansion will be carried on: the solution is expanded in a power series of $\epsilon = \frac{D}{L}$, where we assume D to have a unitary value.

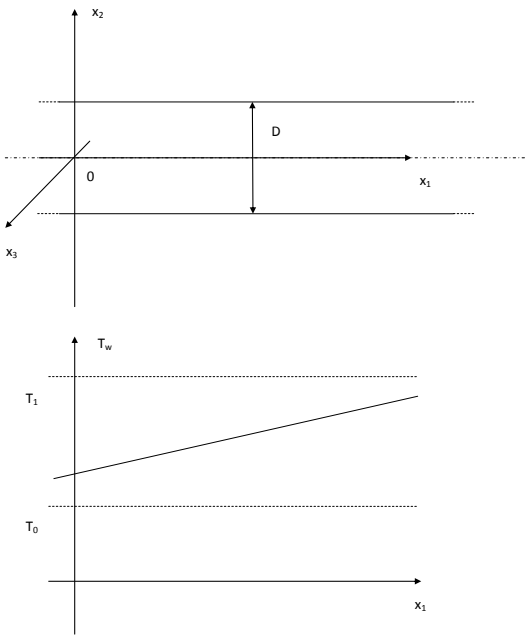

Figure 3.3: Knudsen Pump Conduit

3.5 Applicability of the Hypotheses

The preceding hypotheses plus that of constant gradient of pressure and tempetarure have been applied to study the flow in a circular straight tube. Thereafter, the results have been compared to a series of experiments carried out by Ko Kugimoto, who built an implement made up of several different thin tubes [5]. The boundary conditions that have been used are those of diffuse reflection (that is to say $\alpha = 0$ in the Maxwell-type boundary condition). The results are astonishingly good. The theoretical result perfectly match the results of the experiments for a good range of Knudsen numbers. This results show that this hypotheses are suitable to describe flows that are not as rarefied as one might suppose. In the case of large pressure difference and uniform temperature, for small Knudsen numbers ($Kn \leq 1$) the relative error is really small whereas it increases steeply (it is around 15% at the most) for larger Knudsen numbers. However, the accordance is quite surprising. In

fact, a real wall, in order to be suitable to be modeled with the previously mentioned boundary condition, must meet certain requirements like that of smoothness, uniform pressure, etc. Indeed, it goes without saying that the making of an experiment is an extremely delicate matter, especially when it comes to deal with quantities that are so sensitive to external parameters as those we are trying to describe in the present paper.

4 Solution to the Problem and Numerical Recipes

4.1 Zeroth-order solution

In this chapter, we will go through the procedure used to solve the problem and we will describe how it has been numerically implemented. Unless otherwise specified, the problem is considered steady.

By applying an asymptotic expansion ([7] p. 359) to the adimensionalized ES-Model ([7] pp. 355-359) we get several terms that are to be grouped according to the exponent of k. The adimensionalization is exactly the same as that introduced in the previous chapter. We just need to specify the reference quantities. The reference length in the longitudinal direction is the diameter of the channel whereas the reference length in the axial direction is the length of the channel. Other parameters are specified in [7]. The zeroth-oder equation can be solved ([7] p. 360) by employing a Maxwellian distribution $\hat{F}_{(0)}$ as it has been defined in the previously mentioned paper about the validity of the H-theorem for the ES-Model (section about the case of a polyatomic gas):

$$\hat{F}_{(0)} = \frac{\sigma_{(0)}(t, x_2)\Lambda_\alpha}{\hat{T}_w(x_1)^{\frac{5}{2}}} \frac{1}{\pi^{\frac{3}{2}}} e^{-\frac{v_i^2+\hat{\mathcal{E}}}{\hat{T}_w(x_1)}} \tag{4.1}$$

The solution can be proved to be unique [8] modulo $\sigma_{(0)} = \sigma_{(0)}(t, x_2)$, which is the density computed with a zeroth-order approximation. The solution depends on time and axial coordinate only through this arbitrary function.

A couple of further remarks:

- The gross velocity at the first order is null.
- The density is constant throughout the whole cross section.

4.2 First-order solution

The first order solution ([7] p 361-362) is the main "actor" playing the major role in this paper. The function that we get is the following:

$$v_1 \partial_{x_1} \hat{F}_{(0)} + v_2 \partial_{x_2} \hat{F}_{(1)} = \frac{1}{k} \hat{\mathbb{C}}(\hat{F}_{(0)}, \hat{F}_{(1)}) \tag{4.2}$$

The solution to this equation can be found in Paper 3 for a different model equation. A more specific but less general solution is found in Paper 1. This equation is an inhomogeneous linear equation whose inhomogeneous term is made up of two different parts: one is a function of the density and the other of the temperature. We factorize $\hat{F}_{(1)}$ in the following way $\hat{F}_{(1)} = \hat{F}_{(0)}\phi$ and apply the following properties introduced in the section about the adimensionalized Boltzmann equation (section 1.3), which hold also for the model equations introduced:

- $2\mathcal{J}(1, \phi) = \mathcal{L}(\phi)$;
- $E\mathcal{J}(\phi, \psi) = \hat{\mathbb{C}}(E\phi, E\psi)$.

Last, we have to rescale the velocity, the internal energy state and the longitudinal coordinate: $c = v/\hat{T}_w^{\frac{1}{2}}$, $Y = \frac{\mathcal{E}}{RT_0\hat{T}_w}$ and $x_2 = \frac{X_2}{l}$, where l is the distance between the two plates.

Given that $\hat{F}_{(0)}$ is known, we get a formula in which the linearized collision operator replaces the original one. Not a single approximation has been done. They key step is that of factorizing the solution, which is a quite common trick with these kind of problems. What we finally get is a linear integro-differential equation with only one unknown, that is to say ϕ. Because of the linearity of the problem, the solutions is found to be composed of three different terms that are to be summed. Each one can be found independently. Furthermore, one is an arbitrary function that will be omitted. We obtain the following equation ($K(\hat{t}, x_1) = \frac{K_* \hat{T}_w^{\frac{3}{2}}(x_1)}{\hat{p}_{(0)}(\hat{t}, x_1)\hat{A}_{c(0)}(x_1)D}$, where K_* is the ratio between the reference mean free path and D and $\hat{A}_{c(0)}(x_1)$ is a function appearing in the ES-Model that is used to define a collision frequency and

that we take, without any loss of generality, to have always a unitary value):

$$\begin{aligned}\phi(x_2,c) = \phi^P(x_2,c_1,c_2c_3,\mathcal{E};\hat{T}_w(x_1),\hat{\rho}_{(0)}(x_1),K(x_1))\partial_{x_1}\ln\hat{p}+\\ +\phi^T(x_2,c_1,c_2,c_3,\mathcal{E};\hat{T}_w(x_1),\hat{\rho}_{(0)}(x_1),K(x_1))\partial_{x_1}\ln\hat{T}_w\end{aligned} \tag{4.3}$$

in which ϕ_P and ϕ_T are the solutions to two certain equation. The final solution will be

$$\begin{aligned}\hat{F}_{(1)}(x_2,c) = \hat{F}_{(0)}[\phi^P(x_2,c_1,c_2c_3,\mathcal{E};\hat{T}_w(x_1),\hat{\rho}_{(0)}(x_1),K(x_1))\partial_{x_1}\ln\hat{p}+\\ +\phi^T(x_2,c_1,c_2,c_3,\mathcal{E};\hat{T}_w(x_1),\hat{\rho}_{(0)}(x_1),K(x_1))\partial_{x_1}\ln\hat{T}_w]\end{aligned} \tag{4.4}$$

K might be a function of time and the partial derivative has been used because the temperature and the pressure might also be functions of time in the general case, which we do not take into consideration at the moment.

We can see that ϕ^P corresponds to the solution in the case of uniform pressure gradient (Poiseuille flow), whereas ϕ^T to the solution in the case of uniform temperature gradient along the wall (thermal-transpiration flow). The biggest problem that we will face trying to solve these two equations is that the collision term is an operator acting upon an unknown with many variables, which implies the integration with respect to all of them except the spatial ones (see the definition of the linearized ES-Model). However, by applying a similarity solution (the linearized collision operator related to the ES-Model is spherically symmetric, see section 1.8), we get the solution can be greatly simplified. This point might is of major importance because by reducing the number of variables the memory allocatable for every variable increases and the solution gets more precise. The linearized ES-Model is further simplified. Neglect of this point would probably lead to results which are not sufficiently accurate. This is what we get:

$$\phi^\alpha = \frac{c_1}{c_\rho}\phi_\alpha(y,c_2,c_\rho,Y,k(x_1))\ (\alpha = P,T) \tag{4.5}$$

$$c_\rho = (c_1^2+c_3^2)^{\frac{1}{2}} \tag{4.6}$$

$$c_2\frac{\partial\phi_\alpha}{\partial x_2} = \frac{2}{\sqrt{\pi}}\frac{1}{K}[-\phi_\alpha + 2c_\rho u_\alpha + 2(1-\eta)\nu c_2 c_\rho \Sigma_\alpha] + I_\alpha \tag{4.7}$$

$$u_\alpha = \int_{-\infty}^{\infty}\int_{0}^{\infty}\int_{0}^{\infty} c_\rho^2 Y^{\frac{\delta}{2}-1}\phi_\alpha \tilde{E}_Y dY dc_\rho dc_2 \tag{4.8}$$

$$\Sigma_\alpha = 2\int_{-\infty}^{\infty}\int_{0}^{\infty}\int_{0}^{\infty} c_2 c_\rho^2 Y^{\frac{\delta}{2}-1}\phi_\alpha \tilde{E}_Y dY dc_\rho dc_2 \tag{4.9}$$

$$I_P = -c_\rho,\ I_T = -c_\rho(c_2^2 + c_\rho^2 + Y - \frac{5+\delta}{2}) \tag{4.10}$$

$$\tilde{E}_Y = \Lambda_\delta \pi^{-\frac{1}{2}} exp(-c_2^2 - c_\rho^2 - Y) \tag{4.11}$$

$$\Lambda_\delta^{-1} = \int_0^\infty s^{\frac{\delta}{2}-1} e^{-s} ds \tag{4.12}$$

and the boundary conditions are

$$\phi_\alpha = 0,\ (y = \pm\frac{1}{2}, c_2 \lesseqgtr 0) \tag{4.13}$$

The boundary conditions are not properly those of the ES-Model in general.

By performing an integration, this set of equations can be even more simplified but these are the equations used to perform the first round of computations. Among the several macroscopic quantities that we may want to derive, the most important one for our purposes is the adimensionalized mass-flow rate $\hat{M}_{(1)}$.

$$\hat{M}_{(1)} = a^2 \frac{\hat{p}_{(0)}}{\hat{T}_w^{\frac{1}{2}}}(M_P \partial_{x_1} \ln \hat{p} + M_T \partial_{x_1} \ln \hat{T}_w) \tag{4.14}$$

where a is the distance between the two plates, which is given a unitary value in our computations

$$M_\alpha = M_\alpha(k) = \int_0^a u_\alpha(x_2, k(x_1))dx_2 \; \alpha = P, T \tag{4.15}$$

Recall that $Kn = k\frac{\sqrt{\pi}}{2}$. The utility of this two coefficients, that is M_P and M_T, will be showed in chapter 5. The adimensionalized mass-flow rate, which is an adimensionalized flux,

has been thus defined because the density at the first order $\rho_{(1)}$ is null (it happens to be so because an arbitrary function ϕ_g making up the first order solution together with ϕ_P and ϕ_T has been taken to be zero). Being $\rho_{(1)} = 0$, $\rho = \rho_{(0)} + \rho_{(2)}\epsilon^2 + ...$, we have that the density is constant in the cross section at the first order and the adimensionalized flow-rate is given by the formula above.

4.3 The Collision Term

The collision term is the most delicate one to treat numerically. The method employed in this paper is the Numerical Kernel Method, developed by Professors Yoshio Sone, Taku Ohwada and Kazuo Aoki [6]. The begin with, the domain of definition of ϕ_α, which can be considered as a three-dimensional real domain in our case (velocities c_ρ and c_2 and energy state $\mathcal{E}$), needs discretizing. The discretization process should lead to a non-homogeneous mesh because around the origin the molecular density is typically increasingly steeper with respect to its three variables. We will see later on how to choose a suitable spacing for the grid points. We just assume the mesh to be given:

- I grid points in the direction of the velocity v_ρ: $i_1, i_2, i_3, ..., i_p, ..., i_I$, each at a given velocity c_{ρ_p}.
- J grid points in the direction of the velocity v_2: $j_1, j_2, j_3, ..., j_q, ..., j_J$, each at a given velocity c_{2_q}.
- Z grid points in the direction of the energy state Y: $z_1, z_2, z_3, ..., z_r, ..., z_Z$, each at a given energy state Y_r.

Our discretization, among all the possible ones, will yield $(I-1)(J-1)(Z-1)$ grid points $P_{p,q,r}$ inside the domain such that $P_{p,q,r} = (v_{\rho_p}, v_{2_q}, Y_r)$. We will have a domain made up of several parallelepipeds with non-uniform faces. We must apply a cut-off to the domain of ϕ_α before discretizing.

Next, we shall choose whatever basis functions we prefer to approximate the molecular density in the domain of definition exactly as in the case of the

Finite-Element Method. We will take a Lagrangian polynomial basis of the second order defined on a three dimensional space. Accordingly, the domain of definition of the basis function comprises a subdomain of the whole domain ϕ made up by the following points: $i_{p-1}, i_p, i_{p+1}, j_{q-1}, j_q, j_{q+1}, z_{r-1}, z_r, z_{r+1}$. We need three grid points on each side. The unknowns will be the values of ϕ_α at each grid point. In our case, thanks to the symmetry of the solution, we have that the integration has to be performed with respect to only three variables. A three-dimensional array of all the unknowns is to be defined $\phi_{p,q,r} = \phi(c_{\rho_p}, c_{2_q}, \mathcal{E}_r)$. From now on, whenever these three subscripts will be specified, α will be omitted for the sake of clarity.

Last, we ought to approximate the linearized ES-Model.

$$\mathcal{L}(\phi) = \frac{1}{k}[-\phi_{p,q,r} + 2c_\rho u_\alpha + 2(1-\eta)\nu c_2 c_\rho \Sigma_\alpha] \cong \frac{1}{k}\mathbb{L}_{p,q,r}\phi_{p,q,r} \tag{4.16}$$

where the summation convention used with tensors has to be applied to these arrays. $\mathbb{L}_{p,q,r}$ equals to the value of the linearized ES-Model evaluated in the domain $i_{p-1}, i_p, i_{p+1}, j_{q-1}, j_q, j_{q+1}, z_{r-1}, z_r, z_{r+1}$ for a unitary value of $\phi_{p,q,r}$ and the chosen basis functions.

$$\mathbb{L}_{p,q,r} = 2c_{\rho_p}\overline{u}_\alpha + 2(1-\eta)\nu c_{2_q} c_{\rho_p}\overline{\mathbf{\Sigma}}_\alpha \tag{4.17}$$

For instance, if we take into consideration the central node of the subdomain of definition of the Lagrangian basis, will have that:

$$\begin{aligned}\overline{u}_\alpha = \int_{i_{p-1}}^{i_{p+1}}\int_{j_{q-1}}^{j_{q+1}}\int_{z_{r-1}}^{z_{r+1}} c_{\rho_p}^2 Y_z^{\frac{\delta}{2}-1}\overline{E}_Y \frac{c_\rho - c_{\rho_{p+1}}}{c_{\rho_p} - c_{\rho_{p+1}}}\frac{c_\rho - c_{\rho_{p-1}}}{c_{\rho_p} - c_{\rho_{p-1}}}\times \\ \times \frac{c_2 - c_{2_{q+1}}}{c_{2_q} - c_{2_{q+1}}}\frac{c_2 - c_{2_{q-1}}}{c_{2_q} - c_{2_{q-1}}}\frac{Y - Y_{r+1}}{Y_r - Y_{r+1}}\frac{Y - Y_{r-1}}{Y_r - Y_{r-1}} dY dc_2 dc_\rho\end{aligned} \tag{4.18}$$

$$\overline{\Sigma}_\alpha = 2\int_{i_{p-1}}^{i_{p+1}}\int_{j_{q-1}}^{j_{q+1}}\int_{z_{r-1}}^{z_{r+1}} c_{2_q} c_{\rho_p}^2 Y_z^{\frac{\delta}{2}-1}\overline{E}_Y \frac{c_\rho - c_{\rho_{p+1}}}{c_{\rho_p}-c_{\rho_{p+1}}}\frac{c_\rho - c_{\rho_{p-1}}}{c_{\rho_p}-c_{\rho_{p-1}}}\times \\ \times\frac{c_2 - c_{2_{q+1}}}{c_{2_q}-c_{2_{q+1}}}\frac{c_2 - c_{2_{q-1}}}{c_{2_q}-c_{2_{q-1}}}\frac{Y-Y_{r+1}}{Y_r - Y_{r+1}}\frac{Y-Y_{r-1}}{Y_r-Y_{r-1}} dY\, dc_2 dc_\rho \tag{4.19}$$

$$\overline{E}_Y = \Lambda_\delta \pi^{-\frac{1}{2}} exp(-c_{2_q}^2 - c_{\rho_p}^2 - Y_z) \tag{4.20}$$

$$\Lambda_\delta^{-1} = \int_0^\infty s^{\frac{\delta}{2}-1} e^{-s} ds \tag{4.21}$$

For different nodes, the three-dimensional Lagrange polynomial has to be substituted into the formula. Furthermore, whenever a node is common to multiple subdomains, the basis functions of different subdomains have to be taken into consideration. The treatment is more delicate at the boundaries of the domain.

In the program, there should be a separate module for every integral that has to be evaluated. All the integrals have been evaluated analytically and their expression has been substituted into each module. The hypothesis of diatomic gas makes the integrals analytically solvable. We just mention that the longest part of the program used to solve the problem is dedicated to all the cases that need considering. A good check on the accurateness of the program is that of considering several polynomial functions of c_2 and c_ρ and to find the

$$error = \left| \frac{\mathcal{L}(\phi) - \mathbb{L}_{p,q,r}\phi_{p,q,r}}{\mathcal{L}(\phi)} \right| \tag{4.22}$$

of the approximation.

The reference node is the one marked by the hand-shaped arrow. This node is common to eight different intervals, so the value of the function f assigned to this node equals the value by which the functions of the Lagrangian basis on the eight surrounding intervals should be multiplied to obtain the interpolating function.

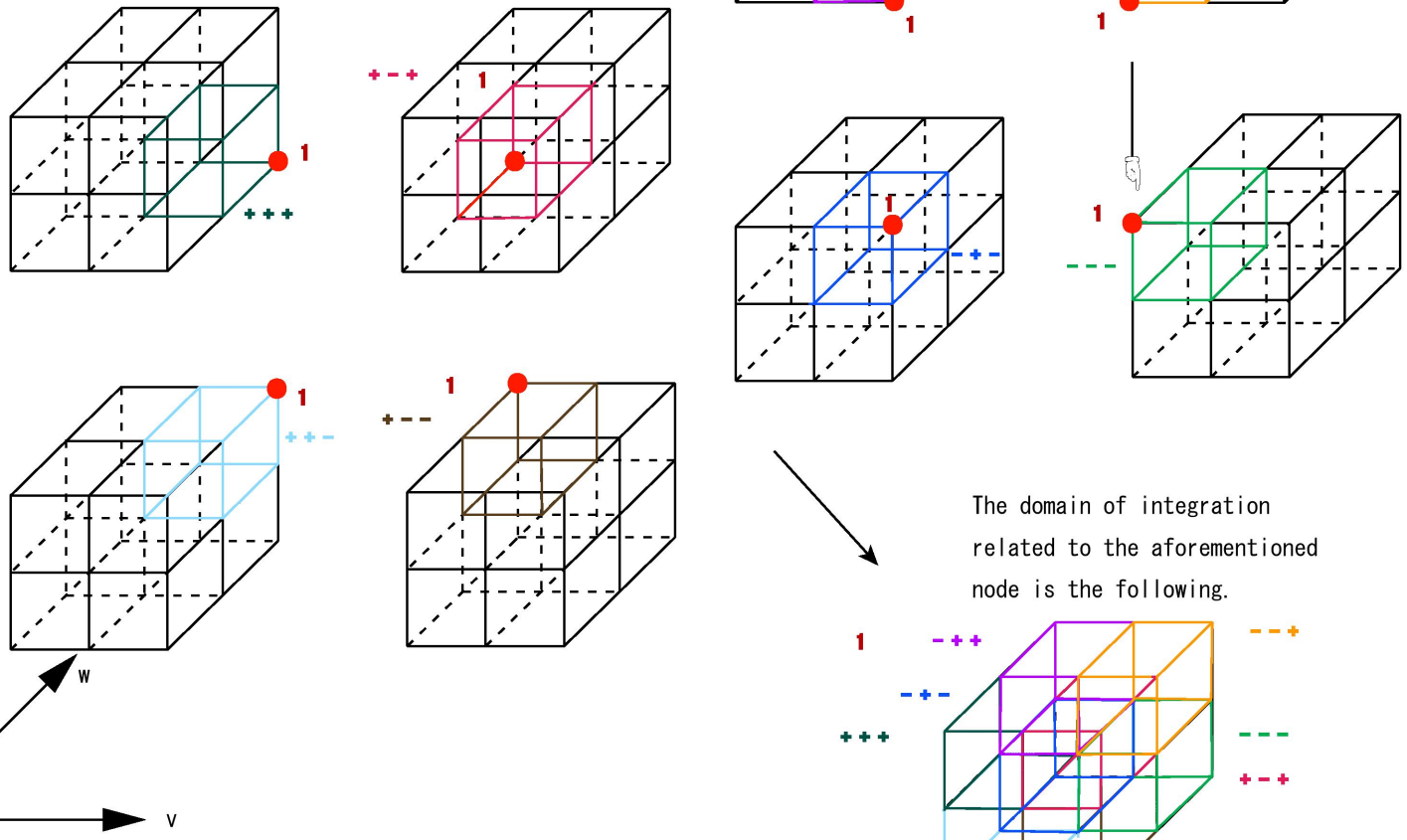

The domain of integration related to the aforementioned node is the following.

The nodes on the boundary need to be dealt with separately due to the fact that they lack certain surrounding intervals. For instance, the value of f at the nodes in the vertices of the domain will be multiplied only by one basis function depending on the vertex they are in, whereas the values of f at the nodes on the edges that are not on the vertices need multiplying by two basis functions. The remaining nodes, that is to say those on the six faces of the domain that are not on the edges, are related to four basis functions. The next figures exemplify this important aspect.

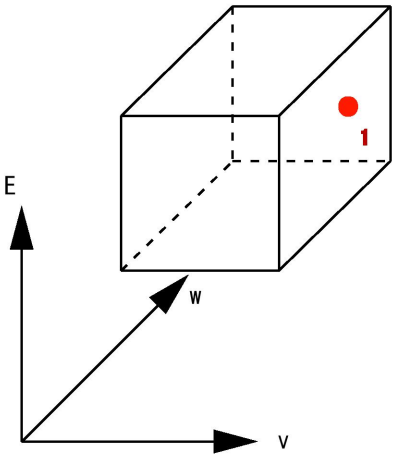

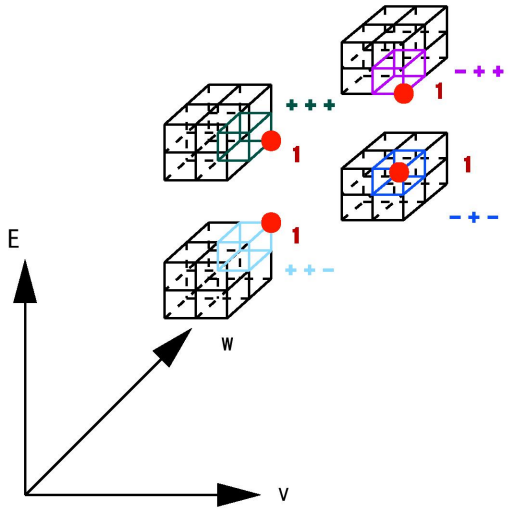

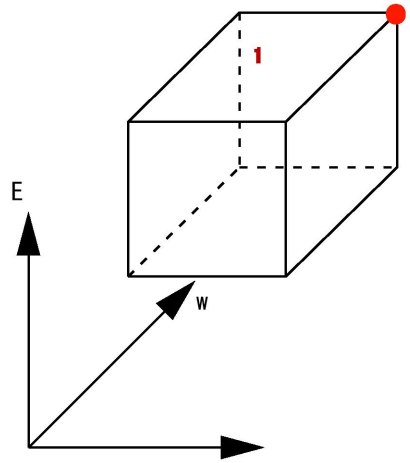

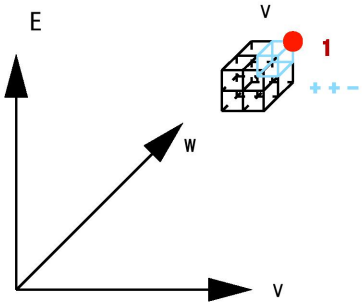

4.4 Second-order upwind scheme

What we have obtained so far is an equation like the following with homogeneous boundary conditions:

$$c_2 \frac{\partial \phi_\alpha}{\partial y} = \frac{1}{k}[-\phi_\alpha + 2c_\rho u_\alpha + 2(1-\eta)\nu c_2 c_\rho \Sigma_\alpha] + I_\alpha \tag{4.23}$$

Given that the problem is symmetric with respect to the plane to which the two axes x_1 and x_2 belong, we need only to deal with the lower half of the domain. Given that the virtual memory allocatable is pretty limited, dealing with half of the domain will allow for a denser grid. The results yielded by the dicretization of the whole domain were not acceptable at all. A finite-difference method has been applied with a second-order upwind scheme. The solution obtained with a first order-upwind scheme was not satisfactory. The reference frame that has been used has the origin lying on the lower plate. The nodes in the longitudinal direction are numbered increasingly x_{2_1}, x_{2_2},..., x_{2_N}(point on the median line),...,$x_{2_{2N}}$. The reason why an upwind scheme has been employed is that the particles are thought of as spheres traveling with a given direction whose interaction determine a change of molecular density for a given range of values of velocity corresponding to that same direction. Therefore, let us say that $c_2 > 0$ (c_ρ is always positive), in this case a second-order backward difference approximates the partial derivative in the node x_i and we would have that

$$\begin{aligned} c_2 D(x_{2_i}, x_{2_{i-1}}, x_{2_{i-2}}, \phi(x_{2_i})_{p,q,r}, \phi(x_{2_{i-1}})_{p,q,r}, \phi(x_{2_{i-2}})_{p,q,r}) = \\ = \tfrac{1}{k}\mathbb{L}_{p,q,r}\phi(x_i)_{p,q,r} + I_\alpha(c_2, c_\rho, Y)\ \forall c_2, c_\rho, Y \end{aligned} \tag{4.24}$$

where D is a second-order backward difference. The expression of D can be easily found by applying a parabolic interpolating polynomial to three points that are not equally spaced. The necessity of using points that are not uniformly spaced in the x_2 direction is a consequence of the discontinuity on the boundary. In the same way, if $c_2 < 0$, we would have that

$$\begin{aligned} c_2 D(x_{2_{i+2}}, x_{2_{i+1}}, x_{2_i}, \phi(x_{2_{i+2}})_{p,q,r}, \phi(x_{2_{i+1}})_{p,q,r}, \phi(x_{2_i})_{p,q,r}) = \\ = \tfrac{1}{k}\mathbb{L}_{p,q,r}\phi(x_i)_{p,q,r}\ \forall c_2, c_\rho, Y \end{aligned} \tag{4.25}$$

Moreover, if $c_2 = 0$, we would have the following

$$0 = \mathbb{L}_{p,q,r}\phi(x_i)_{p,q,r} \ \forall c_2, c_\rho, Y \tag{4.26}$$

The unknown is the array $\phi_{i,p,q,r} = \phi(x_i)_{p,q,r} \ \forall x c_2, c_\rho, Y$.

However, the first two nodes on the lower plate and the last two nodes in the median line between the two plates need considering separately. As far as the latter are concerned, the problem is symmetric, therefore:

- On the last point x_{2_N} in the median line only the first equation (that for $c_2 > 0$ is imposed) and the last one (that for $c_2 = 0$) are imposed. In fact $\phi_\alpha(x_{2_N}, c_2) = \phi_\alpha(x_{2_N}, -c_2)$.
- On the second-last point $x_{2_{N-1}}$, all the previous equations have been imposed, but, in the case of negative c_2, we have that $\phi_\alpha(x_{2_{N-1}}, c_2) = \phi_\alpha(x_{2_{N+1}}, -c_2)$. This allows to compute a second-order backward difference for all the points in the lower half part of the domain.

For what concerns the first two nodes, we should spend a few more words. On the lower boundary we have a discontinuity, so, as already explained (section 1.7), we have $\phi(x_{2_1}, 0^+)$ as well as $\phi(x_{2_1}, 0^-)$. The equations that we impose are:

- $c_2 D(x_{2_{i+2}}, x_{2_{i+1}}, x_{2_i}, \phi(x_{2_{i+2}})_{p,q,r}, \phi(x_{2_{i+1}})_{p,q,r}, \phi(x_{2_i})_{p,q,r}) = \frac{1}{k}\mathbb{L}_{p,q,r}\phi(x_i)_{p,q,r}$ $\forall c_2, c_\rho, Y, \ c_2 < 0$.
- $0 = \mathbb{L}_{p,q,r}\phi(x_i)_{p,q,r} \ \forall c_2, c_\rho, Y, \ c_2 = 0^-$.
- The boundary condition ($\phi_{p,q,r}(x_{i_1}) = 0$) has to be imposed on $c_2 = 0^+$ and $c_2 > 0^-$.

Lastly, on the second point x_{i_2}, we apply the first three equations with a first-order backward difference formula in the case of positive c_2. The mesh should be denser close to the discontinuity. Furthermore, also the nodes close to the origin of the three-dimensional domain originated by c_ρ, c_2 and Y should be denser. A cubic function has been used to determine the spacing of points on the grid, in such a way as to ensure a dense arrangement of points in the "hot zone".

Finally, a matrix A has been assembled. This is a square matrix of size $I \times (J+1) \times Z + (N-1) \times I \times J \times Z$ (we have $\phi(x_{2_1}, 0^+)$ as well as $\phi(x_{2_1}, 0^-)$, therefore the nodes discretizing c_2 for the first spatial point are $J+1$, $q = 1, ..., J+1$ iff $i = 1$). The unknown is a vector ψ whose components are those of the array $\phi_{i,p,q,r}$ disposed in this way:

- $\psi((p-1)\times(J+1)\times Z+q\times Z+r)=\phi_{1,p,q,r}$.
- $\psi(I\times(J+1)\times Z+(i-1)\times I\times J\times Z+(p-1)\times J\times Z+(q-1)\times Z+r)=\phi_{i,p,q,r}$, $i=2,...,N$.

The first conditions to be imposed are those on x_{2_1} in the case of $c_2>0$. Then all the other conditions on this point and those on the others point starting from the second going upwards to the one on the median line. The unknown vector is ψ. The inhomogeneous term b is due to I_α. We get the final system to be solved:

$$A\psi=b \tag{4.27}$$

A is a square matrix and its rows are all linearly independent. That is a consequence of the fact the discretized problem is well-posed. This procedure is not straightforward because of a lack of reference. Actually, at the beginning, the author did know know that this was the procedure to follow. Therefore, what has been explained in the last two chapters is the final result of a long journey that started from the following question "How can I coherently impose the boundary conditions (on the temperature and pressure, which are macroscopic variables) in a discretized problem?". The procedure originally followed was quite different in that the spacing of the grid points, the order of the scheme and many others things were different, but it lead to results that were not accurate enough to draw any conclusions. Step by step, every single change was applied and the program began to take on its actual form. Anytime the author had a problem, several fruitful conversations with Masanari Hattori brought about small but essential changes that finally gave rise to this procedure.

4.5 Solution to the Resolvent System

The whole problem reduces to the solution of a linear system. Usually, when a finite-difference method is applied, a fixed-point iterative procedure is advisable that does not require the assembly of the matrix because the computational cost is relatively small. One of the main shortcomings of an iterative procedure is that the computational time required to have a "good" solution tends to be really long. Usually computations last several hours or even an whole day for such problems. The author, driven by a lack of experience in this field, decided to solve the system. There are two reasons behind this choice:

- the solution can be found in just 6 to 8 hours with a sufficiently good mesh;
- the assembly of the matrix proved itself an extremely propaedeutical introduction to the problem.

Unfortunately, the side effects of this choice all but negligible: the matrix that has to be solved has an enormous size. Even if it happens to be a banded matrix due to the finite-difference method, it is still tough to save. That is why the author decided to store the matrix in two separate files. Although, this choice made the resolvent module slightly more complex. At first, an iterative method seemed preferable, so the author wrote a program to solve the former system using a biconjugate gradient stabilized method. Unfortunately, the results obtained were not satisfactory, and so a Lapack routine to solve linear systems with banded matrices was found to be the best way to get the solution. These brief chapter, though encapsulated in a few lines, has presented one of the biggest problems faced to solve this problem: the size of the data that have to be dealt with. This problem was a big drain on the author's time during the present research. A "usual" matrix A was stored by storing just the coordinates and values of non-zero elements. That required a couple of files of about 8 Gigabytes each. Strenuous efforts were made to save as much virtual memory as possible, but it seemed to be never enough for our purposes. Consider that, in general, the following statements hold:

- An increase in the number of grid points or in the number of variables leads inevitably to an increase of the size of the matrix.
- An increase in the order of the problem implies more non-zero diagonal lines in the matrix.

Those obvious conclusions entail the following question:

"What is the best compromise between order of accuracy, number of variables and number of grid points?"

Actually, the author has not yet found an answer to this question. Therefore, every single session of computations has been separately considered to find the best choice: the biggest the Knudsen number gets, the more the molecular density gets steep, so it is better to increase the number of velocity grid points. However, if the function gets steeper, the cut-off of its domain may be changed: it may be "shrunk" because the wings of the molecular function are closer to the origin. We will partly answer this question in the next section.

4.6 Results Obtained

Unsatisfactory: that is all! This procedure was applied to only a small number of values of the Knudsen number. It was too time-consuming and the error of approximation of the collision term (see section 3.4) was too large. The results can be seen in the next chapter. The error of M_P and M_T is of the order of the error of approximation of the collision term (see next chapter), although the trend of this coefficients as functions of the Knudsen number is good. The "exact" solution is taken to be the one we are about to show how to compute. The error on the collision term, though relatively small in the case of M_P, spoils completely M_T, whose values are significantly smaller.

Once again, we have to overcome the feeling of grief caused by this overt failure. There is a way out of the problem: we could drop a variable. As a consequence, the number of points could be increased up to an acceptable value! The word "acceptable" refers to the fact the the number of grid points used so far, large as it may seem, is still too small compared to the number of points mostly used in this kind of numerical analysis. The procedure through which we solved the problem, that is to say by solving a linear system, is much more consuming in terms of virtual memory than an iterative fixed-point method. Using the same mesh in our procedure would require an enormous demand of memory for allocation.

4.7 How to Drop a Variable: the BKW-Model

The same solution can be worked out in a different way. We introduce a marginal velocity distribution Φ_α ([7] pp. 364-366):

$$\Phi_\alpha = \Lambda_\delta \int_0^\infty Y^{\frac{\delta}{2}-1} \phi_\alpha(x_2, c_1, c_\rho, Y, k(x_2)) e^{-Y} dY \tag{4.28}$$

We write the problem for the marginal velocity distribution and we eventually get that the equation for the thermal-transpiration flow is the same that we would derive by applying the BKW-Model, whereas the molecular density and the macroscopic quantities related to the Poiseuille flow obtained by using the ES-Model are the same that we would have by correcting with a given function of the parameters ν and η and of the coordinate x_2 the data obtained applying the BKW-Model. Moreover, in the general case of a polyatomic gas whose degree of freedom is δ, δ does not appear any more. Therefore, the whole program has been changed to solve the modified equa-

tions with the BKW-Model. Basically, the difference lies in the collision term, in which the integration has to be performed with respect to just two variables. The error of approximation of the collision operator is extremely small.

Furthermore, the same problem has been solved after having applied a Maxwell-type boundary condition for different values of the accommodation coefficient α. Also in this case the same similarity solution holds and we have that the discontinuity at the boundary tends to disappear as α approaches a unitary value. Therefore, after carrying on all the due computations, we obtain that the equations to be solved are the same but that the boundary conditions become:

$$\phi_\alpha(c_2) = (1-\alpha)\phi_\alpha(-c_2), (y = \pm\frac{1}{2}, c_2 \lesseqgtr 0) \tag{4.29}$$

4.8 Second-Order Solution

So far, the flow has been considered steady. Let us try to remove this hypothesis. Because of the last assumption in section 2.4, the flow of gas expected to be slow, which means that $\hat{v}_i$ is of the order of ϵ^2, and so the reference time t is taken to be $\hat{t} = \hat{L}/(2R\hat{T})^{\frac{1}{2}}\epsilon$ and the Strouhal number $Sh = \epsilon^2$. Accordingly, the time derivative appears in the equation to be solved multiplied by $Sh = \epsilon^2$. Surprisingly, we have that all the results obtained up to now are still valid in the time-varying case. However, when it comes to solving the second-order solution, we stumble upon this additional term. Before embarking on new computations, we decide to complete our analysis by finding the value of the macroscopic quantities at the first order, which does not require to find the solution of the second-order equation: we have only to through this equation the conservation of the number of particles. By performing an integration, we get the following problem to be solved ([7] pp. 362-363):

$$\frac{\partial \hat{p}_{(0)}}{\partial t} + \hat{T}_w \frac{\partial \mathcal{M}}{\partial x_2} = 0 \tag{4.30}$$

$$\mathcal{M} = \frac{\hat{p}_{(0)}}{\hat{T}_w^{\frac{1}{2}}} \frac{D}{2} [M_P(K)\partial_{x_1} \ln \hat{p} + M_T(K)\partial_{x_1} \ln \hat{T}_w] \tag{4.31}$$

$$K(\hat{t}, x_1) = \frac{K_* \hat{T}_w^{\frac{3}{2}}(x_1)}{\hat{p}_{(0)}(\hat{t}, x_1)\hat{A}_{c(0)}(x_1)D} \tag{4.32}$$

where K_* is the ratio between the reference mean free path and D and $\hat{A}_{c(0)}(x_1) = 1$ without loss of generality.

This equation is the diffusion-convection equation for the pressure at the zeroth order in ϵ. $\mathcal{M}$ is the dimensionless first-order mass flux: $\frac{M}{\hat{\rho}}(2R\hat{T})^{\frac{1}{2}} = \frac{D}{2}\mathcal{M}\epsilon + O(\epsilon^2)$, where the reference longitudinal length is taken to be 1 and M is the original dimensional mass-flow rate.

4.9 Flow between Two Tanks at Different Pressure

The last problem we are going to deal with is that of a flux driven by a difference of pressure between two tanks and a constant gradient of temperature imposed along the thin conduit joining those two tanks. It might be modeled as follows:

- The thin conduit is a tube just like the ones analyzed in depth in the latter sections.
- The two tanks are filled with the same fluid as the one inside the linking tube and closed with a valve, which is a kind of tiny "faucet" that, when opened, lets the fluid out. The two valves are opened simultaneously.
- Being the tube long and narrow and the two tanks extremely larger, the effect of the joint are omitted.
- The flow, after it transfers from the tube to tank, as soon as it has passed the valve, is thought to instantaneously modify the pressure inside the whole tank, in which the pressure is considered constant. The tank keeps passing from an equilibrium condition to the next one.
- The temperature of the tank is that of the cross section of the pipe in contact with the valve.

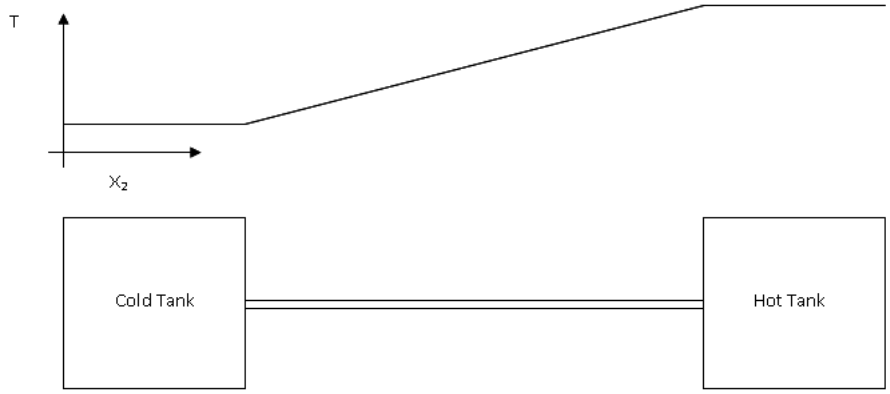

Accordingly, the pressure is a function of time and x_2, whereas the temperature is a given function of x_2 only. The only unknown happens to be the pressure.

4.9.1 Case of Given Pressure at the Extremities of the Tube

At first, we consider the case in which the pressure at the extremities of the tube, that is to say inside the tanks, is given. At the initial time, the pressure through the tube is thought to be linear. The equations that have to be used are those of the second-order solution with the coefficients of M_p and M_T previously found. The solution to this highly non-linear equation does not present us with any problems. First, we substitute the expression of $\mathcal{M}$ into $\frac{\partial \hat{p}_{(0)}}{\partial t} + \hat{T}_w \frac{\partial \mathcal{M}}{\partial x_2} = 0$. Second, we discretize it using a second-order backward finite difference for the time derivative and second-order central finite difference for the derivative with respect to x_2. At the extremities of the tube, we apply a first order finite-difference approximation. From now on we will omit the caps. We have that the adimensionalized mass-flow rate coefficients are functions of $K = K(T, p)$. For a given time t_j, where t_j is a point of the uniform time grid ($j = 1, ..., T$ and $t_j - t_{j-1} = \Delta t$, $j = 2, ..., T$), we get this system of equations (we omit the caps):

$$A(p_j)p_j = r_j \tag{4.33}$$

in which:

- p_j is a vector such that $p_{j_i} = (x_{2_i}, t_j)$, where x_{2_i} is a point of the uniform spatial grid ($i = 1, ..., S$ and $x_i - x_{i-1} = \Delta x$, $i = 2, ..., S$).
- $A(p_j)$ is a matrix such that$A_{1,1} = 1$, $A_{S,S} = 1$, $A_{i,i-1} = \frac{h}{(\Delta x)^2} - \frac{g}{\Delta x}$, $A_{i,i} = \frac{3}{2\Delta t} + f - \frac{2h}{(\Delta x)^2}$, $A_{i,i+1} = \frac{g}{\Delta x} - \frac{h}{(\Delta x)^2}$ and all the other elements are 0. f, g and h are thus defined:

$$f = \frac{1}{R^2 T^{\frac{1}{2}}} \frac{\partial M_T}{\partial x} \frac{dT}{dx} - \frac{3}{2} M_T (\frac{dT}{dx})^2 \frac{1}{R^2 T^{\frac{3}{2}}} + M_T \frac{d^2T}{dx^2} \frac{1}{R^2 T^{\frac{1}{2}}} \tag{4.34}$$

$$g = \frac{M_T}{R^2 T^{\frac{1}{2}}} \frac{dT}{dx} - \frac{1}{2} M_P \frac{dT}{dx} \frac{1}{R^2 T^{\frac{3}{2}}} + \frac{T^{\frac{1}{2}}}{R^2} \frac{dM_P}{dx} \tag{4.35}$$

$$h = M_P \frac{T^{\frac{1}{2}}}{R^2} \tag{4.36}$$

- r_j is a vector such that $r_{j_i} = \frac{2}{\Delta t} p_{i,j-1} - \frac{1}{2\Delta t} p_{i,j-2}$.

All the element of A_j can be found by analytical derivation (in case of derivation of the temperature) or numerical integration (in case of the mass-flow rate coefficients we will employ a finite-difference formula). The data for the pressure in the preceding time step are used to compute the vector r_j. However, A_j is a function of the pressure through M_P and M_T. Newton-Raphson's method can be promptly applied. In fact, we are looking for p such that $F(p_j) = A_j p_j - r_j = 0$. Once the Jacobian of $F(p_j)$, that is $J_F(p)$, has been computed, we iteratively solve the following problem:

$$p_j^{(k)} = p_j^{(k-1)} - J_F^{-1}(p_j^{(k-1)})(A(p_j^{(k-1)})p_j^{(k-1)} - r_j) \tag{4.37}$$

where k is the counter of the iterations.

The analytical computation of the Jacobian matrix is tedious and the steps are omitted but, with a little of patience and much care not to make any mistakes, it is easy to get the result. After a number of iterations has been carried out, p_j is taken to be equal to $p_j^{(k)}$. As far as the inversion of the Jacobian matrix is concerned, we know that it is tridiagonal, therefore a method devised by Emrah Kilic [9] to invert a diagonal matrix by use of backward continued fractions has been applied.

This procedure is followed for every time step. The pressure in the tanks before the time in which the valves are opened is thought to be constant and

to coincide with the pressure of the tanks at the time of the opening of the valves. This assumption allows us to apply a second-order finite-difference formula for the time derivative since the beginning of the computation.

4.9.2 Pressure at the Extremities Unknown

In this case, the problem is exactly like the one introduced at the beginning of the chapter. The pressure at the extremities and through the tube is known only at the initial time step. The procedure is pretty much the same as that in the previous subsection. However, the pressure at the extremities is computed at every time step. It is determined by the pressure at the previous time step plus a variation that is a function of a parameter m and of the net mass which has entered the tank. Once again, the mass-flow rate must agree with the gradients of temperature and pressure at the joints between the tubes and the tanks.

The evaluation of m is not straightforward. It must be such as to grant the conservation of mass, that is to say that M flowing through the junction to the tank must equal M entering the tank and vice versa. Supposedly, the tanks will go through successive equilibrium states. First of all the dimensional mass-flow rate must be computed:

$$M = \frac{\rho_0}{(2RT)_0^{\frac{1}{2}}}\frac{D}{2}[\mathcal{M}\epsilon + O(\epsilon^2)] \cong \frac{\rho_0}{(2RT_0)^{\frac{1}{2}}}\frac{D}{2}\mathcal{M}\epsilon \tag{4.38}$$

We must pay attention to the fact that the problem is bidimensional and the dimension of ρ_0 is $[\frac{M}{L^2}]$ and to the fact that the reference longitudinal length is taken to be unitary according to the previous analysis.

Then, given that the volume of a tank V is constant, we may claim that

$$\mathfrak{M}_\mathfrak{j} = \mathfrak{M}_{j-1} + M_j\Delta T_j \tag{4.39}$$

where $\mathfrak{M}$ is the total mass of fluid inside the tank and M_j and ΔT_j are respectively the dimensional mass-flow rate and the difference of temperature at $t = t_j$. Therefore $\rho_{tank_j} \cong \rho_{tank_{j-1}} + \frac{M_j\Delta T_j}{V}$. Recall that $p = \rho RT$ for a fluid that can be modeled with kinetic theory, and so

$$p_{1,j} = p_{tank_j}RT_j \cong (\rho_{tank_{j-1}} + \frac{M_j\Delta T_j}{V})RT_j = p_{tank_{j-1}} + m\mathcal{M}_j\Delta T_j \tag{4.40}$$

where T_j and $\mathcal{M}_j$ are respectively the temperature and the non-dimensional

mass-flow rate at $t = t_j$ and $m = \frac{\rho_0}{(2RT_0)^{\frac{1}{2}}} \frac{D}{2} \epsilon \frac{\Delta T_j}{V} R$. The symbol of "approximately equal to" may be substituted by the symbol "equal to" in case of first-order accuracy. Another way to solve the same problem could have been that of modeling the tank as a tube with a "huge" distant between the parallel plates. The term "huge" refers to the relative size of the tank and the thinner tube.

One more essential remark has to be made: the direction of the flow driven by the temperature is directed towards the region of higher temperature whereas the flow driven by he pressure gradient is opposite to the gradient itself. Therefore, whenever we compute the Poiseuille or thermal-transpiration flow at the boundary, its direction (which determines its sign) has to be found.

4.9.3 Single-stage Knudsen Pump

The same program detailed in the previous section has been slightly changed (the boundary condition on the cold tank on the left side has been changed) to suit the following problem.

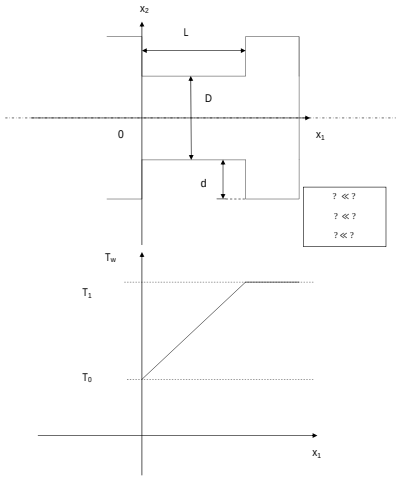

Figure 4.1: Single-stage Knudsen Pump

The pressure on the cold tank is kept constant so has to have a single-stage Knudsen pump.

5 Data Obtained

5.1 ϕ_p and ϕ_T computed imposing the Diffuse-Reflection Boundary Condition

5.1.1 BKW-Model

The plot in this section represent some of the functions ϕ_p and ϕ_T, where ϕ_α is redefined as $\phi_\alpha = E\Phi_\alpha = \pi^{-3/2}\exp(-\hat{v}_i^2)\Phi_\alpha$ (Φ_α is the marginal distribution function), obtained for different values of the Knudsen number Kn at the boundary and on the median line. The reason behind the rescaling the function ϕ_α lies in the fact that $\hat{F}_{(1)}$ was factorized using the solution $\hat{F}_{(0)}$, which is proportional to the following Maxwellian function:

$$\widetilde{E} = \frac{1}{\pi^{\frac{3}{2}}} - \frac{\hat{v}_i^2 + \hat{\mathcal{E}}}{T_w(x_1)} \tag{5.1}$$

(see the form of the solution in the previous chapter).

In fact, the same procedures could be followed employing the BKW-Model since the beginning. That would have led to a solution $\hat{F}_{(0)}$ proportional to E.

Given that the BKW-Model has been applied, the data do not reflect the diatomic structure of Nitrogen. As predicted in the first chapter, on the boundary occurs a discontinuity. While going through these data, one should pay attention to the fact that ϕ_T might have negative values, which does contrast with the definition of molecular density as a positive function. This can be promptly justified by looking at the solution of the first-order equation: ϕ_P and ϕ_T can have negative values as long as the overall formula of the molecular density yields a positive value.

5.1.1.1 $Kn = 10^{-2}$

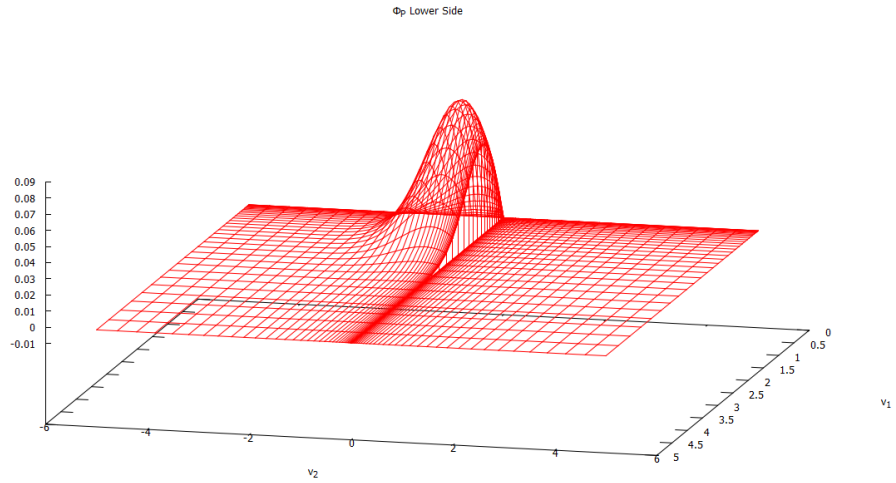

Figure 5.1: ϕ_P Lower Side

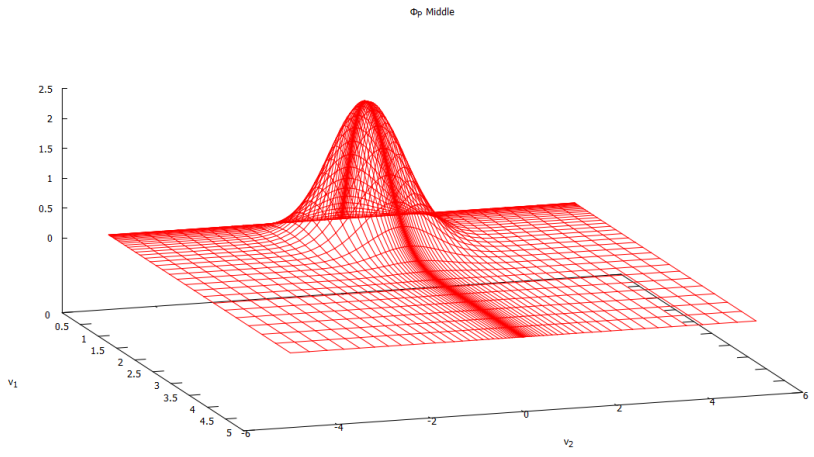

Figure 5.2: ϕ_P Middle

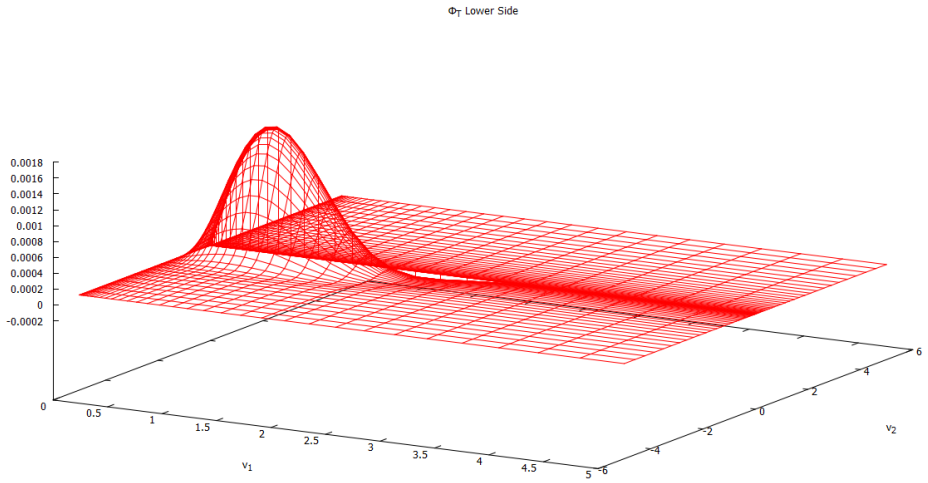

Figure 5.3: ϕ_T Lower Side

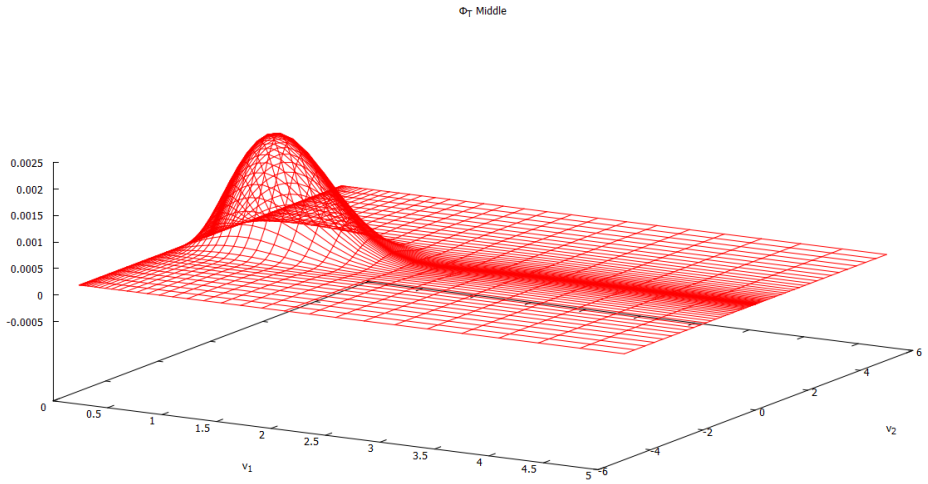

Figure 5.4: ϕ_T Middle

5.1.1.2 $Kn = 3 \times 10^{-2}$

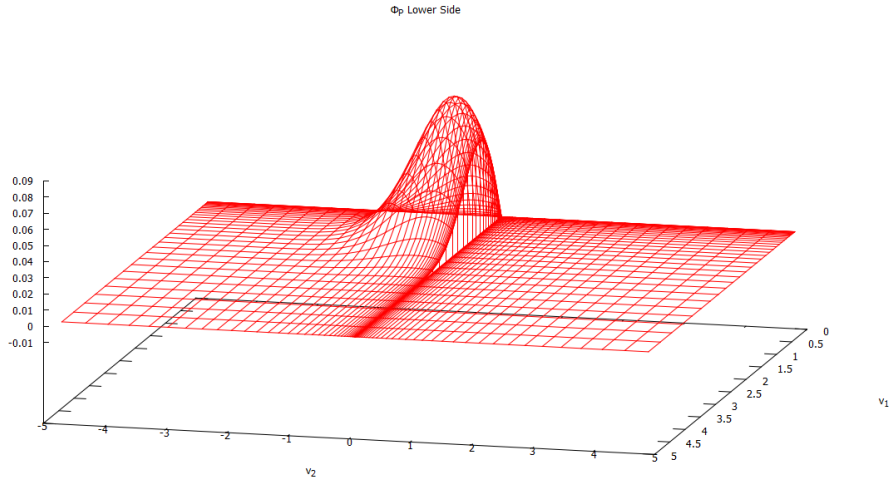

Figure 5.5: ϕ_P Lower Side

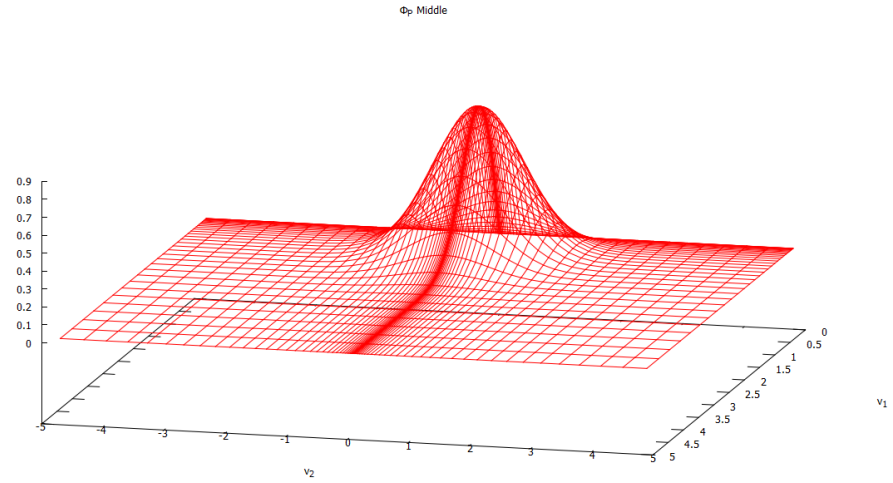

Figure 5.6: ϕ_P Middle

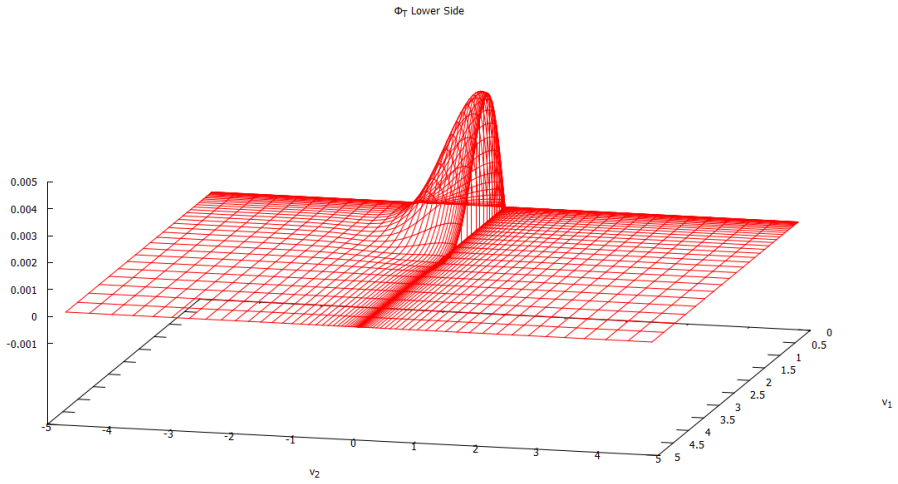

Figure 5.7: ϕ_T Lower Side

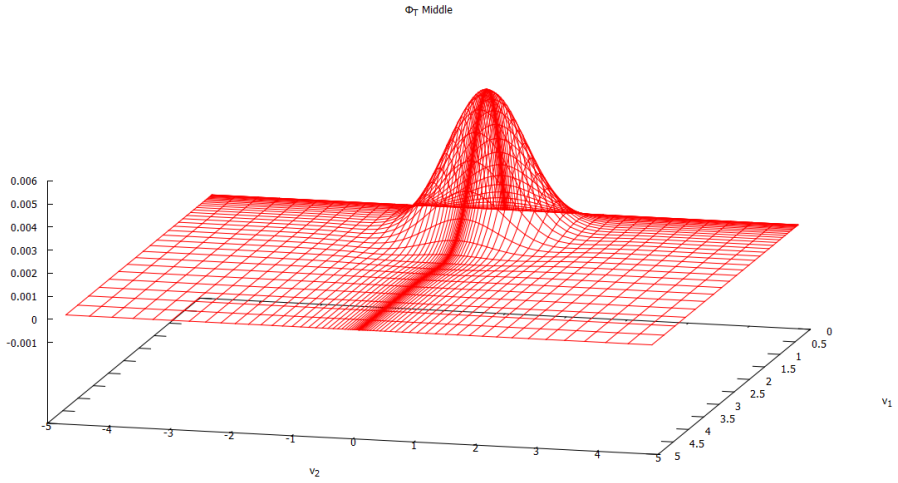

Figure 5.8: ϕ_T Middle

5.1.1.3 $Kn = 6 \times 10^{-2}$

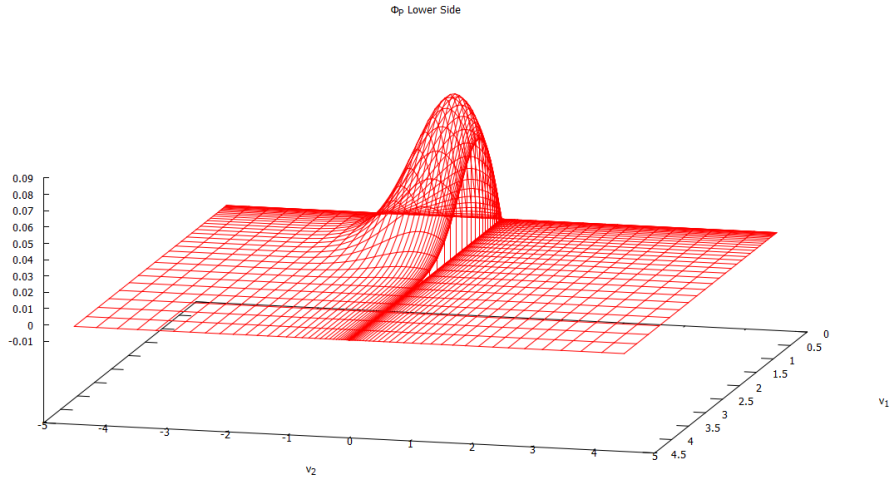

Figure 5.9: ϕ_P Lower Side

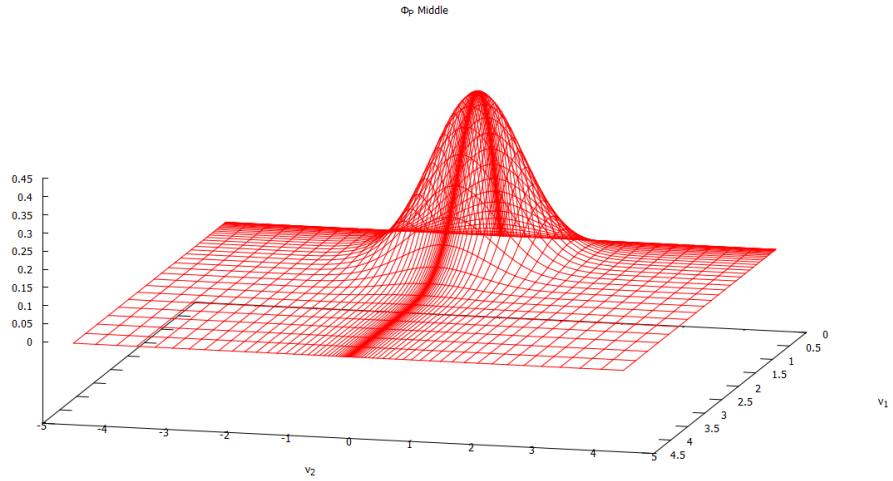

Figure 5.10: ϕ_P Middle

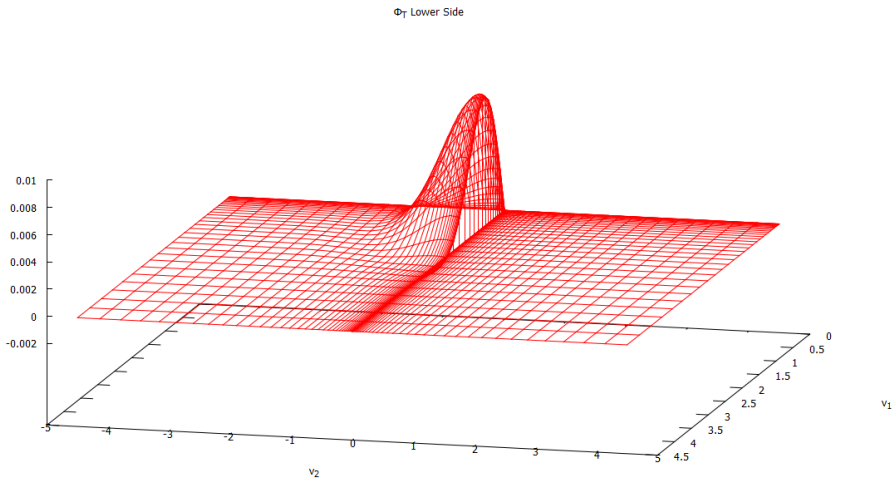

Figure 5.11: ϕ_T Lower Side

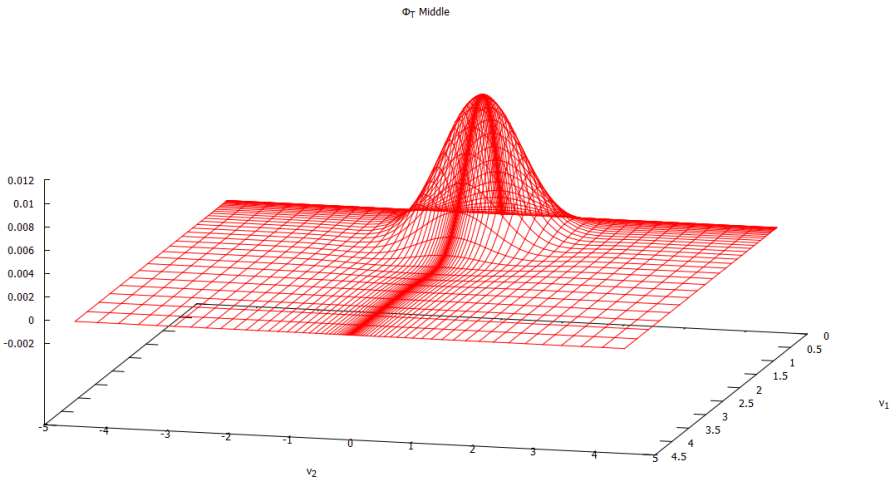

Figure 5.12: ϕ_T Middle

5.1.1.4 $Kn = 10^{-1}$

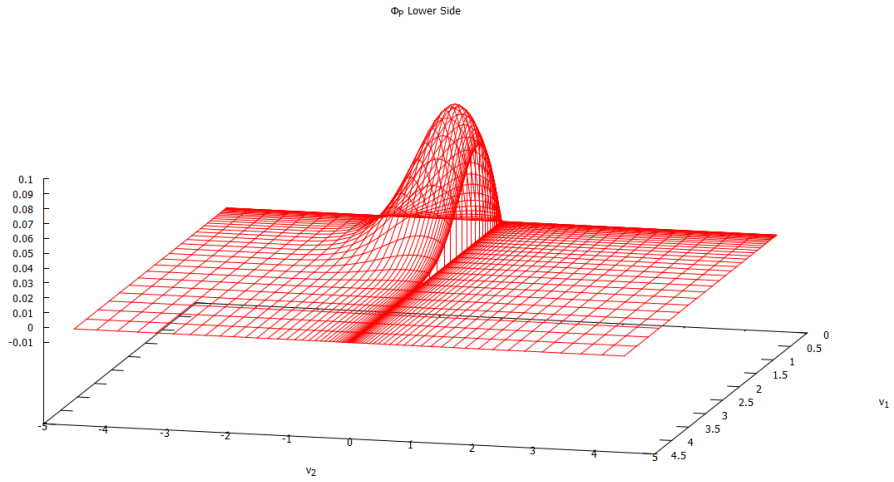

Figure 5.13: ϕ_P Lower Side

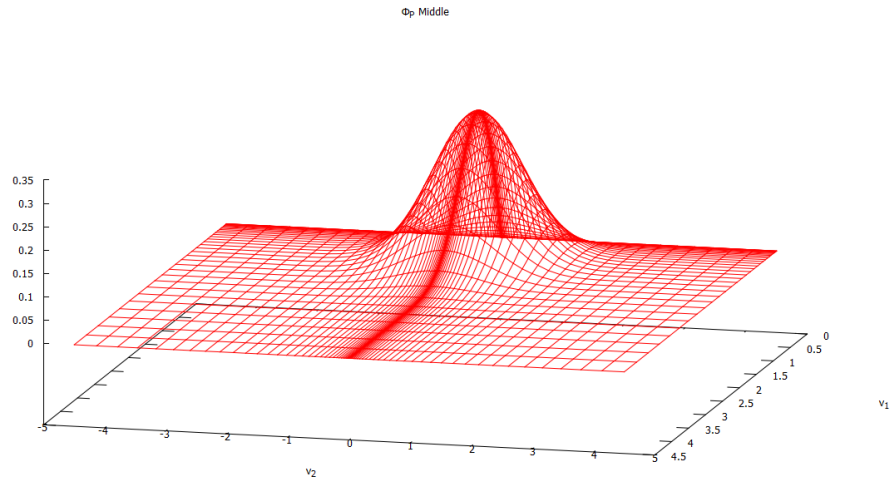

Figure 5.14: ϕ_P Middle

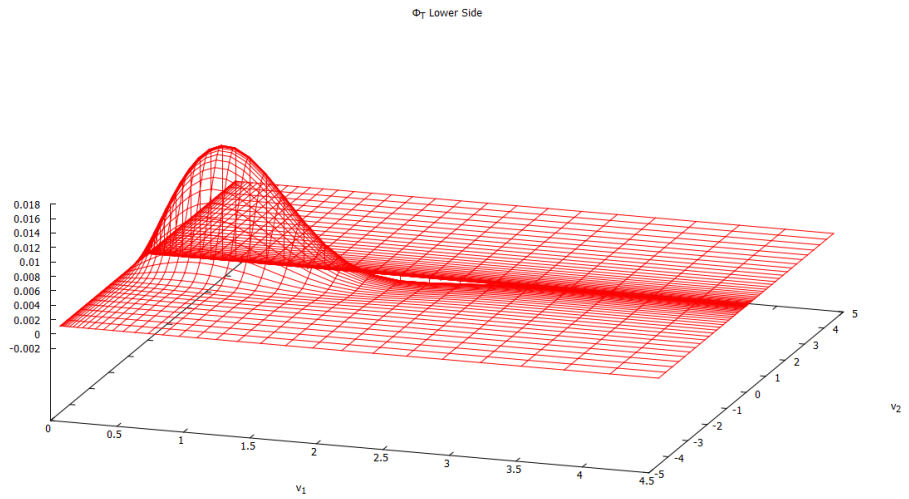

Figure 5.15: ϕ_T Lower Side

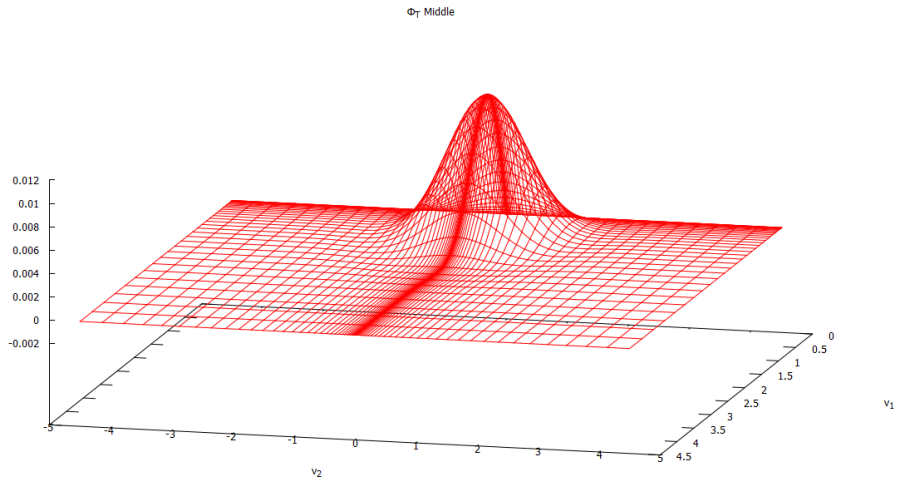

Figure 5.16: ϕ_T Middle

5.1.1.5 $Kn = 3 \times 10^{-1}$

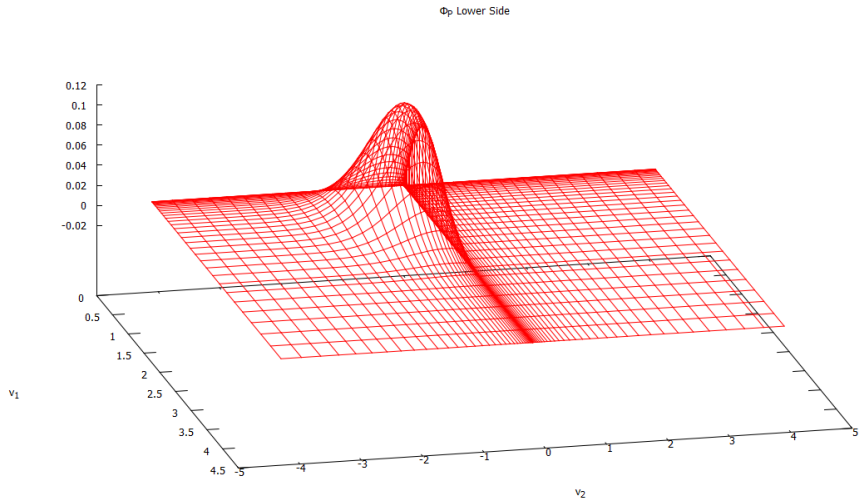

Figure 5.17: ϕ_P Lower Side

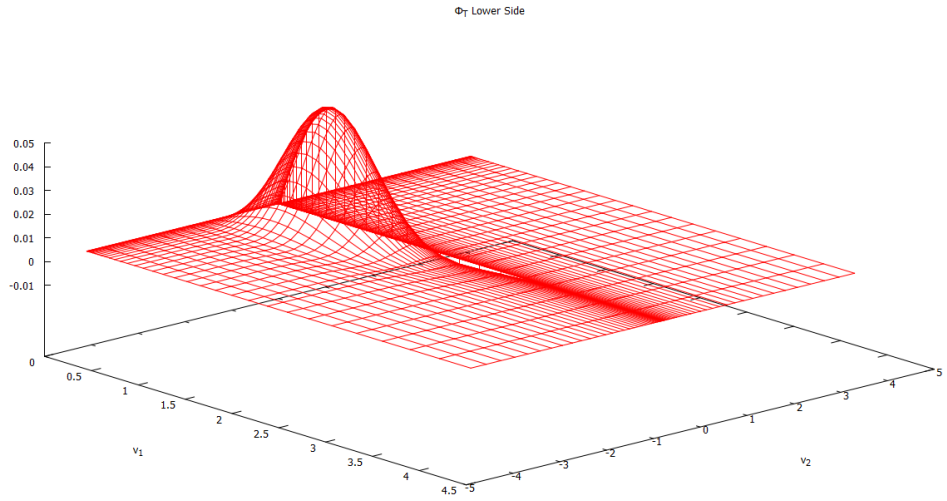

Figure 5.18: ϕ_T Lower Side

5.1.1.6 $Kn = 8 \times 10^{-1}$

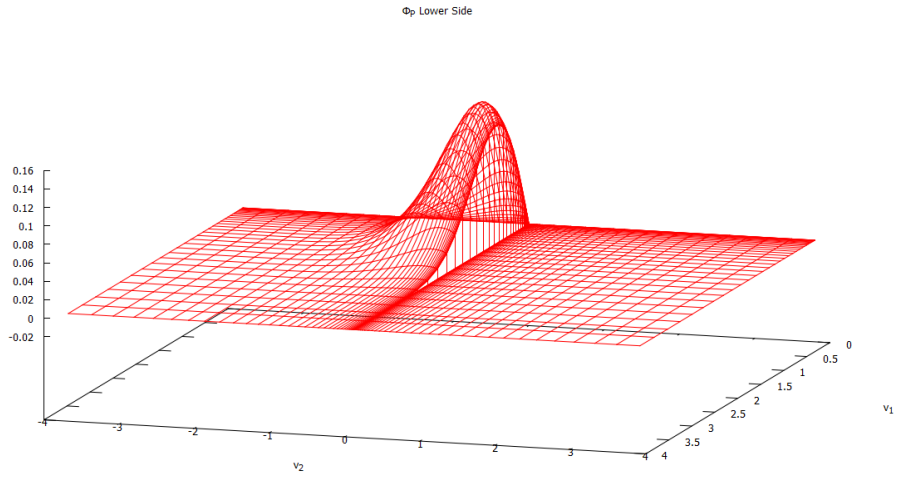

Figure 5.19: ϕ_P Lower Side

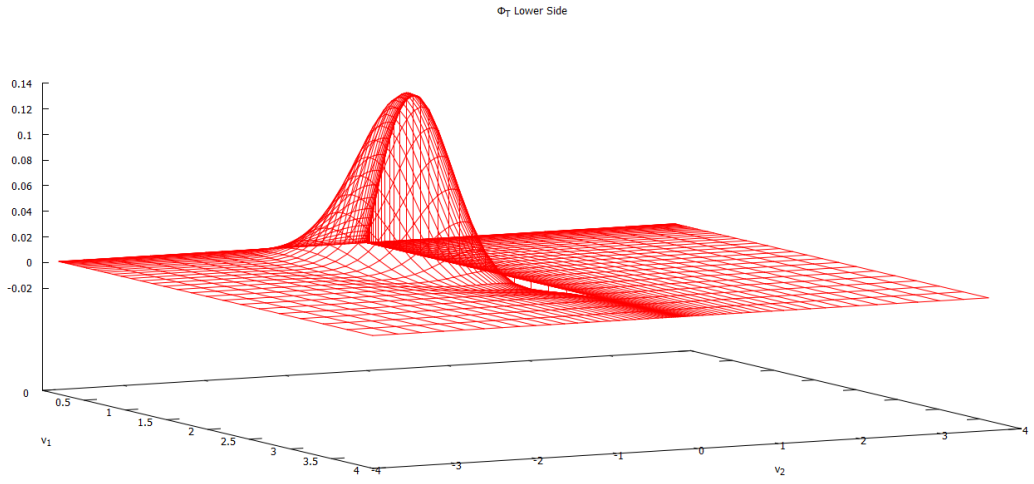

Figure 5.20: ϕ_T Lower Side

5.1.1.7 $Kn = 10^2$

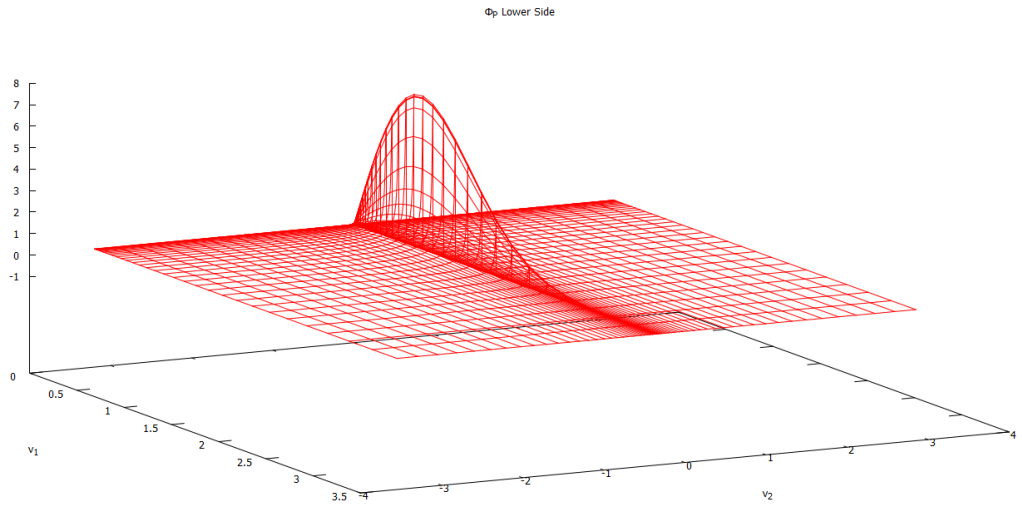

Figure 5.21: ϕ_P Lower Side

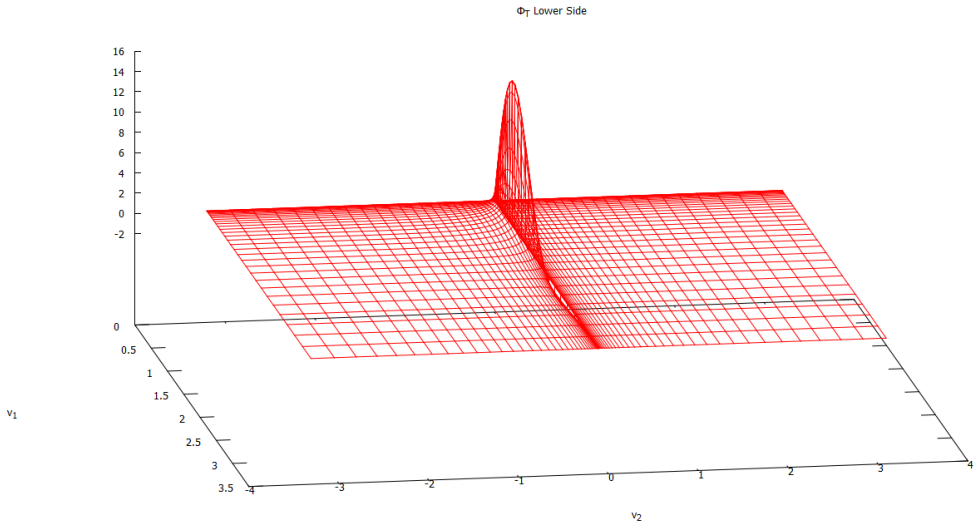

Figure 5.22: ϕ_T Lower Side

5.1.2 ES-Model

The following plots are those of ϕ_P and ϕ_T redefined in the following way: $\phi_\alpha = \tilde{E}\Phi_\alpha$. Indeed, the original functions of the ES-Model are functions of three variables (c_2, c_ρ and Y). We will show the marginal distributions derived from the original functions multiplied by a given Maxwellian.

5.1.2.1 $Kn = 4 \times 10^{-1}$

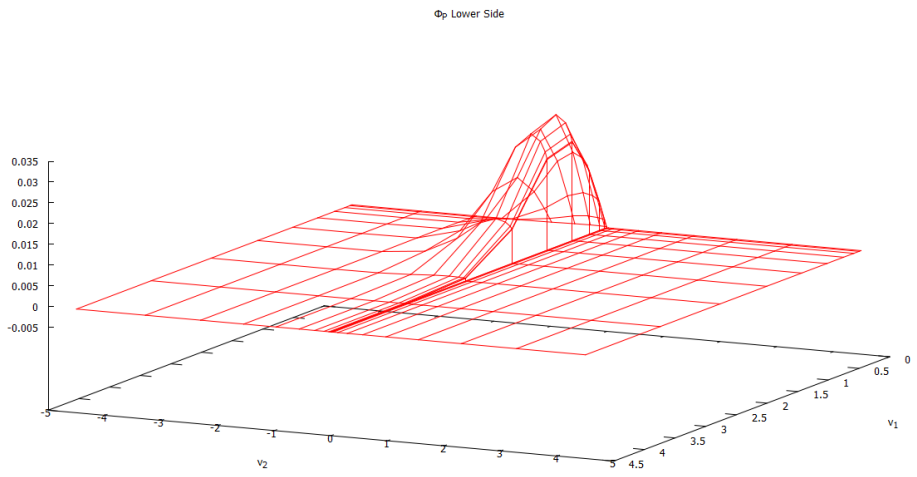

Figure 5.23: ϕ_P Lower Side

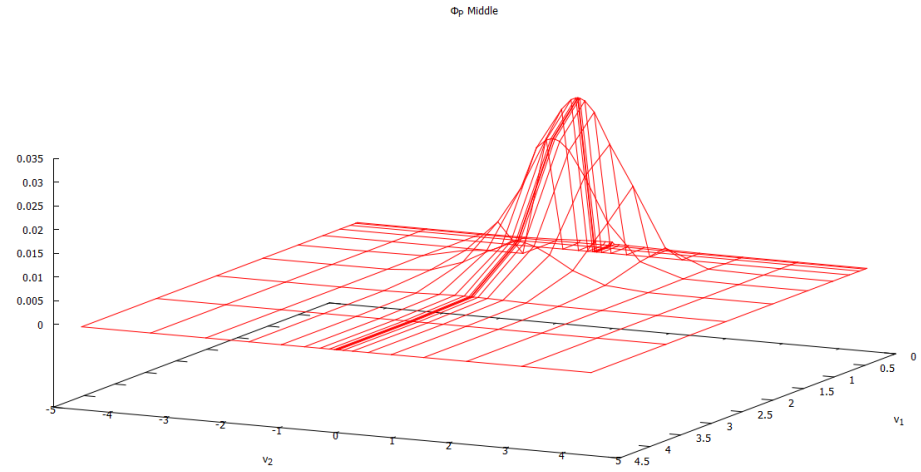

Figure 5.24: ϕ_P Middle

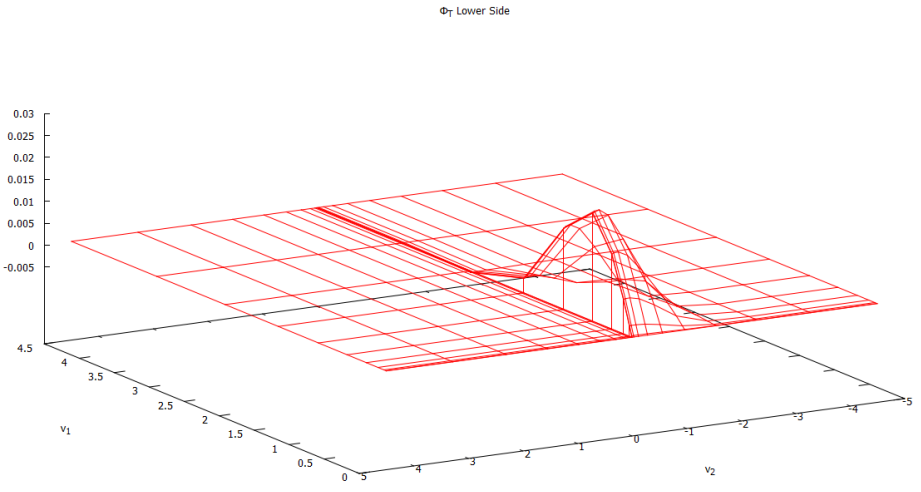

Figure 5.25: ϕ_T Lower Side

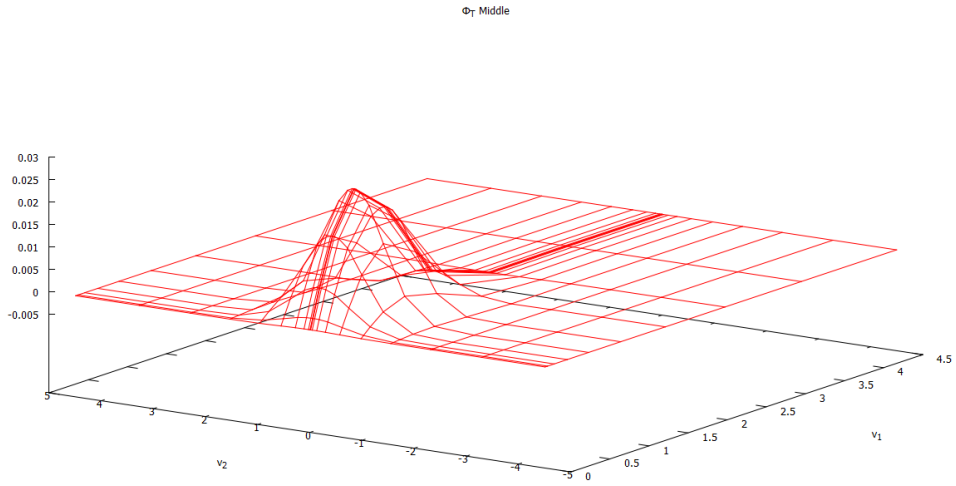

Figure 5.26: ϕ_T Middle

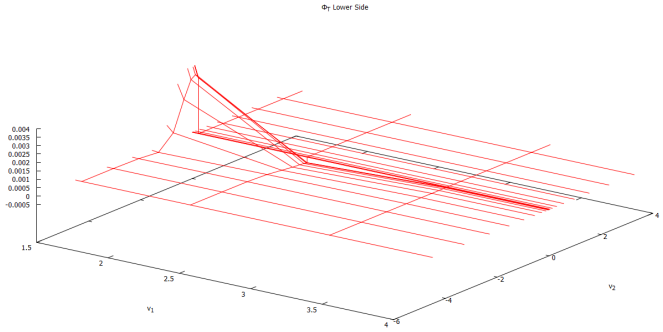

Figure 5.27: ϕ_T Lower Side (close-up)

By looking carefully at the plot on the left it can be noticed that there's the "hollow" that appears also in the data obtained by employing the BKW-Model.

5.1.2.2 $Kn = 6 \times 10^{-1}$

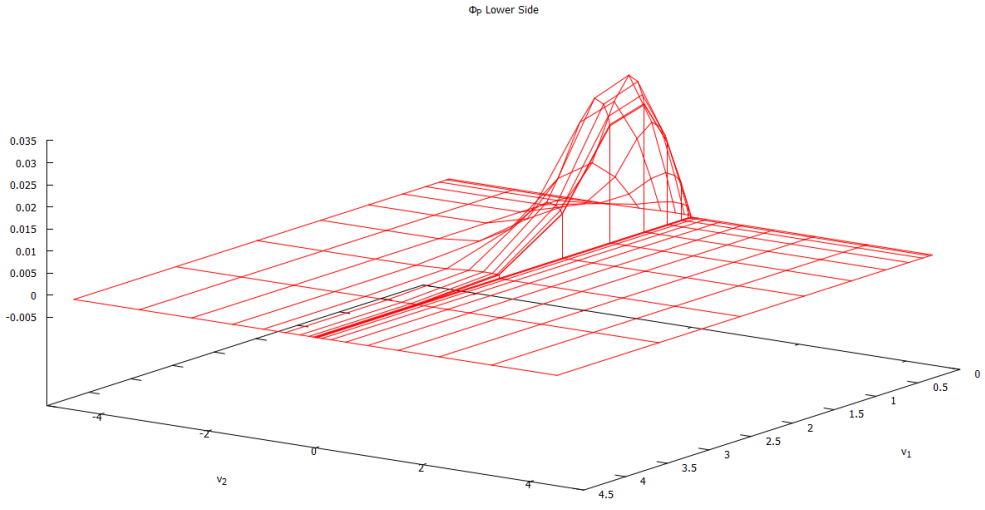

Figure 5.28: ϕ_P Lower Side

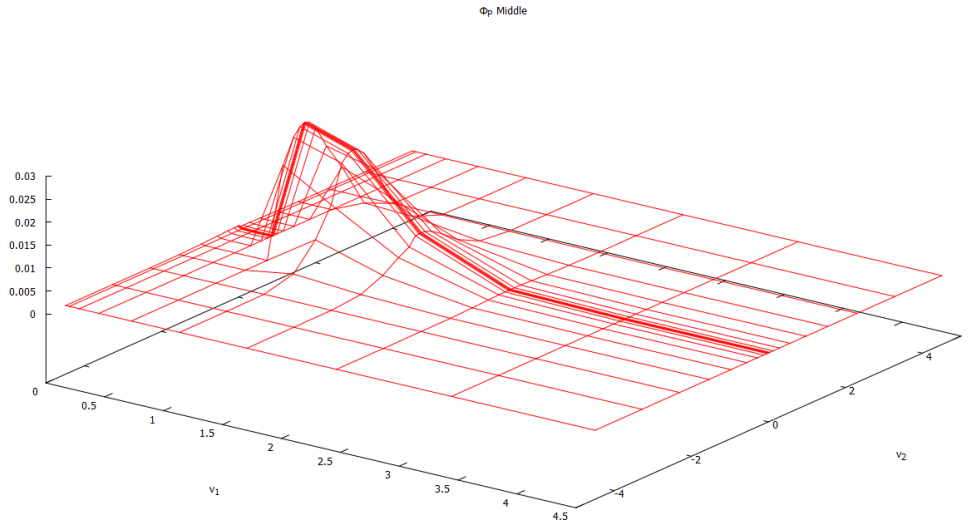

Figure 5.29: ϕ_P Middle

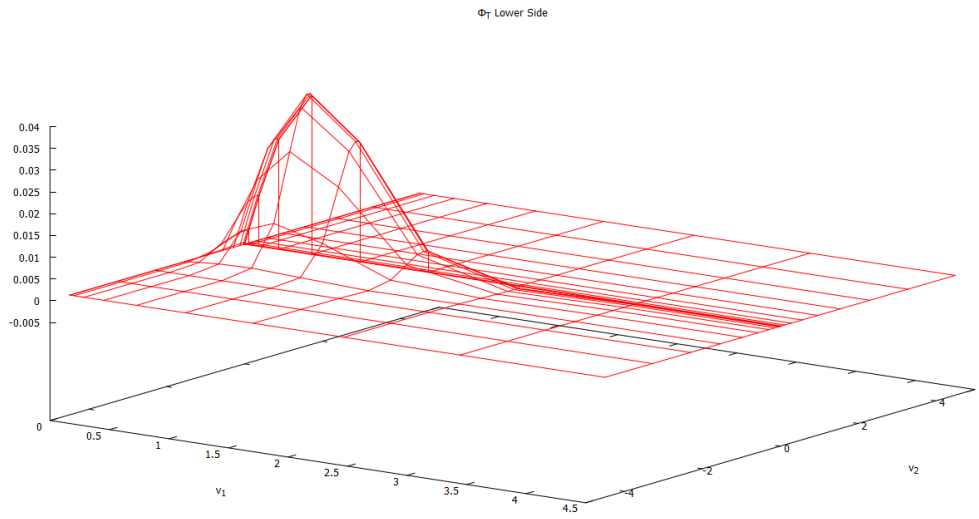

Figure 5.30: ϕ_T Lower Side

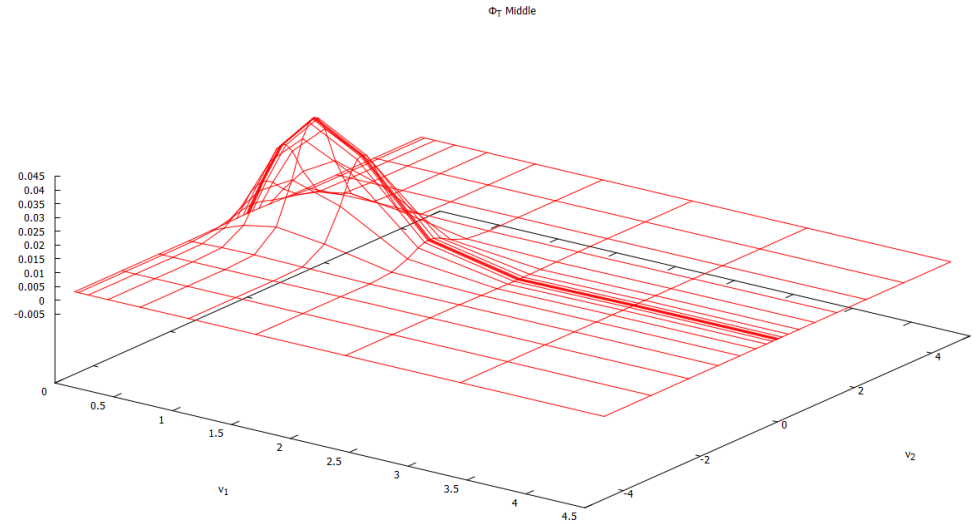

Figure 5.31: ϕ_T Middle

5.2 Gross Velocity (u_{α_1}) Profiles computed imposing the Diffuse-Reflection Boundary Condition

5.2.1 BKW-Model

Given that the rate of flow per unit area has been computed, we may employ the term flux. The two fluxes have a given velocity profile which basically shows what has been previously anticipated: the flows have opposite direction.

5.2.1.1 u_{P_1}

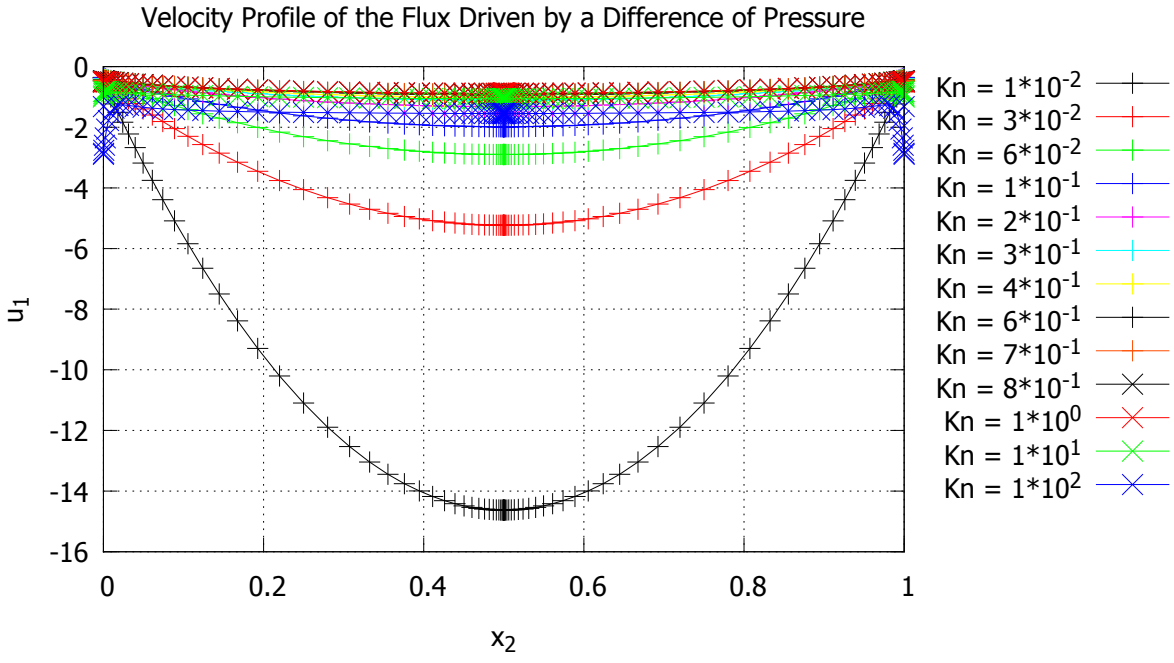

Figure 5.32: u_{P_1}

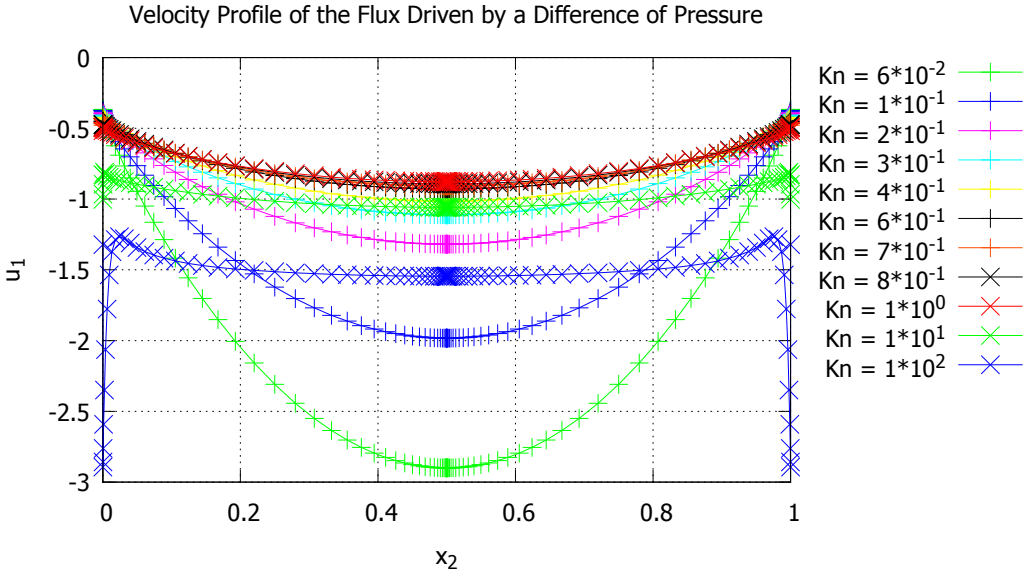

Figure 5.33: u_{P_1}

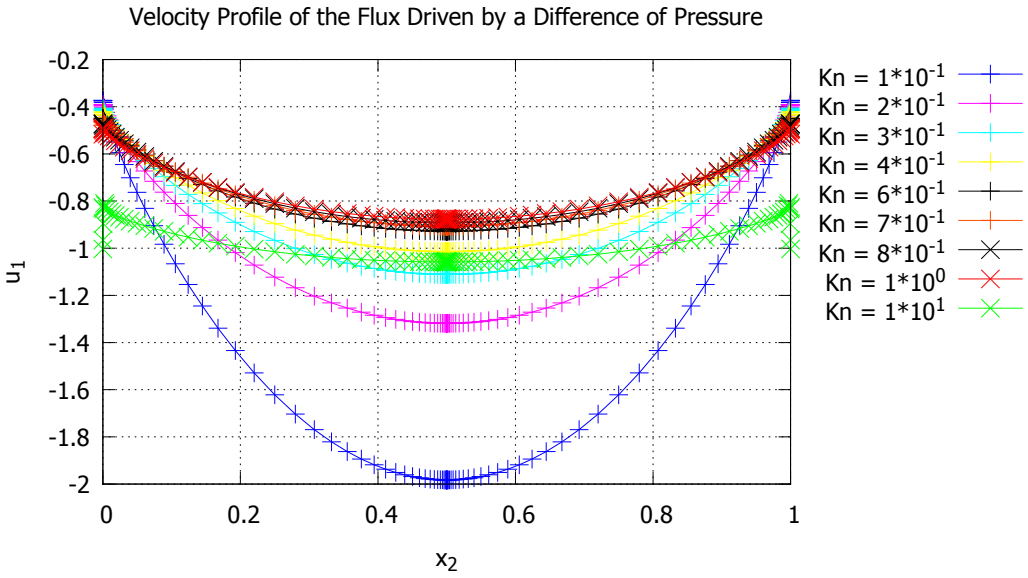

Figure 5.34: u_{P_1}

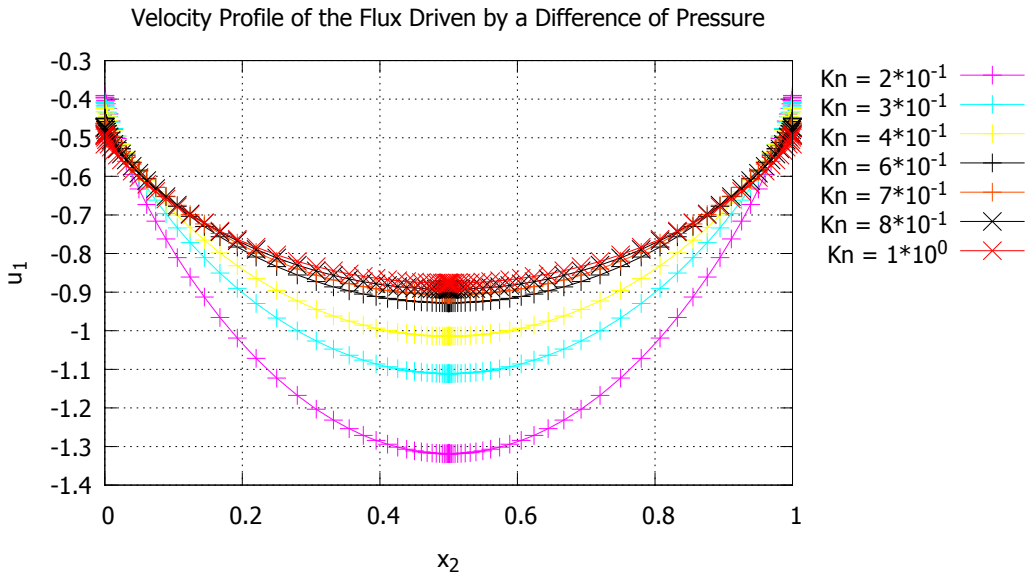

Figure 5.35: u_{P_1}

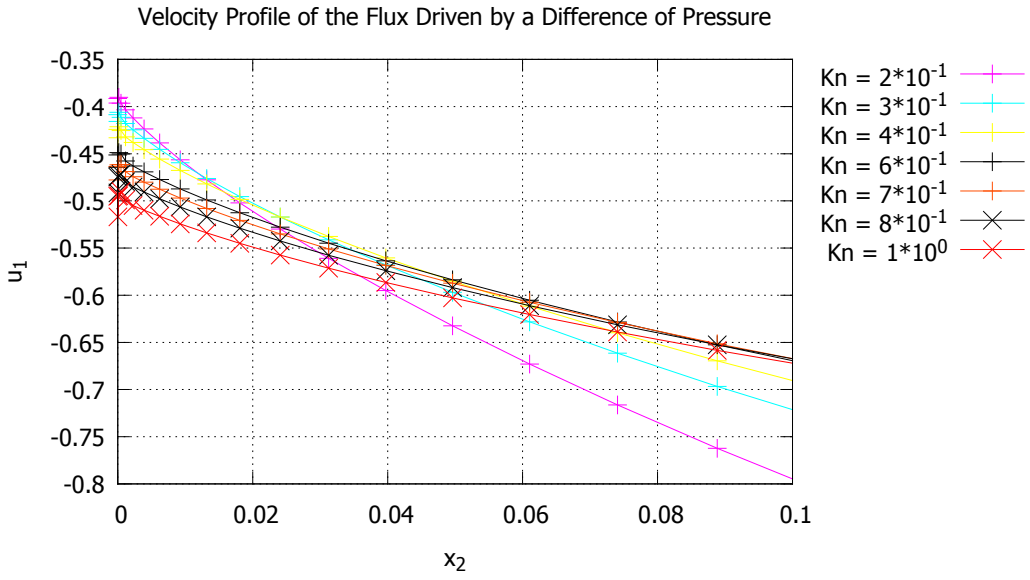

Figure 5.36: u_{P_1}

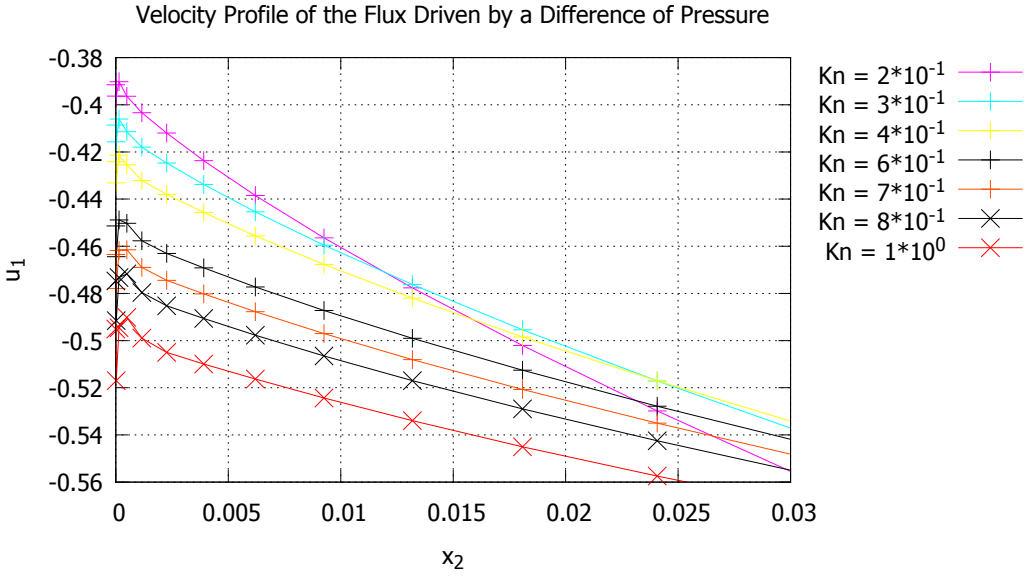

Figure 5.37: u_{P_1}

The velocity exhibits a strange behavior at the boundary. Its profile zigzags towards the borderline. That is due to the finite-difference method that "clashes" with the discontinuity. Moreover, in the second picture of this section one may notice that in the case of $Kn = 10^2$ the gross velocity rises abruptly on the boundary. Such an high value of the Knudsen number causes the molecular density to get "thinner" around the origin, which means that the gas is more rarefied. The overall system of particle is less responsive to the effect of the collisions. As a consequence the gross velocity is more uniform in the innermost part of the tube and suddenly changes at the boundary to suit the boundary conditions. This effect does not have anything to do with our method. It reflects a "true" physical phenomenon. One more noteworthy remark has to be made: the velocity profile in the case of $Kn = 10$ is lower than the profile found for $Kn = 1$. This counter-intuitive behavior reflects the presence of a minimum of the mass flow-rate around a unitary value of the Knudsen number.

5.2.1.2 u_{T_1}

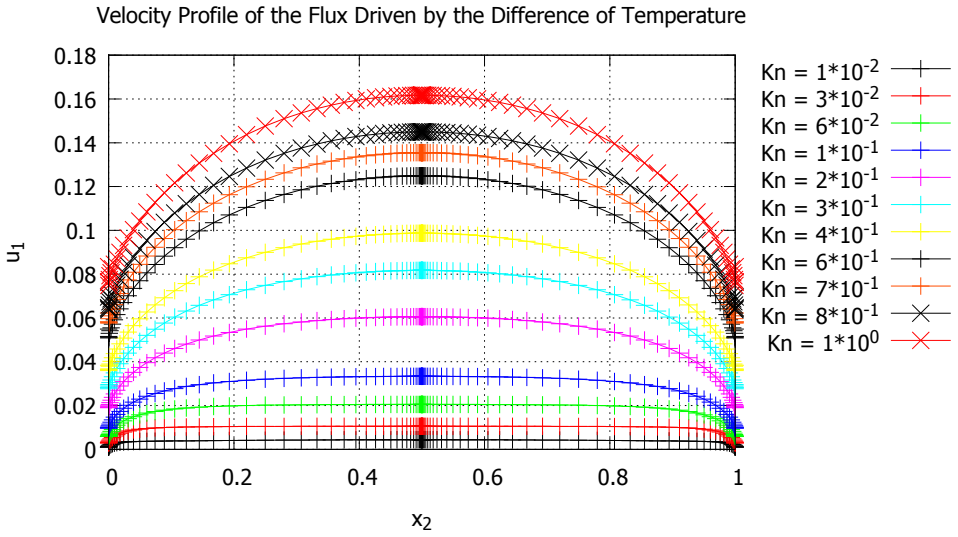

Figure 5.38: u_{T_1}

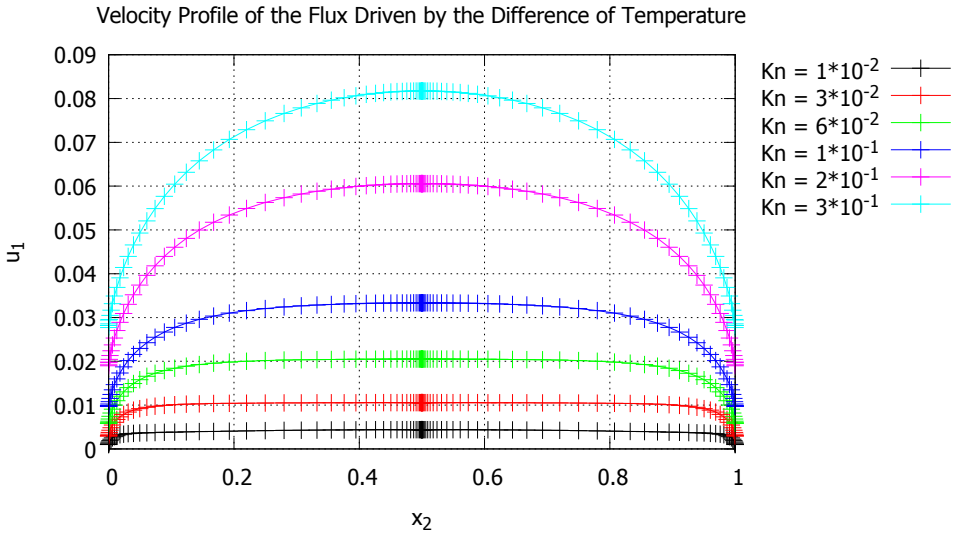

Figure 5.39: u_{T_1}

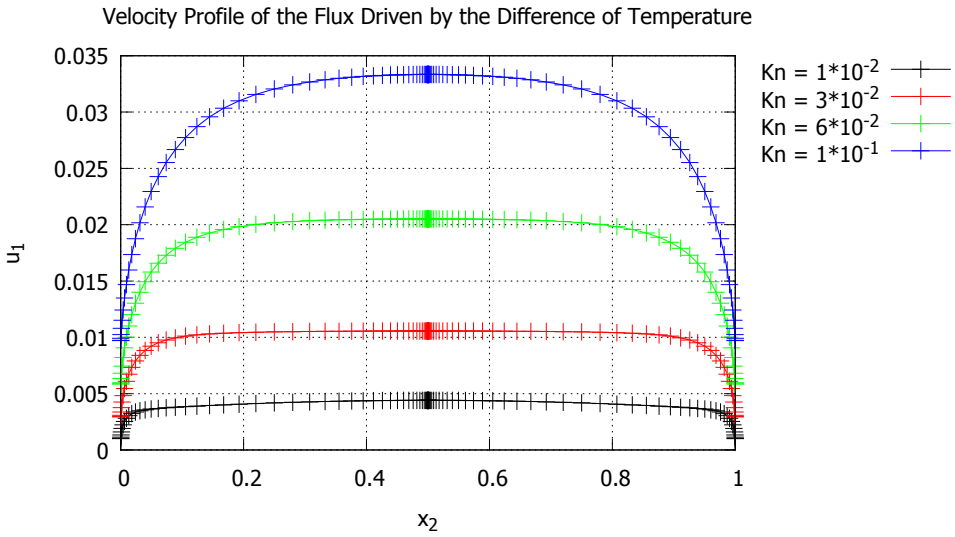

Figure 5.40: u_{T_1}

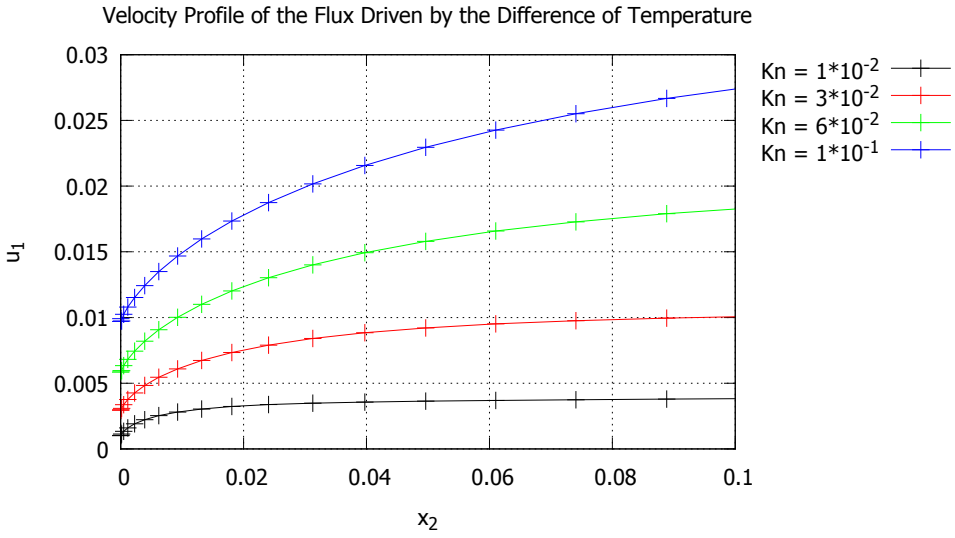

Figure 5.41: u_{T_1}

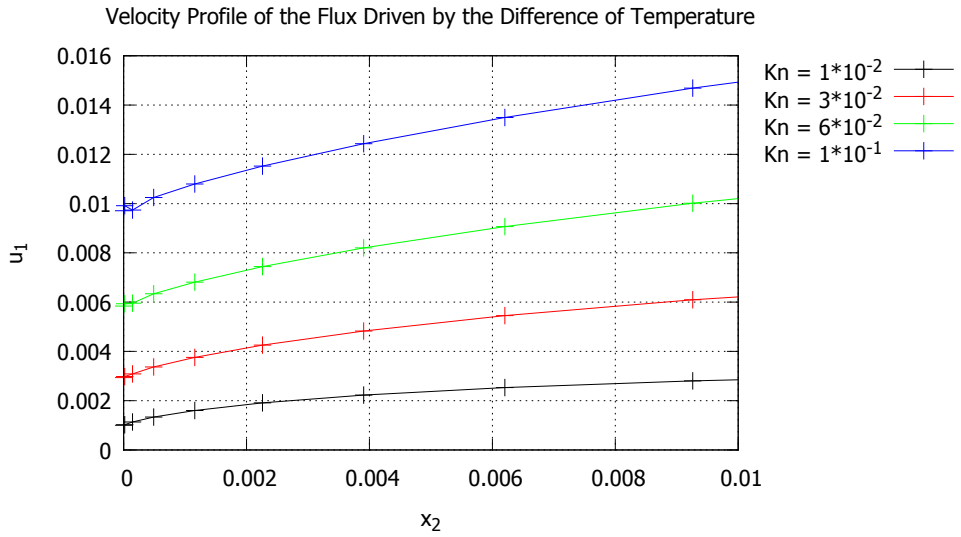

Figure 5.42: u_{T_1}

5.2.2 ES-Model

5.2.2.1 u_{P_1}

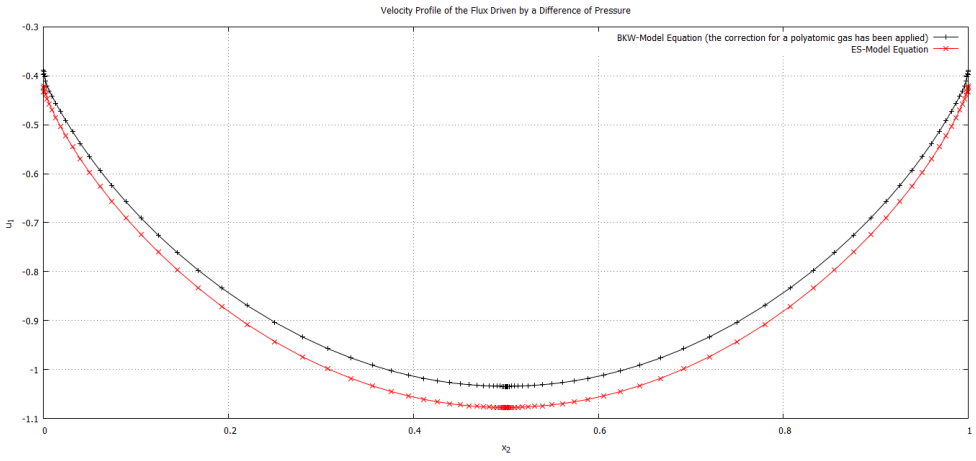

Figure 5.43: u_{P_1}, $Kn = 4 \times 10^{-1}$

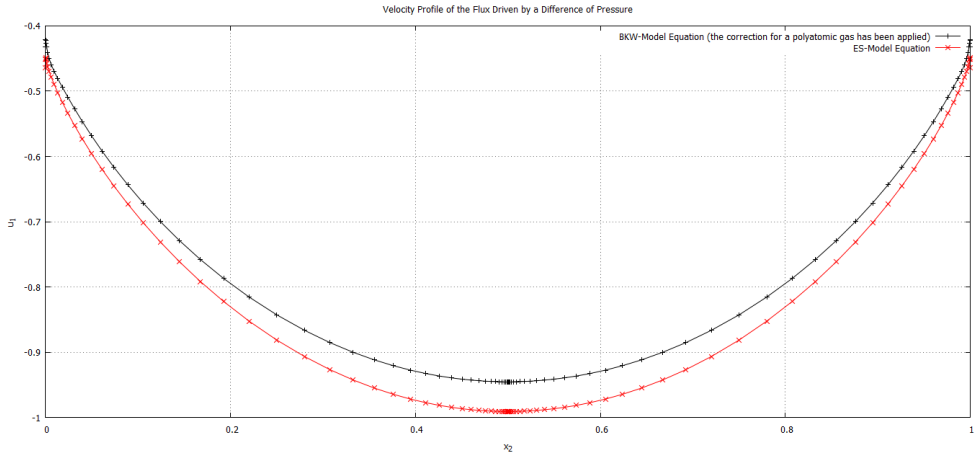

Figure 5.44: u_{P_1}, $Kn = 6 \times 10^{-1}$

5.2.2.2 u_{T_1}

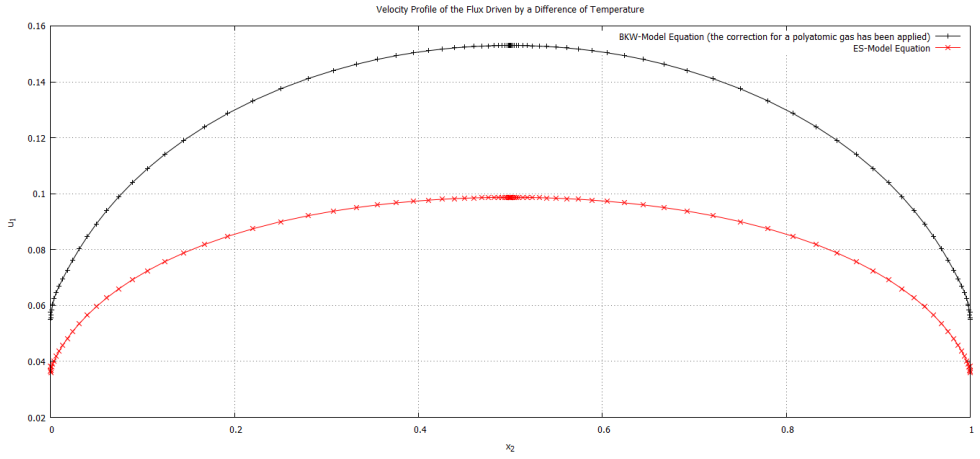

Figure 5.45: u_{T_1}, $Kn = 4 \times 10^{-1}$

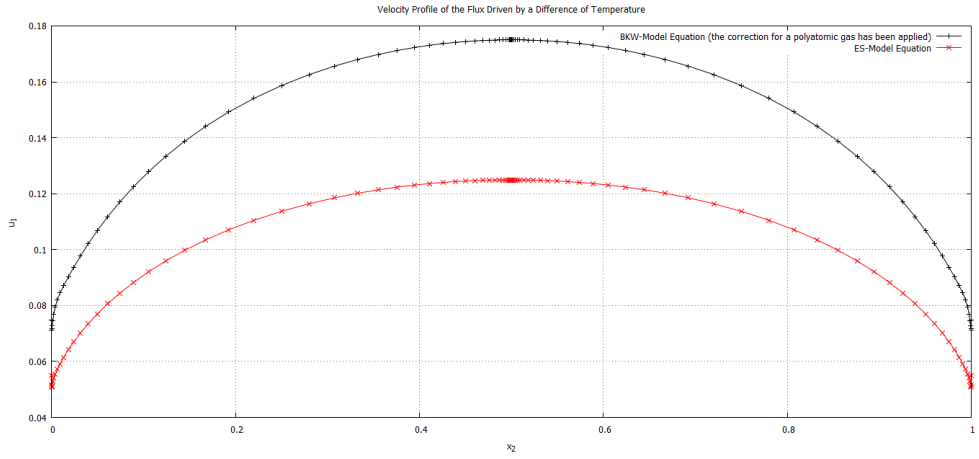

Figure 5.46: u_{T_1}, $Kn = 6 \times 10^{-1}$

5.3 ϕ_p and ϕ_T computed imposing the Maxwellian-Type Boundary Condition

ϕ_α has the same meaning as in section 4.1.1. We will show some of the outcomes of the computations.

5.3.1 $\alpha = 4 \times 10^{-1}$ and $Kn = 10^{-1}$

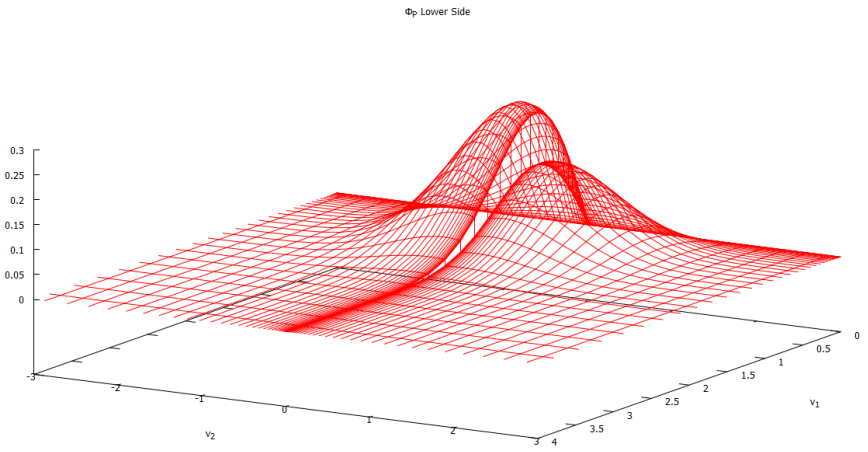

Figure 5.47: ϕ_P Lower Side

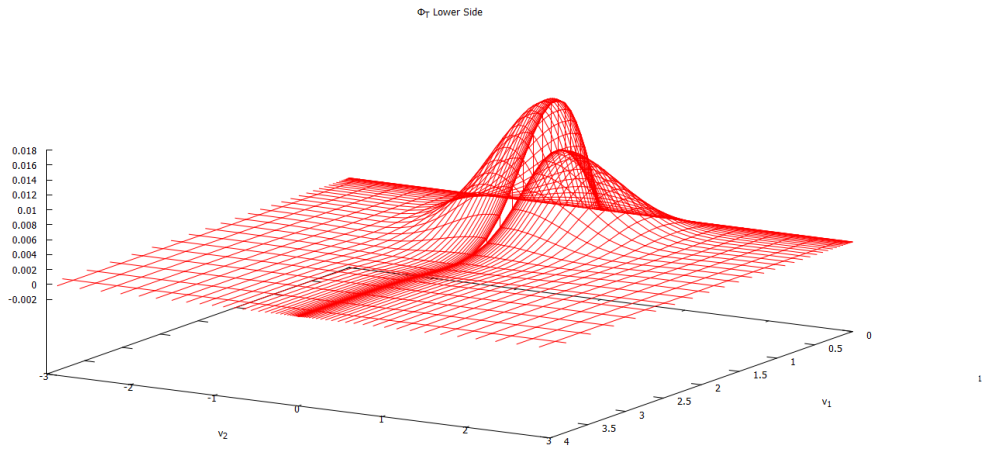

Figure 5.48: ϕ_T Lower Side

5.3.2 $\alpha = 2 \times 10^{-2}$ and $Kn = 10^{-1}$

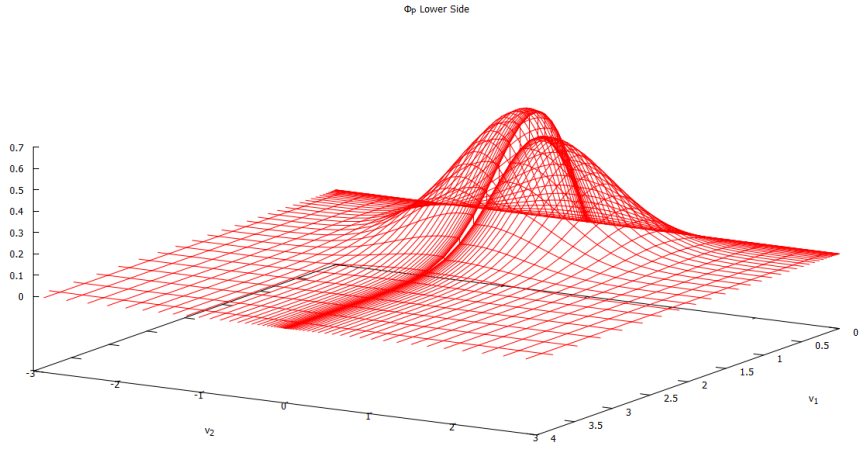

Figure 5.49: ϕ_P Lower Side

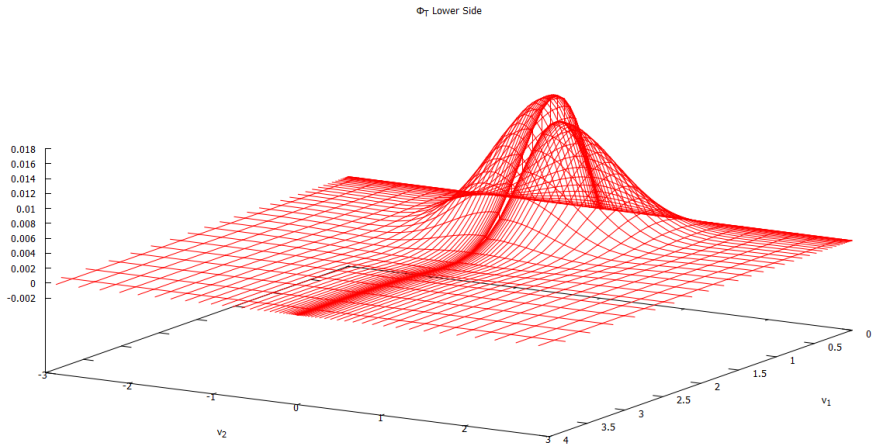

Figure 5.50: ϕ_T Lower Side

5.3.3 $\alpha = 10^{-2}$ and $Kn = 10^{-1}$

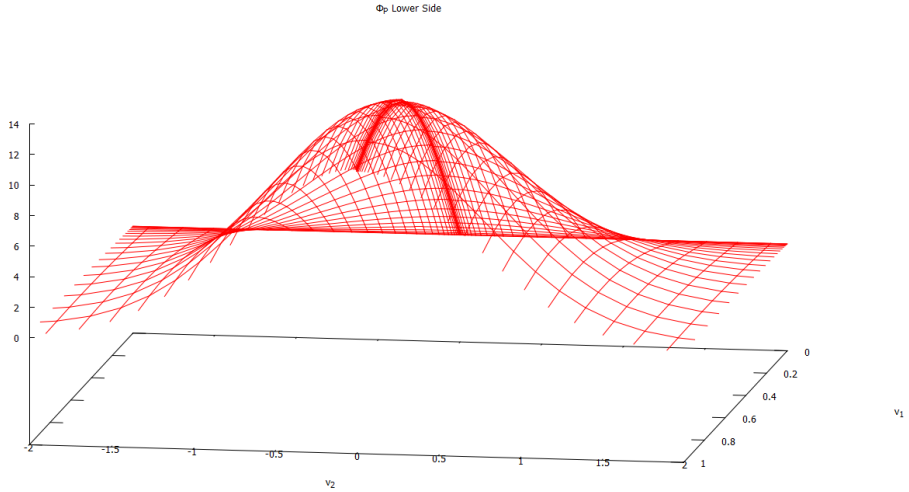

Figure 5.51: ϕ_P Lower Side

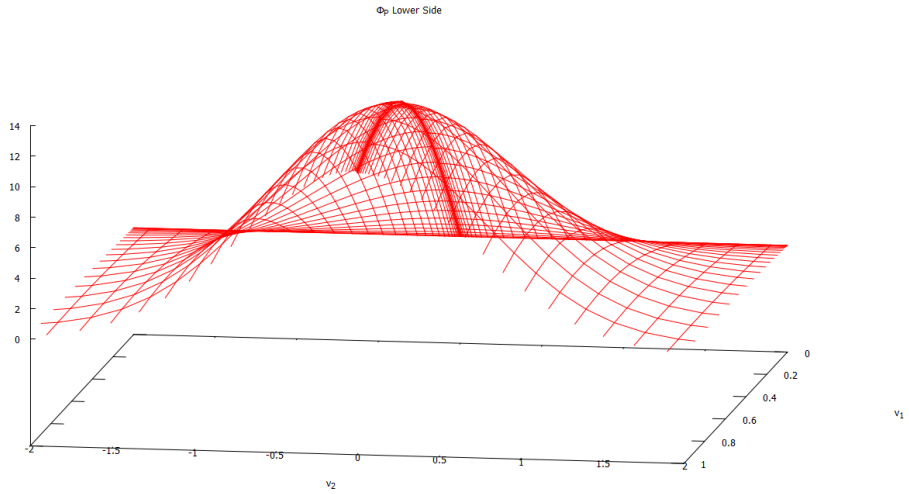

Figure 5.52: ϕ_P Lower Side

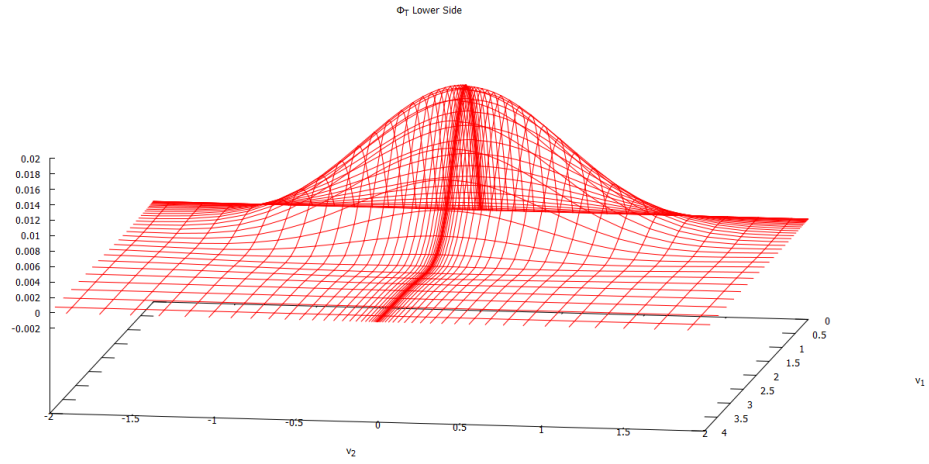

Figure 5.53: ϕ_T Lower Side

5.4 M_T and M_P

We compare now the mass-flow rates obtained. It is noteworthy that there is a database available online on the personal website of Professor Sone [10] where data for these two coefficients can be found in the case of flow through a cylinder and between two parallel plates. However, these data have been

found by applying only the BKW-Model, which, as already explained, is not a limiting condition, and diffuse-reflection boundary conditions. The data found in this paper, as well as those resulting from similar computations (see for the case of a flow inside a thin cylindrical conduit), are thought to be slightly more accurate than those found some years ago by Sone because of the ongoing continuous improvement of computational media. The results obtained for the Poiseuille flow show good accordance for all Knudsen numbers. In both this computations and those in [5], as far as the thermal-transpiration flow is concerned, the relative difference is small for higher values of the Knudsen number, whereas in case of lower Knudsen numbers ($Kn \leq 10^{-1}$), the relative difference is not negligible any more. Also the computation in case of large Knudsen numbers ($Kn \geq 10^{2}$) might yield slight different results.

Kn	$-M_{P_{Sone}}$	$-M_P$	$M_{T_{Sone}}$	M_T
1×10^{-2}	9.916	9.91637958588908	0.00335365	0.004060362164873696
3×10^{-2}	3.6559	3.65603894464242	0.0098094	0.01009631585877536
6×10^{-2}	2.1004	2.10070954005793	0.0188694	0.01904252863978931
1×10^{-1}	1.48745	1.48751271803829	0.0297971	0.02993366274276359
2×10^{-1}	1.04345	1.04354838548154	0.052255	0.05236761848361676
3×10^{-1}	0.90625	0.906405723990694	0.069765	0.06987919978034930
4×10^{-1}	0.84395	0.844092217677563	0.08408	0.08419076357268261
6×10^{-1}	0.79175	0.791904667206507	0.10675	0.106888610183851
7×10^{-1}	0.7806	0.780728294950862	0.116095	0.116213100798656
8×10^{-1}	0.7741	0.774241969773390	0.1245	0.124678954963663
1	0.76925	0.769227542192666	0.139182	0.139802239856045
10^1	0.99505	0.994484098946172	0.33503	0.338602477173270
10^2	1.4946	1.49643622164889	0.60245	0.609082237673433

Table 5.1: BKW-Model, Mass-Flow Rates

Nevertheless, given that the accuracy of the results hereby obtained is subject to a relative error on the collision term which worsens the solution since an integration over the whole cross section is carried out (the last digits of the given data might be utterly insignificant in physical term), we may claim that, as far as the results are comparable to those obtained by Sone (conditions listed above):

- For higher Knudsen numbers, the results given by Sone and those here obtained show perfect accordance;

- For lower Knudsen numbers, the results obtained in this paper and in [5] are likely to be more accurate.

As already explained, the ES-Model implemented in this way (see section 3.7) does not lead to good results. For instance, let us take a look at the following table.

Kn	$-M_P$		M_T	
	BKW-Model*	ES-Model	BKW-Model	ES-Model
4×10^{-1}	0.780468551	0.848042311029	0.0841907635	0.128770089430
6×10^{-1}	0.749488889	0.797031291033	0.1068886101	0.149253507377

* The due correction has been applied.

Table 5.2: ES-Model, Mass-Flow Rates

A couple of remarks have to be made:

- Given that the error on the collision term is the same in the two cases, the relative error on the thermal-transpiration flow i much larger than that on the Poiseuille flow.
- These data are impressively good if compared to the poor mesh used to compute them. The author was expecting to obtain much worse data.
- The Prandtl number applied in the correction, corresponding to the one used in ES-Model by setting the values of its two parameters, is slightly different from the experimental one (see [5], Chapter 5).

We will now show a comparison between the data obtained with different values for the accomodation coefficient α. These are the data obtained in case of $\alpha = 0.8$.

Kn	$-M_P$	M_T
1×10^{-1}	1.71594065102258	0.02852942283308928
2×10^{-1}	1.26792373216702	0.05093826225624633
3×10^{-1}	1.12907193158461	0.06927613436466019
4×10^{-1}	1.06638610642821	0.08490972819031831
6×10^{-1}	1.01555611899100	0.110818132886805
7×10^{-1}	1.00559961171446	0.121871009084524
8×10^{-1}	1.00055813625851	0.131971411048076
1	0.998606092280372	0.150681874415117
10^1	1.32310512304153	0.420133273434314
10^2	2.04131790611601	0.80987726987361

Table 5.3: BKW-Model, $\alpha = 0.8$, Mass-Flow Rates

The following table show the data obtained in case of $\alpha = 0.4$.

Kn	$-M_P$	M_T
1×10^{-1}	2.83892411030098	0.02555419721768168
2×10^{-1}	2.38190353781178	0.04785734492856788
3×10^{-1}	2.23923198125151	0.06803290146520063
4×10^{-1}	2.17578219289462	0.08663895901304167
6×10^{-1}	2.12830249145230	0.120374576071962
7×10^{-1}	2.12144360401964	0.135823667620900
8×10^{-1}	2.11995134946993	0.150666036468581
1	2.12591533382829	0.179283026556779
10^1	2.78574100573617	0.708484684766731
10^2	4.41363806160725	1.62552294251066

Table 5.4: BKW-Model, $\alpha = 0.4$, Mass-Flow Rates

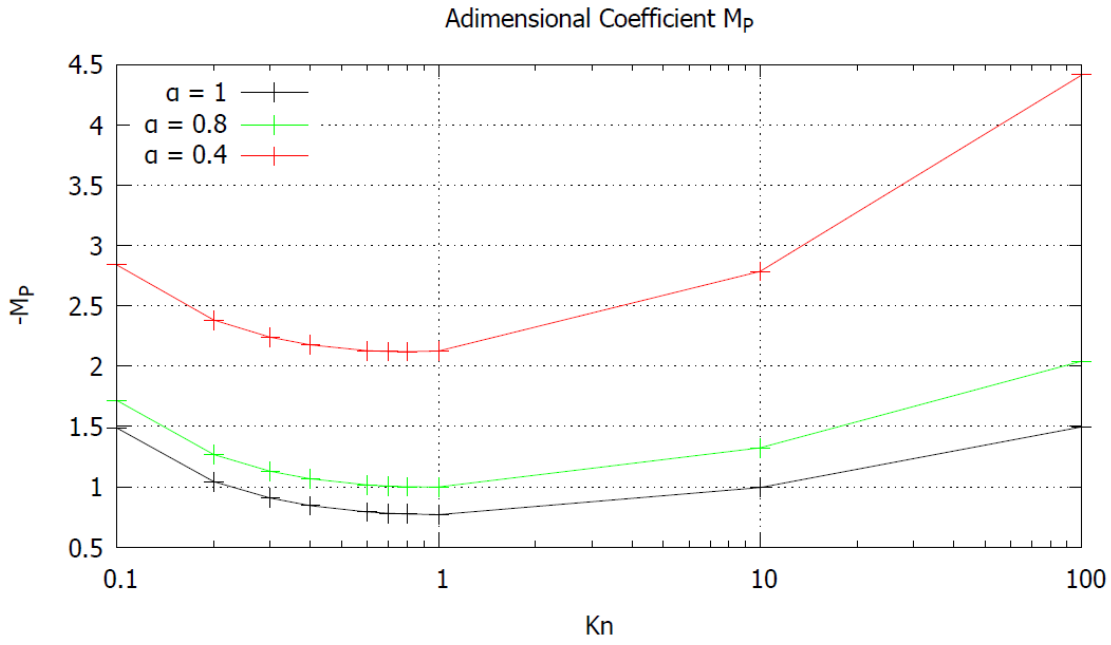

Figure 5.54: M_P

The last plot displays a minimum, which accounts for the behavior of the Poiseuille flow previously showed (subsection 4.2.1.1). The more α is increased, the more the flow grows. This is due to the fact that the imposition of the temperature on the tube is achieved through the boundary condition.

Unfortunately, the temperature does not appear in the pure reflection boundary condition ($\alpha = 0$). Therefore the temperature cannot be enforced on a given cross section and the problem is not well-posed any more. Accordingly, also the pressure cannot be imposed, as one can see by going through all the steps of the solution (see formula (35) of [8]). As a consequence, the smaller gets α, the harder it becomes to impose a given temperature and the wall gets more "slippery", which corresponds to an increasing non-zero right side of ϕ_α at the lower boundary that can be observed in the previous plots. As far as the Poiseuille flow is concerned, this effect leads to an increase in M_p (a decrease in $-M_P$). The plot of u_P for $Kn = 10^{-2}$ is perfectly coherent with what has just been claimed.

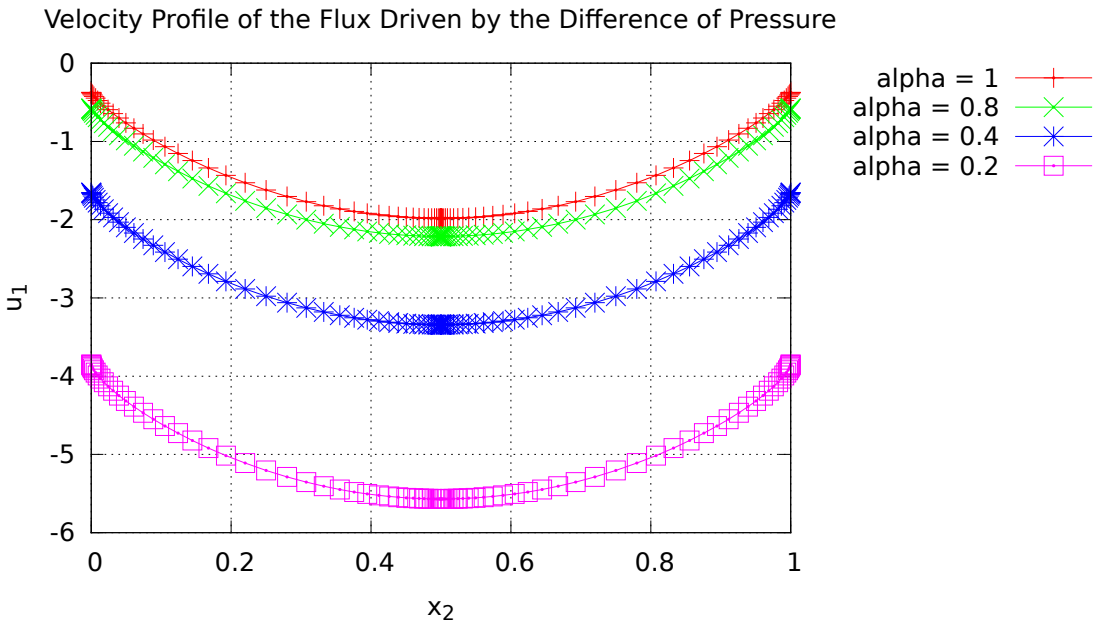

Figure 5.55: u_P, $Kn = 10^{-2}$

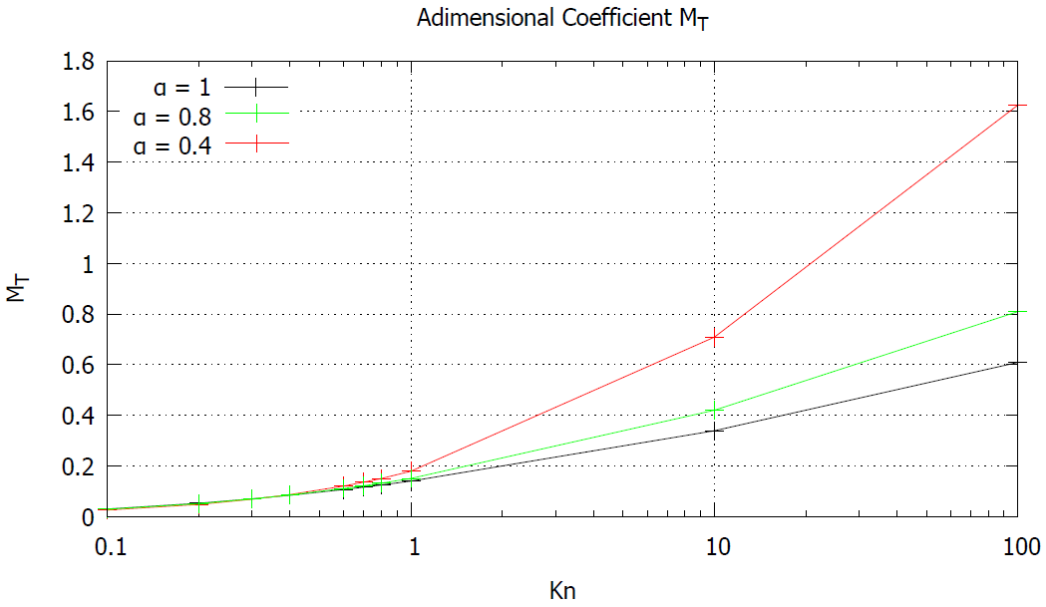

Figure 5.56: M_T

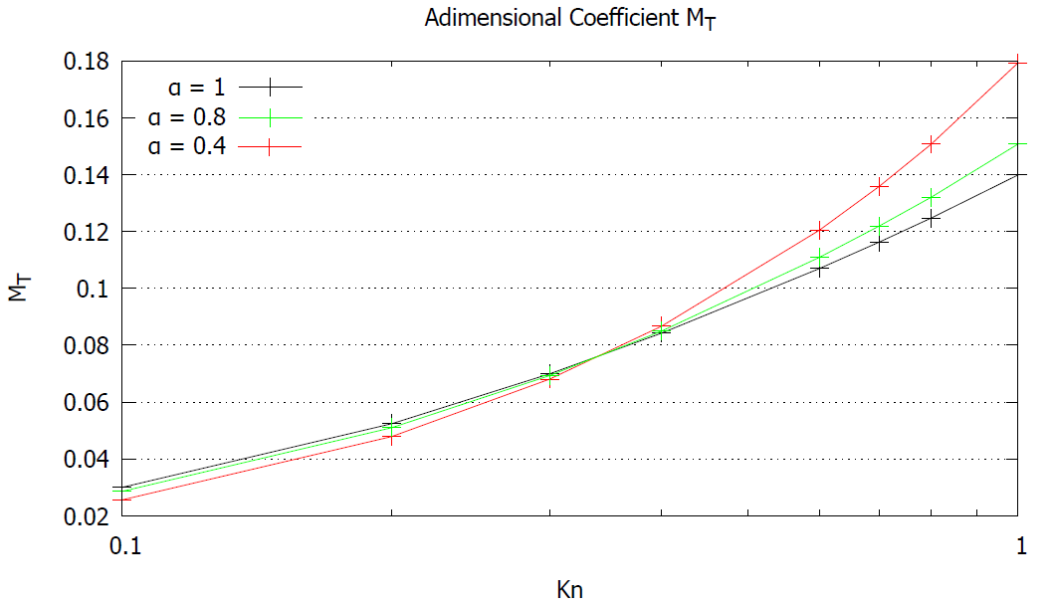

Figure 5.57: M_T

The thermal-transpiration flow is an effect of rarefaction, so for small Knudsen numbers the flow gets smaller. As long as the Knudsen number

is large enough, the trend of the plots is the same as in the previous case, whereas a close-up of the plots for small Knudsen numbers exhibits an inversion in the behavior of the gas, as can be observed in the following plot of u_T for $Kn = 10^{-2}$.

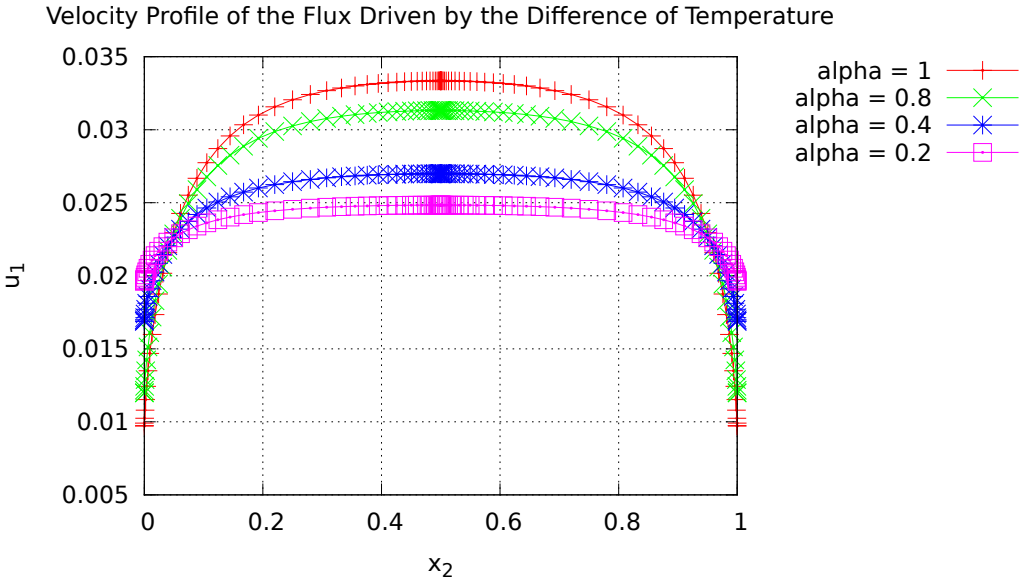

Figure 5.58: u_T Lower Side

In order to fathom this odd behavior, these further data have been computed for $Kn = 10^{-2}$.

α	$-M_P$	M_T
0.2	5.06321581092534	0.02409793982331023
0.01	89.2974758176483	0.02725724635982697

Table 5.5: BKW-Model, $Kn = 10^{-2}$, Mass-Flow Rates

We can definitely affirm that for small Knudsen numbers, the trend of the thermal-transpiration flow is reversed. However, the introduction about the thermal-transpiration flow (section 2.2) was based upon the hypothesis of diffuse-reflection boundary condition. Footnote 7 at page 9 of the aforementioned book by Sone points out that the analysis carried out fails to hold with general boundary conditions because some terms cancel out. As a reference, Sone gives a book by K. Aoki, T. Inamuro, and Y. Onishi [11].

Therefore, two points should be made clearer by a further detailed analysis: the reason for this reversal of behavior and the location of the point of intersection between all the curves.

The following are the data of M_P with the due correction applied. These data will be employed for the computation of the second-order solution.

Kn	$\alpha = 1$	$\alpha = 0.8$	$\alpha = 0.4$
1×10^{-1}	1.74139803061821	1.96982596360250	3.09280942288090
2×10^{-1}	1.17049104177150	1.39486638845698	2.50884619410174
3×10^{-1}	0.991034161517332	1.21370036911125	2.32386041877815
4×10^{-1}	0.907563545822542	1.12985743457319	2.23925352103960
6×10^{-1}	0.834218885969826	1.05787033775432	2.17061671021562
7×10^{-1}	0.816997625319421	1.04186894208302	2.15771293438820
8×10^{-1}	0.805977633845879	1.03229380033100	2.15168701354242
1	0.794616073450658	1.02399462353836	2.15130386508628
10^1	0.997022952071971	1.32564397616733	2.78827985886197
10^2	1.49669010696147	2.04157179142859	4.41389194691983

Table 5.6: BKW-Model, Mass-Flow Rates

5.5 Second-Order Solution

The following data refer to the problem of a flow between two tanks when the pressure in unknown (see section 4.9.2). The following parameters have been set:

- initial pressure gradient $a = 0.2$;
- constant temperature gradient $\beta = 1.5$;
- $L = 10^{-2}$;
- $R = 10^{-4}$;
- $K_* = 1$;
- $m = 2$.

All these parameters may be arbitrarily chosen. The following plot show what we get for three values of α in case of Nitrogen . As time goes on, the steepness of the curves decreases, which reflects the trends to equilibrium.

An increase in the accomodation coefficient leads to smaller mass-flow rate coefficients, and so to a drop in the overall responsiveness of the system.

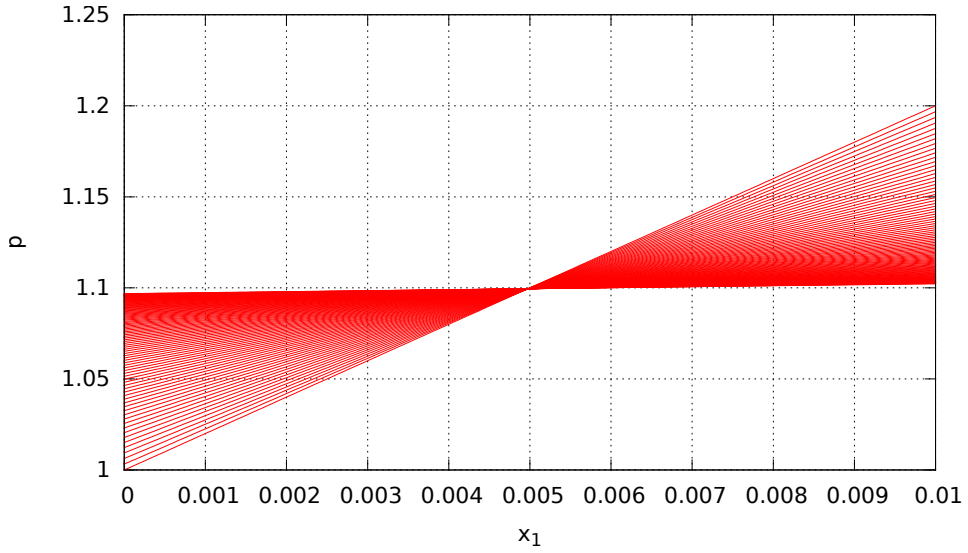

Figure 5.59: $\alpha = 1$

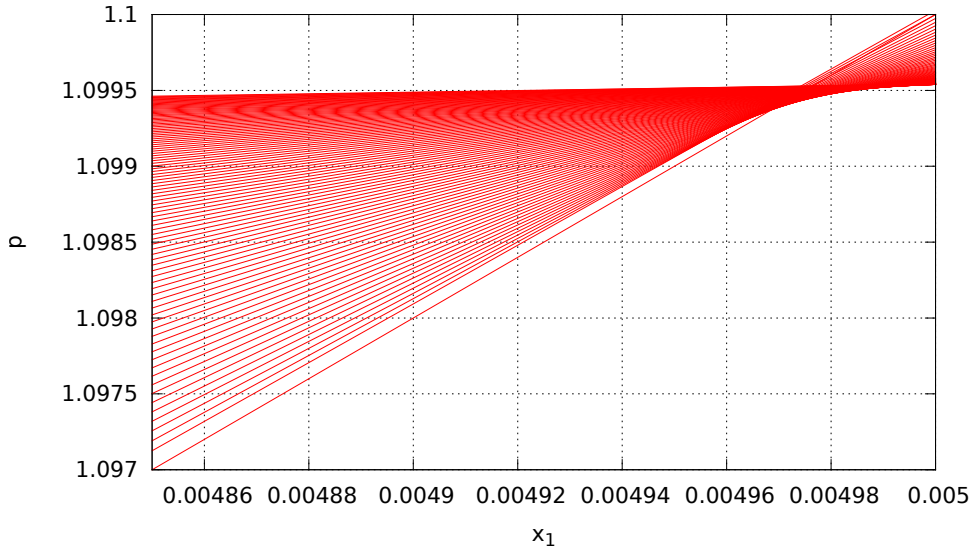

Figure 5.60: $\alpha = 1$

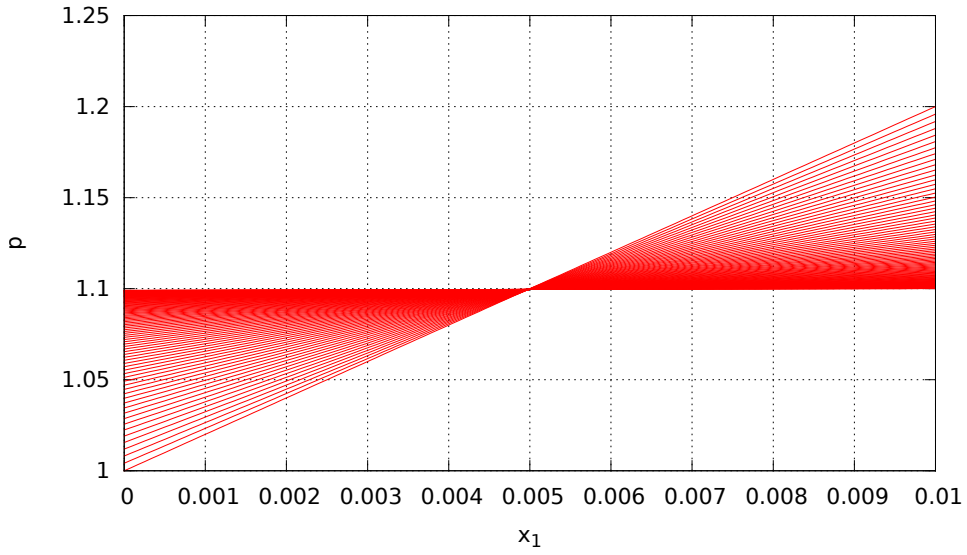

Figure 5.61: $\alpha = 0.8$

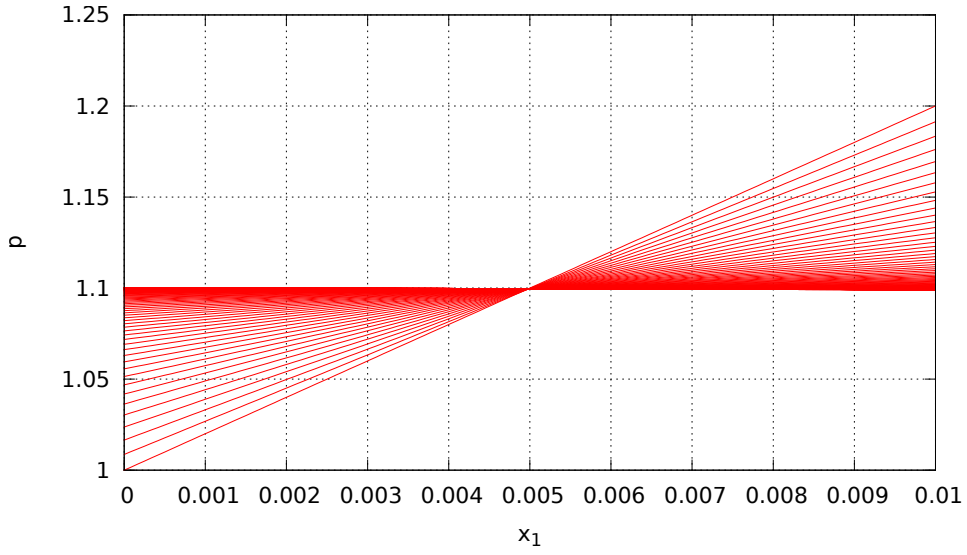

Figure 5.62: $\alpha = 0.4$

Once the effect of a variation of the boundary conditions through α has been illustrated, we want to conclude with a few simulations of a single-stage Knudsen pump (see section 4.9.3) just to show a practical application of the data obtained. Actually, in order to have a good rate of compression, the difference of temperature between the two tanks should be large. Otherwise, several stages are to be arranged in series. Given that we will employ just one stage, we have two choices to attain a satisfactory difference of temperature: increasing the gradient or lengthening the conduit. We will adopt the second solution and set the parameters as shown below:

- $\alpha = 1$;
- initial pressure gradient $a = 0$;
- constant temperature gradient $\beta = 1.5$;
- $L = 1$;
- $R = 10^{-4}$;
- $m = 1$.

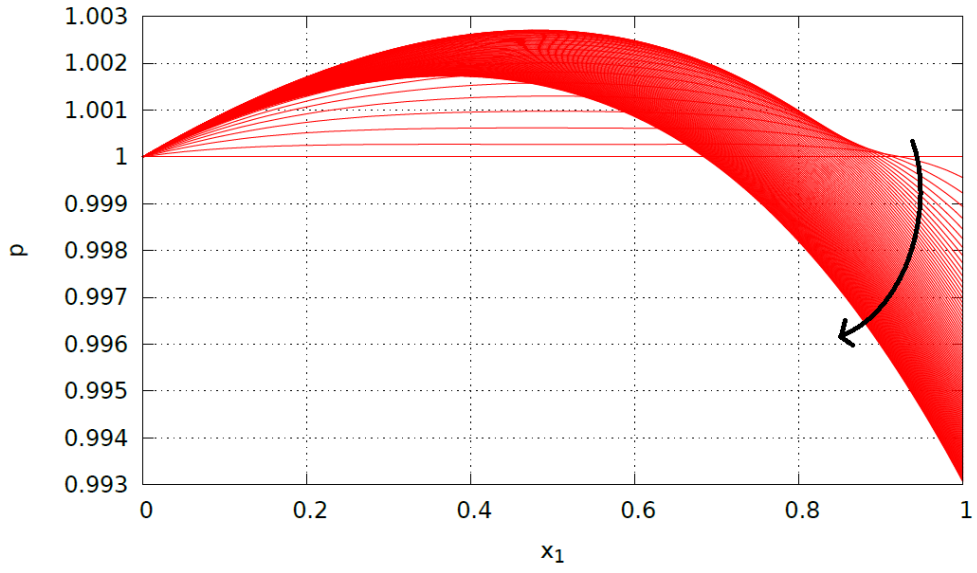

Figure 5.63: $Kn = 0.1$

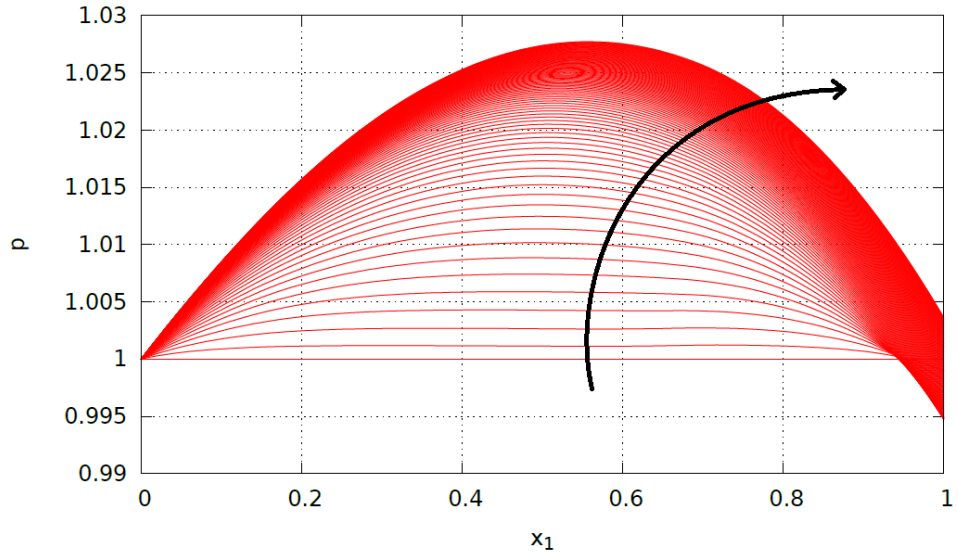

Figure 5.64: $Kn = 0.5$

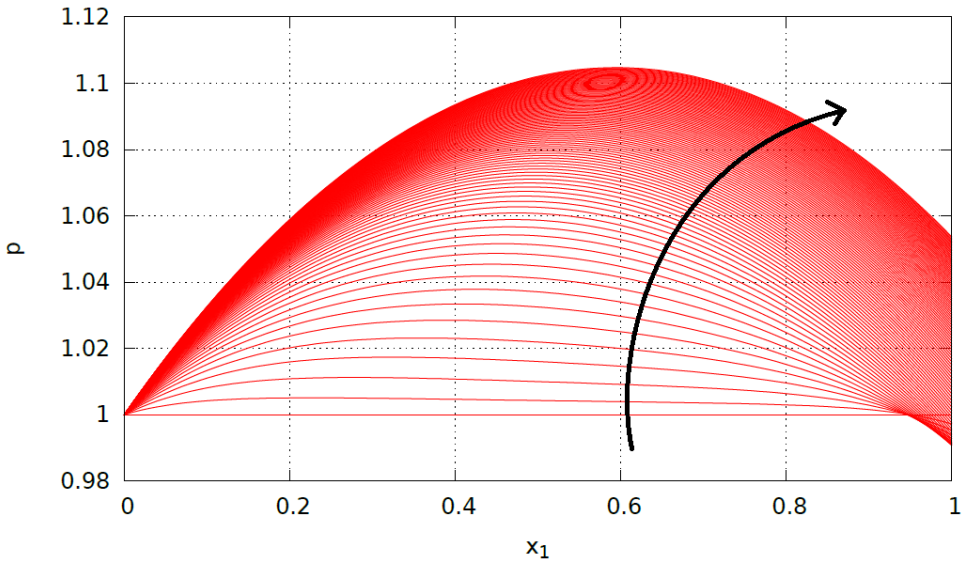

Figure 5.65: $Kn = 10$

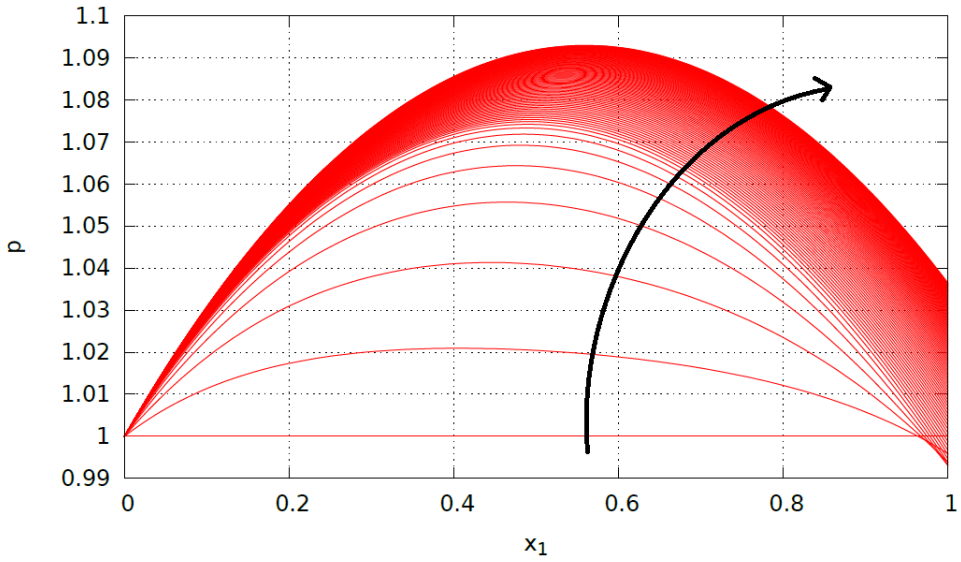

Figure 5.66: $Kn = 35$

The plot of Figure 5.63 does not display the behaviour we expect because of the low Knudsen number. For such a low value the Poiseuille flow is predominant over the thermal-transpiration flow: the compressive effect characteristic of the Knudsen pump proper is reversed. One last point is worth of mention: the compression ratio is greater at $Kn = 10$ than at $Kn = 35$. The fact that the compression ratio is not a monotone function of the Knudsen number has already been pointed out before both numerically and experimentally for gas flowing in circular tubes [5].

6 Bibliography

[1] C. Truesdell & R.G. Muncaster
Pure & Applied Mathematics, V. 83. (Eds.)
Fundamentals of Maxwell's Kinetic Theory of a Simple Monatomic Gas: Treated as a Branch of Rational Mechanics
Academic Press, 1980

[2] C. Cercignani
Applied Mathematics 1st Edition, C. T. (Ed.)
Rarefied Gas Dynamics: From Basic Concepts to Actual Calculations
Cambridge University Press, 2000

[3] P. Andries, P. Le Tallec, J. Perlat & B. Perthame
The Gaussian-BGK model of Boltzmann equation with small Prandtl number
Eur. J. Mech. B-Fluids 19, pp. 813-830, 2000

[4] Y. Sone
Modeling and Simulation in Science, Engineering & Technology (Eds.)
Molecular Gas Dynamics: Theory, Techniques, and Applications
Birkhäuser, 2007

[5] H. Funagane, S. Takata, K. Aoki & T. Kugimoto
Poiseuille flow and thermal transpiration of a rarefied polyatomic gas through a circular tube with applications to microflows
Bollettino dell'Unione Matematica Italiana Ser. 9, 4(1), 19–46, 2011

[6] K. Aoki & S. Takata
Fluid models and simulations of internal rarefied gas flows
Riv. Mat. Univ. Parma, Serie 8, Vol. 1, 1–69, 2009

[7] S. Takata, H. Funagane & K. Aoki
Fluid modeling for the Knudsen compressor: Case of polyatomic gases
Kinetic and Related Models 3(2), 353–372, 2010

[8] K. Aoki, P. Degond, S. Takata & H. Yoshida
Diffusion models for Knudsen compressors
Phys. Fluids 19(11), 117103-1–21, 2007

[9] E. Kilic
Explicit formula for the inverse of a tridiagonal matrix by backward continued fractions
Applied Mathematics and Computation, 197(1):345-357, 2008

[10] Y. Sone
http://fd.kuaero.kyoto-u.ac.jp/download/p1
[11] K. Aoki, T. Inamuro & Y. Onishi
Slightly rarefied gas flow over a body with small accommodation coefficient
J. Phys. Soc. Jpn 47, 663–671, 1979
[12] Y. Sone
Modeling and Simulation in Science, Engineering & Technology
Kinetic Theory and Fluid Dynamics
Birkhauser, 2002
[13] K. Aoki, P. Degond, L. Mieussens, S. Takata, & H. Yoshida
A diffusion model for rarefied flows in curved channels
SIAM MMS 6(4), 1281-1316 (2008)
[14] S. Takata & H. Umetsu
Numerical study on effective configurations of the Knudsen pump for separation and compression
AIP Conference Proceedings 05/2011; 1333(1):998-1003